On the spectra of mapping classes and the 4-genera of positive knots

Inauguraldissertation

der Philosophisch-naturwissenschaftlichen Fakultät
der Universität Bern

vorgelegt von

Livio Liechti

von Landiswil

Leiter der Arbeit:

Prof. Dr. Sebastian Baader

Mathematisches Institut
der Universität Bern

On the spectra of mapping classes and the 4-genera of positive knots

Inauguraldissertation

der Philosophisch-naturwissenschaftlichen Fakultät
der Universität Bern

vorgelegt von

Livio Liechti

von Landiswil

Leiter der Arbeit:

Prof. Dr. Sebastian Baader

Mathematisches Institut
der Universität Bern

Von der Philosophisch-naturwissenschaftlichen Fakultät angenommen.

Bern, 6. Juni 2017

Der Dekan:
Prof. Dr. Gilberto Colangelo

Contents

Preface

This thesis comprises the results I have obtained during my PhD studies under the supervision of Sebastian Baader at the Mathematical Institute of the University of Bern. During my PhD studies, which I started in January 2014, I have been supported by the Swiss National Science Foundation (project no. 137548 and 159208). I have been focusing mainly on pseudo-Anosov mapping classes and on fibred knots and their role in four-dimensional topology, subjects which are connected via the Alexander polynomial and the signature function.

Some of the content of this thesis is available in published form or accepted for publication: Theorem 5.2 originally appeared in the Osaka Journal of Mathematics [**39**], the content of Chapter 6 originally appeared in the Mathematical Proceedings of the Cambridge Philosophical Society [**40**], and the content of Chapter 4 is accepted for publication in the Proceedings of the American Mathematical Society [**41**]. The rest of Chapters 3–7 contains new material and is not yet available elsewhere.

During my PhD studies, I have had the great pleasure and privilege to work with many other mathematicians. Some of the results obtained in collaboration are mentioned in this thesis. However, with the exception of Section 3.2 in Chapter 2, which describes a result jointly obtained with Peter Feller and which has appeared as an appendix to [**39**], proofs of these results are not included in this thesis. I refer to the originals [**6, 7, 10, 11, 31**] instead.

Livio Liechti
Bern, June 2017

Acknowledgements

I am extremely grateful for the privilege to have been encouraged and inspired by so many people during the course of my PhD studies.

First and foremost, I would like to thank my advisor Sebastian Baader. The great amount of inspiration and enthusiasm for mathematics he has shared with me, as well as his confidence in my work and the freedom and the possibilities he has given me during my PhD studies, have been tremendous.

During my PhD studies, I have been invited to two research stays in the US. I warmly thank Eriko Hironaka for these opportunities and her encouragement, as well as for the great amount of mathematics I have learned and for the excellent times I have had during these stays.

This thesis has been read and co-refereed by Michel Boileau and Stefan Friedl. For this, as well as for suggestions and corrections on a preliminary version of this thesis, I am very grateful.

Much of the mathematics I know I have learned through discussions and collaborations. I thank Robert Billet, Pierre Dehornoy, Peter Feller, Josh Greene, Lukas Lewark and Filip Misev for the constant mathematical stimulation.

For comments and suggestions that found their way into this thesis, I thank Norbert A'Campo, Erwan Lanneau and Balázs Strenner.

I thank everybody at the Mathematical Institute of the University of Bern for the great time I have had there. It is a particular pleasure for me to thank Annina Iseli, Johannes Josi and Luca Studer for the crucial amount of mathematics and fun we shared.

Finally, I thank Cilgia, Walter, Luca and Karla for basically everything.

Teaser

In the following few pages, we aim to present an example which illustrates the flavour of many ideas coming together in this thesis. We are not always precise and it is not necessary to read these pages in order to understand the rest of the thesis.

Consider the closed surface Σ depicted in Figure 0.1. It consists of rectangles with parallel identifications of horizontal sides and vertical sides, as indicated in Figure 0.1 by small diagonal bars. As we will see, there is a unique choice of the side lengths of the rectangles so that the ratio of length and width of each annulus obtained by identifying the sides of the rectangles is $r \approx 2.074$. In our example, there are four vertical and two horizontal annuli.

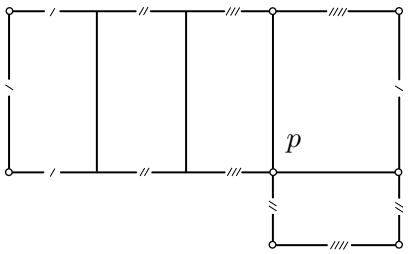

FIGURE 0.1. A closed surface Σ built from rectangles. The vertex p and all the other vertices which get identified with p are highlighted.

Figure 0.2 depicts the action of two self-homeomorphisms f and g of Σ. The map f fixes the vertical sides of the rectangles pointwise, preserves other vertical lines and sends horizontal lines to lines with slope $-r$. In particular, f can be locally written as an affine map with linear part $\left(\begin{smallmatrix} 1 & 0 \\ -r & 1 \end{smallmatrix}\right)$. Similarly, g fixes the horizontal sides of the rectangles pointwise, preserves other horizontal lines and sends vertical lines to lines with slope $1/r$. In particular, g can be locally written as an affine map with linear part $\left(\begin{smallmatrix} 1 & r \\ 0 & 1 \end{smallmatrix}\right)$. It follows that the composition $g \circ f$ can be locally written as an affine map with linear part

$$D = \begin{pmatrix} 1 & r \\ 0 & 1 \end{pmatrix} \begin{pmatrix} 1 & 0 \\ -r & 1 \end{pmatrix} = \begin{pmatrix} 1 - r^2 & r \\ -r & 1 \end{pmatrix}.$$

The linear part D of $g \circ f$ possesses two real eigenvalues $\lambda \approx -1.722$ and $1/\lambda$, and corresponding eigendirections. There exists a pair of transverse, $(g \circ f)$-invariant foliations of Σ, given by lines parallel to the eigendirections of D, see Figure 0.3. There is one singularity of the foliations: the point p, around which the total angle is 6π.

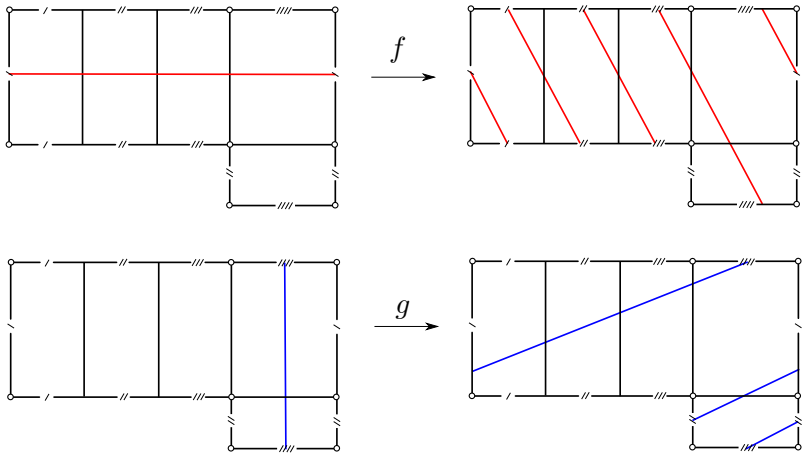

FIGURE 0.2. The action of two affine homeomorphisms f and g on the surface Σ.

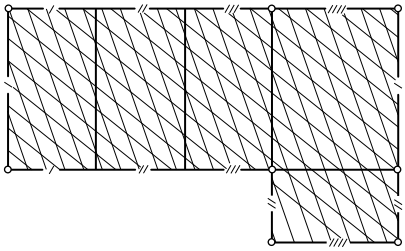

FIGURE 0.3. Two foliations parallel to the eigendirections to $1/\lambda$ and λ. The map $(g \circ f)$ stretches these foliations by $|\lambda|$ and $|1/\lambda|$, respectively.

This means that p is a singularity of the foliations and has the type of a 6-saddle, see Figure 0.4. Furthermore, $g \circ f$ stretches one of the two foliations by $|\lambda|$ and the other

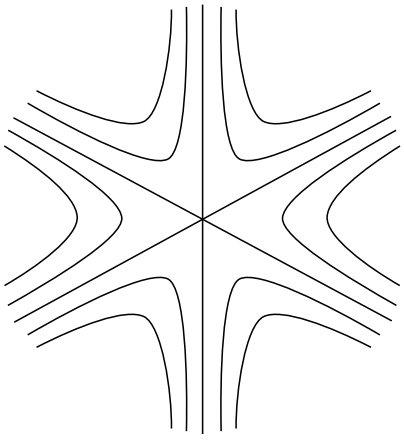

FIGURE 0.4. A foliated neighbourhood of the point p.

by $|1/\lambda|$. The number $|\lambda|$ is called the dilatation of $g \circ f$ and is algebraic. The minimal

polynomial of the number $|\lambda|$ is given by $t^4 - t^3 - t^2 - t + 1$ and its Galois conjugates are $|1/\lambda|$ and $z, \bar{z} \in \mathbf{S}^1$, where $z \approx -0.651 + 0.759i$.

A crucial observation concerns the number r. As we will see, r turns out to be the Perron-Frobenius eigenvalue of the geometric intersection matrix Ω of the curves $\{\alpha_1, \alpha_2, \beta_1, \beta_2, \beta_3, \beta_4\}$, which are depicted in Figure 0.5, and the widths of the rectangles

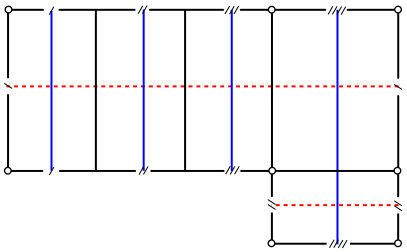

FIGURE 0.5. Dashed red horizontal simple closed curves α_i and blue vertical simple closed curves β_j in Σ.

can be read off from the entries of the Perron-Frobenius eigenvector. In particular, there is a close connection between the Galois conjugates of the dilatation λ and the eigenvalues of Ω, all of which are real numbers, since Ω is symmetric. For many pseudo-Anosov products of two multitwists, think of examples like $g \circ f$, we will make this connection precise and deduce that the Galois conjugates of the dilatation are contained in $\mathbf{R}_{>0}$ or in $\mathbf{R}_{>0} \cup \mathbf{S}^1$, depending on whether the two twists are of opposite sign or of the same sign, respectively (Theorem 3.1). For slightly more general products of two multitwists, we will be able to provide an analogue of this statement for the action induced on the first homology of the surface (Theorem 3.2).

Considering Figure 0.6, we now adopt a different perspective on the surface Σ and the self-homeomorphism $g \circ f$: after removing a small disc around each of the vertices of the rectangles (there are three vertices up to identifications), what is left is a surface Σ' consisting of annuli which retracts to the union of the curves α_i and β_j. Furthermore, Figure 0.6 highlights the fact that the curves α_i and β_j intersect with the pattern of a tree $\Gamma_{\widetilde{X}}$, depicted in Figure 0.7. More precisely, their geometric intersection matrix Ω equals the adjacency matrix $\mathrm{A}(\Gamma_{\widetilde{X}})$ of the tree $\Gamma_{\widetilde{X}}$. As a side remark, Figure 0.6 might also make plausible that the construction we are considering could be carried out for any finite tree Γ.

Something peculiar happens if we consider the mapping torus of the map $g \circ f$ restricted to our new surface Σ', that is, the product of Σ' and the unit interval $[0, 1]$, with the top and bottom copies of Σ' identified by the map $g \circ f$. Using the theory of fibred links, one can show that this mapping torus is homeomorphic to $\mathbf{S}^3 \setminus L$, where L is the link given by the boundary of the surface Σ' embedded in $\mathbf{S}^3$ with one positive full twist in every annulus, see Figure 0.8. As a mapping torus of a pseudo-Anosov homeomorphism, $\mathbf{S}^3 \setminus L$ is also a complete hyperbolic 3-manifold by a theorem of Thurston [**70**].

Now that we have a link L at hand, we might as well consider two of its classic invariants: the Alexander polynomial Δ_L and the signature $\sigma(L)$. In the case of fibred

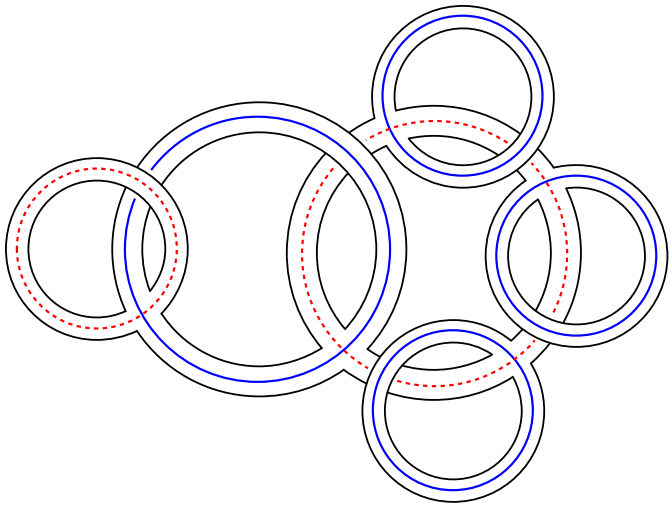

FIGURE 0.6. The surface Σ' is obtained from the surface Σ by removing small neighbourhoods of the three vertices.

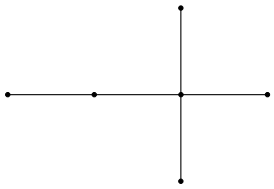

FIGURE 0.7. The tree $\Gamma_{\widetilde{X}}$, whose adjacency matrix $\mathrm{A}(\Gamma_{\widetilde{X}})$ equals the geometric intersection matrix Ω of the curves α_i and β_j.

links, like L, the Alexander polynomial equals the characteristic polynomial of the homological action of the identification map, in our case $g \circ f$. Using this fact and our previously mentioned result on the eigenvalues of the homological action of a product of two multitwists yields a similar distribution result for the zeroes of the Alexander polynomial, which we will generalise to a broader class of links, for example including links as in Figure 0.8 but with multiple positive full twists in each annulus (Theorem 5.4). The signature of an example arising in the same way, but for an arbitrary finite tree Γ, is given by the signature of the matrix $2I + \mathrm{A}(\Gamma)$. In our specific example, the signature of the matrix $2I + \mathrm{A}(\Gamma_{\widetilde{X}})$ is 4, while its dimension is 6. We will show that the signature is always at least two thirds of the dimension, for any finite tree Γ (Theorem 5.2). This result is optimal by the very example we are considering.

The Alexander polynomial Δ_L equals $(-1+t)^2(1+t-t^2+t^3+t^4)$. We observe that the number of zeroes of Δ_L on $\mathbf{S}^1$ exactly equals the signature of the matrix $2I + \mathrm{A}(\Gamma_{\widetilde{X}})$, a phenomenon which we will prove for any finite tree Γ (Proposition 5.6). As an application, we will obtain monotonicity of the signature function $[0,1] \to \mathbf{Z}$, where the value at 1 is the signature of the matrix $2I + \mathrm{A}(\Gamma_{\widetilde{X}})$ (Theorem 5.1). The signature function is of interest in the context of 4-dimensional topology, since many of its values bound from below the first Betti numbers of locally-flat surfaces in $\mathbf{B}^4$

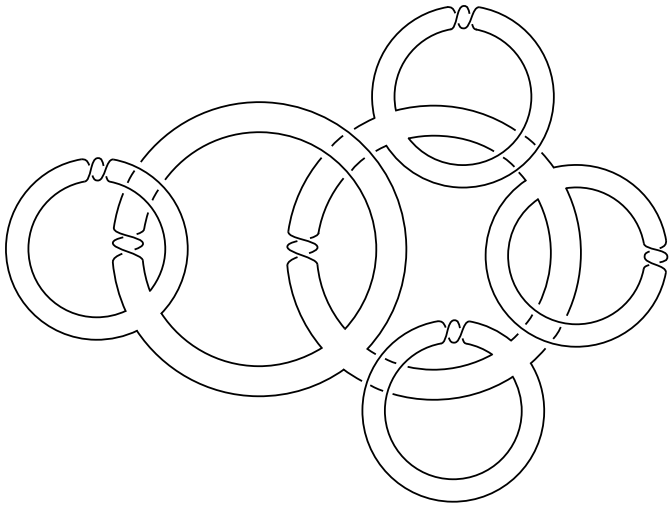

FIGURE 0.8. The link L is the boundary of the surface Σ' embedded in $\mathbf{S}^3$ so that every band has one positive full twist. It has three components.

with boundary $L \subset \mathbf{S}^3$. For example, a locally-flat surface in $\mathbf{B}^4$ with boundary L must have first Betti number greater than or equal to 4. It is possible to show that there exists such a surface with first Betti number 4 as follows. Figure 0.9 depicts a simple closed red curve in the abstract surface Σ', whose homology class evaluates to zero under the quadratic form given by $2I + \mathrm{A}(\Gamma_{\widetilde{X}})$. Furthermore, the depicted dashed

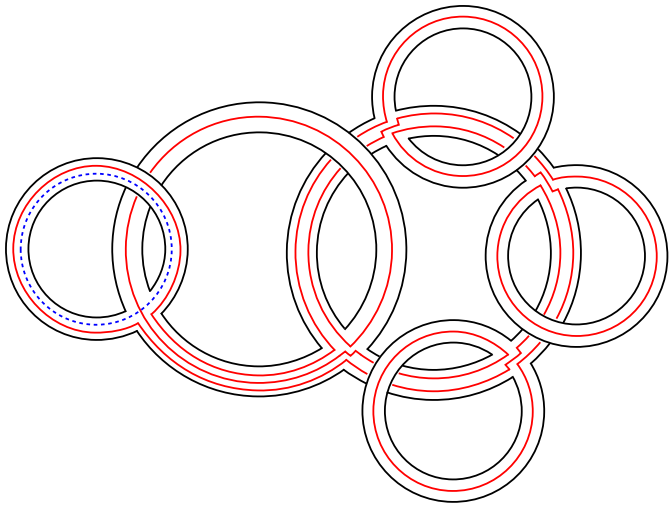

FIGURE 0.9. In our chosen embedding of Σ' into $\mathbf{S}^3$, the boundary of the punctured torus defined by the union of the thickened red and dashed blue curves bounds a locally-flat disc in $\mathbf{B}^4$. This figure is taken from [**7**].

blue curve intersects the red curve exactly once. One can show that the boundary of the punctured torus defined as the union of annular neighbourhoods of both curves

defines a knot with Alexander polynomial 1 via our chosen embedding of the surface Σ' into $\mathbf{S}^3$. By a theorem of Freedman, this knot bounds a locally-flat disc in $\mathbf{B}^4$ [**24**]. In particular, we obtain a locally-flat surface in $\mathbf{B}^4$ with boundary L and first Betti number 4 by cutting out the punctured torus and glueing back the locally-flat disc in $\mathbf{B}^4$. We will see that such a surgery procedure can be carried out for any tree Γ for which the difference of signature and the number of vertices is greater than or equal to two (Proposition 6.5).

We allow ourselves one last angle of looking at the link L. This time, we consider L as the closure of the positive braid on four strands given by the positive braid word $w = \sigma_1^2\sigma_2^2\sigma_1\sigma_3\sigma_2^2\sigma_3$. A geometric representation of w and its closure are depicted in Figure 0.10. Clearly, there exist many positive braid words which have w as a subword.

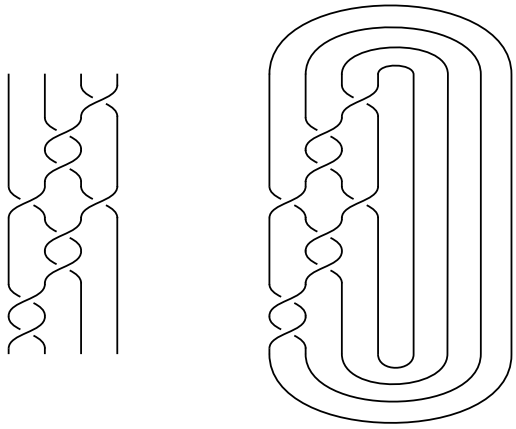

FIGURE 0.10. A geometric representation of the braid word w on the left, and its closure on the right.

What we will remark is that their fibre surfaces have our chosen embedding of Σ' as an incompressible subsurface. In particular, we will see that a surgery procedure as described above works for the fibre surface of all these positive braid links. Using this remark for $\Gamma_{\widetilde{X}}$ and three other well-chosen trees $\Gamma_{\widetilde{T}}$, $\Gamma_{\widetilde{E}}$ and $\Gamma_{\widetilde{Y}}$, we will be able to show the following: if the signature of a positive braid knot does not equal the first Betti number, then a surgery procedure as described above can be carried out on its fibre surface (Theorem 6.1). In fact, we will even show that for prime positive braid knots K, the minimal possible number of such surgery procedures grows linearly with the minimal number of strands necessary to represent K as a positive braid (Theorem 7.3).

CHAPTER 1

Introduction

In the last decades, the study of low-dimensional topological objects has been strongly influenced by ideas of Thurston and Freedman, with many of them reaching as far back as the 70s or the 80s. Important instances are the classification of surface mapping classes due to Thurston [**69**] and Thurston's Geometrisation Conjecture, proved by Perelman in 2003 [**51, 52, 53**] and confirmed in more detail by many others, see, for example, [**12**]. Another important instance is the huge discrepancy of the smooth and the locally-flat category in dimension 4, perceivable through the work of Donaldson [**17**] and Freedman [**24**], puzzling and intriguing researchers up to this day. The goal of this thesis is to illustrate some of these ideas and ponder their consequences in the context of certain examples in knot theory. We mainly use two important concepts in order to bridge the dimensions 2, 3 and 4. The first concept is fibredness of knots, that is, the case of knots whose complement in the 3-sphere fibres over the circle and thus can be described by a mapping class on a surface. The second concept is the topological 4-genus of a knot, that is, the minimal genus of a surface which is properly, locally-flatly embedded in the 4-ball and has the given knot as boundary.

The rest of this chapter is devoted to the statement and description of the main results of this thesis. It is divided into three sections, according to a rough topical division: spectra of mapping classes, the signature of positive links and the topological 4-genus of positive braid knots.

1. Spectra of mapping classes

Thurston's classification divides surface mapping classes into three categories: reducible, periodic and pseudo-Anosov [**69**], with pseudo-Anosov being the generic case in a certain sense [**55**]. A mapping class is *pseudo-Anosov* if it has a representative for which there exists a pair of transverse, invariant singular measured foliations such that the representative stretches one of them by a number $\lambda > 1$ and the other one by $1/\lambda$. The number λ is called the *dilatation* or *stretch factor* of the mapping class, is algebraic and can be seen as a measure for how much the surface gets distorted when the mapping class is applied [**69**]. Mapping classes with large dilatation are easy to construct, simply by iterating a given pseudo-Anosov mapping class. On the other hand, it is difficult to describe which mapping classes have small dilatation. For example, the minimal dilatation among pseudo-Anosov mapping classes on a surface of fixed type is known only for very few surfaces, see, for example, [**36**]. In this context, we study a construction of pseudo-Anosov mapping classes due to Penner [**50**]. More precisely, we determine for every closed surface the minimal dilatation one can obtain among such

mapping classes. Due to a result of Leininger, it is known that their dilatations are uniformly bounded from below by $\sqrt{5}$, see the appendix of [**37**].

THEOREM 4.1. *On an orientable closed surface Σ_g of genus $g \geq 1$, the minimal dilatation λ_g among mapping classes arising from Penner's construction is*

$$1 + 2\cos^2\left(\frac{\pi}{2g+1}\right) + 2\sqrt{\cos^2\left(\frac{\pi}{2g+1}\right) + \cos^4\left(\frac{\pi}{2g+1}\right)}.$$

Furthermore, the dilatation λ_g is realised by the Coxeter mapping class associated to the Coxeter graph $(A_{2g}, \pm)$ with alternating signs.

As the dilatation of a pseudo-Anosov mapping class is an algebraic number, it is natural to ask about its Galois conjugates. For Penner's construction, they lie dense in the complex plane by a result of Strenner [**67**]. The situation is very different for pseudo-Anosov mapping classes arising from a construction due to Thurston [**69**]: the Galois conjugates of their dilatations are contained in $\mathbf{R} \cup \mathbf{S}^1$ by a result of Hubert and Lanneau [**32**]. We give a stronger version of this result in the case where the mapping class in Thurston's construction is given as a product of exactly two multitwists, a case which is interesting in the context of fibred links.

THEOREM 3.1. *If a product of two multitwists in Thurston's construction is pseudo-Anosov, then all Galois conjugates of its dilatation are contained in*

(a) $\mathbf{R}_{>0}$ *if the two twists are of opposite sign,*
(b) $\mathbf{R}_{>0} \cup \mathbf{S}^1$ *if the two twists are of the same sign.*

We also obtain a version for the eigenvalues of the action on the first homology of the surface induced by a product of two multitwists. In this case, we do not have to assume the mapping class to be pseudo-Anosov.

THEOREM 3.2. *Let $\phi : \Sigma \to \Sigma$ be the product of two multitwists. Then all eigenvalues of the homological action ϕ_* are contained in*

(a) $\mathbf{R}_{>0}$ *if the two twists are of opposite sign,*
(b) $\mathbf{R}_{<0} \cup \mathbf{S}^1$ *if the two twists are of the same sign.*

Since the Alexander polynomial of a fibred link equals the characteristic polynomial of the action induced on the first homology by its monodromy, Theorem 3.2 directly implies an equivalent statement for the zeroes of the Alexander polynomial of fibred links with a product of two multitwists as their monodromy. We extend this statement to a broader class of links (Theorem 5.4) and deduce log-concavity of the coefficient sequence of the Conway polynomial (Corollary 5.5). Theorems 3.1 and 3.2 as well as Theorem 5.4 and Corollary 5.5 contain several special cases which have already been treated by A'Campo [**1, 2**], Hirasawa and Murasugi [**30**] and Hironaka and the author [**31**].

2. The signature of positive links

The signature $\sigma(L)$ of a link L is a link invariant introduced by Trotter [**72**]. It is closely related to the Alexander polynomial and constitutes a lower bound for the topological 4-genus [**33, 49**]. We are interested in the signature invariant of *positive links*, that is, links which have a projection with only positive crossings. Rudolph was the first to study the signature invariant of closures of positive braids, a subclass of positive links. He found that it is always positive [**57**]. Stoimenow proved that it is bounded from below by an increasing function of the first Betti number, and conjectured this to be true for the more general class of positive links [**66**]. Feller showed that for positive braids, this increasing function could be chosen to be linear with slope $\frac{1}{100}$, and conjectured an optimal slope of $\frac{1}{2}$ for such a linear bound [**20**]. Recently, the linear bound has been improved to slope $\frac{1}{24}$ and at the same time extended to the more general class of positive links by Baader, Dehornoy and the author [**6**], proving Stoimenow's conjecture. Again more specifically, Feller has improved the slope to $\frac{1}{8}$ for closures of positive braids [**22**]. Here, we consider the signature of positive arborescent Hopf plumbings. These links are positive but not necessarily closures of positive braids. They are fibred and their monodromy arises from Thurston's construction. We give the optimal signature bound for positive arborescent Hopf plumbings in terms of the first Betti number.

THEOREM 5.2. *The signature of a positive arborescent Hopf plumbing is greater than or equal to two thirds of the first Betti number.*

Levine and Tristram extended the definition of the signature invariant to a signature function $[0,1] \to \mathbf{Z}$, where the value at 1 is the ordinary signature invariant [**38, 71**]. The signature function shares many properties with the ordinary signature, for instance with respect to concordance, see, for example [**54**]. In particular, one would like to know where the signature function attains its maximum. We answer this question for the signature function of a Murasugi sum of two Seifert surfaces with symmetric, positive definite Seifert form, a class of links which contains positive arborescent Hopf plumbings, but also many links which are not fibred. We show that the signature function of such a link is monotonically increasing and hence attains its maximum at 1.

THEOREM 5.1. *The signature function of a Murasugi sum of two Seifert surfaces with symmetric, positive definite Seifert form is monotonic.*

3. The topological 4-genus of positive braid knots

There are numerous notions of 4-genera for knots. Analogously to the topological 4-genus g_4^{top}, one can define the *smooth 4-genus* g_4^{smooth}, where the embedding of the surface in $\mathbf{B}^4$ is required to be smooth instead of locally-flat. The methods used to give lower bounds for both g_4^{top} and g_4^{smooth} have led to variations of these concepts. For example, the algebraic unknotting number, studied in this context by Borodzik and Friedl [**13**], or the algebraic genus, introduced by Feller and Lewark [**23**]. Furthermore,

stable versions of these notions have been studied, for example by Livingston [**43**] and Baader and Lewark [**9**].

In the context of this thesis, we study the topological 4-genus of positive braid knots. More precisely, we show that the difference $g - g_4^{\text{top}}$ of the ordinary genus and the topological 4-genus grows linearly with the minimal number b of strands needed in order to represent a positive braid knot as a positive braid.

THEOREM 7.3. *For a prime positive braid knot of positive braid index b,*

$$g - g_4^{\text{top}} \geq \frac{1}{16}b - 1.$$

By the resolution of the Thom conjecture due to Kronheimer and Mrowka [**35**] and Rudolph's extension [**59**], we have $g = g_4^{\text{smooth}}$ in the context of Theorem 7.3. In particular, showing that the corresponding difference in the locally-flat category grows linearly with the positive braid index accentuates the discrepancy between the locally-flat and the smooth category in dimension 4. In order to prove Theorem 7.3, we use Freedman's disc theorem [**24**] and carry out a careful study of the fibre surfaces of positive braid knots. More precisely, we define fibre surfaces $\widetilde{T}$, $\widetilde{E}$, $\widetilde{X}$ and $\widetilde{Y}$ such that whenever the fibre surface of a positive braid knot contains one of them as a surface minor, the difference $g - g_4^{\text{top}}$ grows by at least one. In this context, a *surface minor* is an *incompressible* subsurface, that is, the embedding is assumed to be injective on the level of the fundamental group. We also show that among positive braid knots, as soon as the signature invariant is not maximal, already the fibre surface contains a surface minor $\widetilde{T}$, $\widetilde{E}$, $\widetilde{X}$ or $\widetilde{Y}$. This leads to the following theorem.

THEOREM 6.1. *For a positive braid knot K, the equality $g_4^{\text{top}}(K) = g(K)$ holds exactly if $|\sigma(K)| = 2g(K)$.*

In particular, using Baader's classification of positive braid knots with maximal signature invariant [**3**], we obtain that the only positive braid knots with $g_4^{\text{top}}(K) = g(K)$ are the torus knots $T(2,n)$, $T(3,4)$ and $T(3,5)$ (Corollary 6.2). On a more abstract note, we use Theorem 7.3 to show that for any $c \geq 0$, there exists a finite number of surface minors which yield a complete obstruction to $g - g_4^{\text{top}} \leq c$ for the fibre surfaces of positive braid knots.

THEOREM 7.1. *Among prime positive braid knots, $g - g_4^{\text{top}} \leq c$ is characterised by finitely many forbidden surface minors for any $c \geq 0$.*

Our methods also allow us to deduce the result of Theorem 7.1 for the signature difference $2g - |\sigma| \leq c$ (Theorem 7.2).

CHAPTER 2

Background

1. Pseudo-Anosov mapping classes

Let Σ be a surface of finite type, possibly with punctures and boundary. A *mapping class* ϕ on Σ is a self-homeomorphism of Σ fixing the boundary of Σ pointwise and permuting the punctures, up to isotopy fixing the boundary and the punctures pointwise. The *mapping class group* is the group of mapping classes with composition, and is denoted by $\mathrm{Mod}(\Sigma)$.

1.1. Dehn twists and multitwists. Let $\gamma \subset \Sigma$ be a simple closed curve in Σ. Thinking of the simple closed curve γ as coming together with an annular neighbourhood, we define the Dehn twists along the curve γ. The *positive Dehn twist* T_γ^+ *along* γ is the mapping class on Σ with a representative supported in an annular neighbourhood of γ that sends an arc crossing γ to an arc crossing γ but also winding around γ once in the counterclockwise sense. This only depends on the orientation of Σ, not on the orientation of γ, and is well-defined by the Alexander trick, see, for example, [**18**]. The definition of a *negative Dehn twist* T_γ^- *along* γ is obtained by replacing "counterclockwise" by "clockwise". Figure 2.1 shows an annular neighbourhood of a simple closed curve γ as a rectangle with top and bottom identified. Thinking of the annular neighbourhood like this, we can describe a specific representative of the positive Dehn twist T_γ^+ along γ in the following way: it fixes the vertical boundary of the rectangle pointwise, preserves vertical lines and sends horizontal lines to lines with slope $-r$, where r is the ratio of length and width of the rectangle, as shown in Figure 2.1.

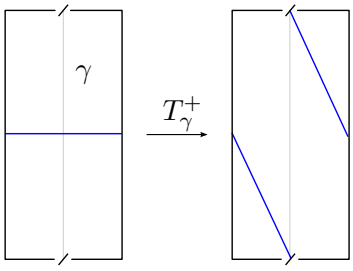

FIGURE 2.1. An affine representative of a positive Dehn twist along a curve γ, depicted in grey.

A *multicurve* $\alpha \subset \Sigma$ is a disjoint union of finitely many simple closed curves $\alpha_1 \dot\cup \cdots \dot\cup \alpha_n \subset \Sigma$. The *positive multitwist* T_α^+ *along* α is the product of all positive Dehn twists $T_{\alpha_i}^+$ along the curves α_i. Since the curves α_i are disjoint, this product

does not depend on the order of multiplication. The *negative multitwist* T_α^- *along* α is defined analogously. A pair of multicurves α and β *fills* a surface Σ if the complement of $\alpha \cup \beta$ consists of discs, once-punctured discs and boundary-parallel annuli.

1.2. Measured foliations. A *foliation* of a surface Σ is an atlas $\mathcal{A} = \{(U_\alpha, \psi_\alpha)\}$ with transition maps of the form

$$\psi_\alpha \circ \psi_\beta^{-1}(x, y) = (h_{\alpha\beta}(x, y), c_{\alpha\beta} + f_{\alpha\beta}(y)).$$

Given an atlas of this kind, the standard horizontal foliation of the plane descends to a decomposition of Σ into disjoint 1-dimensional manifolds, the *leaves*. A *measured foliation* of a surface Σ is a foliation of Σ where for all transition maps, $f_{\alpha\beta}(y) = \pm y$. In this case, the vertical measure $|dy|$ in the plane induces a measure μ on arcs transverse to the leaves. This measure μ is invariant under isotopies keeping an arc transverse to the foliation and its endpoints in a fixed leaf at all times.

A mapping class acts on the set of foliations by composing every chart of the atlas with a representative. Usually, foliations are considered up to isotopy (and Whitehead equivalence in the case below of singular measured foliations), see, for example, [**19**]. However, in our examples, we choose good representatives of the mapping classes so that the invariance is clear. Furthermore, if the induced action of a mapping class fixes a foliation $\mathcal{F}$, the mapping class also induces an action on the set of measures on $\mathcal{F}$ by pullback of arcs transverse to $\mathcal{F}$.

1.3. Anosov mapping classes. A mapping class ϕ on the torus is called *Anosov* if there exists a pair of transverse, ϕ-invariant measured foliations $(\mathcal{F}^u, \mu^u)$ and $(\mathcal{F}^s, \mu^s)$, such that the action of ϕ induced on the measures μ^u and μ^s is given by $\phi_*(\mu^u) = \lambda\mu^u$ and $\phi_*(\mu^s) = (1/\lambda)\mu^s$, respectively, for a real number $\lambda > 1$.

There is an easier description of this definition, since mapping classes of the torus are in one-to-one correspondence with matrices in $\mathrm{SL}(2, \mathbf{Z})$. The action of a matrix $A \in \mathrm{SL}(2, \mathbf{Z})$ on the plane $\mathbf{R}^2$ descends to a mapping class ϕ_A of the torus $\mathbf{R}^2/\mathbf{Z}^2$, since A preserves the integer lattice. Furthermore, one can show that every homeomorphism of the torus lifts to a map which is $\mathbf{Z}^2$-invariantly isotopic to a map induced by a matrix $A \in \mathrm{SL}(2, \mathbf{Z})$, see, for example, [**18**].

Remark 2.1. If a matrix $A \in \mathrm{SL}(2, \mathbf{Z})$ has an eigenvalue $|\lambda| > 1$, then automatically λ is real and the other eigenvalue is $1/\lambda$. It follows that there exists a pair of transverse, A-invariant measured foliations of $\mathbf{R}^2$, namely the ones defined by the lines parallel to the eigendirections of the eigenvalues $1/\lambda$ and λ. The measures on arcs are defined by projecting to the eigendirections of the eigenvalues λ and $1/\lambda$, respectively, and taking the difference of the starting and the end point: The action of A multiplies the measures by λ and $1/\lambda$, respectively. This pair of transverse, A-invariant measured foliations of $\mathbf{R}^2$ descends to a pair of transverse, ϕ_A-invariant measured foliations of the torus $\mathbf{R}^2/\mathbf{Z}^2$, and the action of ϕ_A multiplies the measures by λ and $1/\lambda$, respectively. Summarising, we have that a mapping class ϕ_A of the torus is Anosov exactly if A has an eigenvalue outside the unit circle, or, equivalently, $|\mathrm{trace}(A)| > 2$.

EXAMPLE 2.2. Let $A = \left(\begin{smallmatrix} 2 & 1 \\ 1 & 1 \end{smallmatrix}\right) \in \mathrm{SL}(2, \mathbf{Z})$. The eigenvalues of the matrix A are φ^2 and φ^{-2}, where φ is the golden ratio. Furthermore, the eigendirections are spanned by the vectors $(\varphi, 1)$ and $(1, -\varphi)$, respectively. Figure 2.2 shows the action of the matrix A on the plane, and how the foliations by lines parallel to the eigendirections are stretched by the factor φ^2 or φ^{-2} by this action.

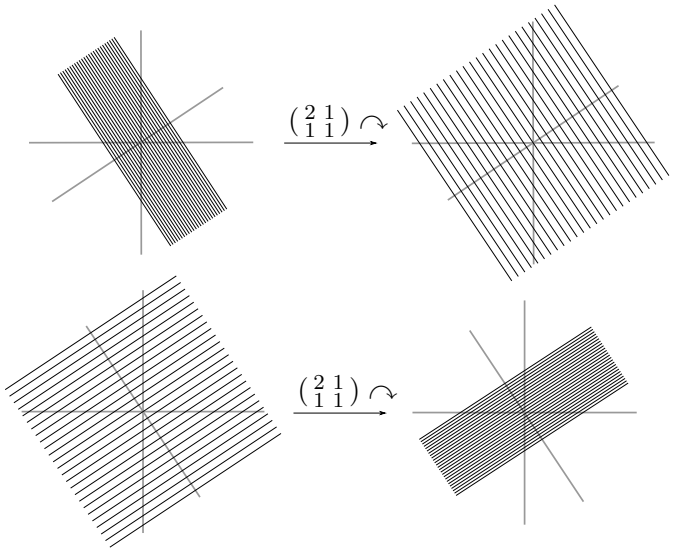

FIGURE 2.2. The effect of matrix multiplication by A on the foliations of $\mathbf{R}^2$ by lines parallel to the eigendirections of A.

1.4. Singular measured foliations and pseudo-Anosov homeomorphisms. A *singular measured foliation with singular points* $p_1, \ldots, p_r$ of a surface Σ is a measured foliation of the surface $\Sigma \setminus \{p_1, \ldots, p_r\}$, with the additional condition that around each point p_j, there exists a chart of Σ in which the foliation is given by the level sets of a standard i-saddle, where $i \geq 3$, as depicted in Figure 2.3 for $i = 3, 4$.

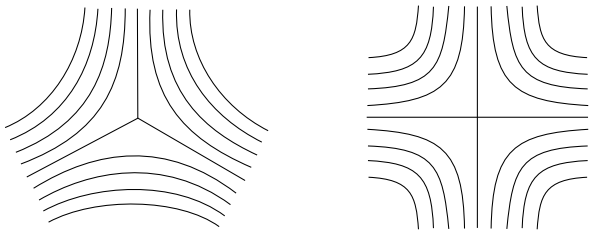

FIGURE 2.3. Level sets of the standard 3-saddle on the left and of the standard 4-saddle on the right.

A measure μ on arcs transverse to the foliation can be defined as in the case without singularities, the difference being that "transverse" now means "transverse outside the singularities".

A mapping class ϕ on a surface Σ is called *pseudo-Anosov* if there exists a pair of transverse, ϕ-invariant singular measured foliations $(\mathcal{F}^u, \mu^u)$ and $(\mathcal{F}^s, \mu^s)$, such that the action of ϕ induced on the measures μ^u and μ^s is given by $\phi_*(\mu^u) = \lambda\mu^u$ and $\phi_*(\mu^s) = (1/\lambda)\mu^s$, respectively, for a real number $\lambda > 1$. The number λ is the *dilatation* of the mapping class ϕ and it is algebraic [**69**].

By the Nielsen-Thurston classification, mapping classes on compact surfaces can be decomposed along invariant multicurves into pieces that are either periodic or pseudo-Anosov [**69**]. In particular, a mapping class not fixing a multicurve up to isotopy is either periodic or pseudo-Anosov. While the Nielsen-Thurston classification indicates that pseudo-Anosov mapping classes are numerous, we consider very specific examples in the following.

1.5. Thurston's construction. We describe a construction of pseudo-Anosov mapping classes due to Thurston. Details for this construction can also be found in Thurston's article [**69**] or in the books [**18, 19**]. Let $\{R_i\}$ be a finite collection of rectangles in $\mathbf{R}^2$ with sides parallel to the vertical and horizontal directions. Furthermore, fix some identification of the sides via translations and rotations by π in the plane, so that no side remains unidentified. In particular, horizontal sides get identified with horizontal sides and vertical sides get identified with vertical sides. Furthermore, identified sides must be of the same length. The quotient after such identifications is a closed surface Σ carrying a Euclidean structure outside the vertices of the rectangles. These vertices might be singular, that is, the total angle around them might be different from 2π. Furthermore, a normal frame is induced by the horizontal and vertical directions of the plane. With respect to this frame, it makes sense to talk of *affine homeomorphisms* of the surface Σ, that is, homeomorphisms ϕ locally given as affine maps, with a globally defined differential $D_\phi \in \mathrm{PSL}(2, \mathbf{R})$. Note that since we allow rotations by π for the identifications, the normal frame on Σ is only defined up to a sign. This is the reason why the differential is well-defined in $\mathrm{PSL}(2, \mathbf{R})$ but not in $\mathrm{SL}(2, \mathbf{R})$

LEMMA 2.3. *If the total angle around each vertex is at least 2π and the differential of an affine homeomorphism ϕ has an eigenvalue λ outside the unit circle, then ϕ is pseudo-Anosov with dilatation $|\lambda|$. Furthermore, the ϕ-invariant stable and unstable singular measured foliations are given by lines parallel to the eigendirections of the differential.*

If the total angle around a vertex is π, an affine homeomorphism as in Lemma 2.3 is *generalised pseudo-Anosov*, as described in [**19**]. This notion allows for a 1-saddle. We do not need to deal with this notion, as we assume the multicurves α and β to *intersect minimally* in Theorem 2.5, that is, we assume the multicurves α and β to minimise the number of unsigned intersection points within their homotopy classes.

PROOF. The argument works exactly as in Remark 2.1, since locally the situation is the same. There is one exception: after the identification, each vertex has an even number $2n$ of outgoing edges, with $n \geq 2$. The total angle around such a vertex is $n\pi$.

For a vertex with $2n > 4$ of outgoing edges, the vertex is a singularity of the foliation by parallel lines. More precisely, it has the type of an n-saddle. □

Let Σ be a surface as above and think of it at the same time as a union of horizontal annuli H_i and as a union of vertical annuli V_j, which are in turn obtained by the identification of all the vertical sides or all the horizontal sides, respectively, of the rectangles. Furthermore, assume that the ratio of the length and the width is equal to a fixed number $r \geq 1$ for each horizontal and vertical annulus (we justify this assumption in Lemma 2.4). Then, the positive multitwist T_H along the horizontal annuli is an affine homeomorphism with differential $\left(\begin{smallmatrix} 1 & r \\ 0 & 1 \end{smallmatrix}\right) \in \mathrm{PSL}(2, \mathbf{R})$ and the positive multitwist T_V along the vertical annuli is an affine homeomorphism with differential $\left(\begin{smallmatrix} 1 & 0 \\ -r & 1 \end{smallmatrix}\right) \in \mathrm{PSL}(2, \mathbf{R})$. This construction yields a whole group of examples of affine homeomorphisms of Σ, namely the group generated by T_H and T_V. This group always contains an affine homeomorphism ϕ whose differential D_ϕ has an eigenvalue outside the unit circle, or, equivalently, $\mathrm{trace}(D_\phi) > 2$. For example $\phi = T_H \circ T_V^{-1}$, whose differential D_ϕ is given by

$$D_\phi = \begin{pmatrix} 1 & r \\ 0 & 1 \end{pmatrix} \begin{pmatrix} 1 & 0 \\ r & 1 \end{pmatrix} = \begin{pmatrix} 1 + r^2 & r \\ r & 1 \end{pmatrix}.$$

LEMMA 2.4. *It is possible to change the width of each annulus H_i and V_j so that the ratio of length and width is a fixed number $r \geq 1$ for each horizontal and vertical annulus. Furthermore, r is unique.*

PROOF. Let $\Omega = \left(\begin{smallmatrix} 0 & X \\ X^\top & 0 \end{smallmatrix}\right) \geq 0$ be the geometric intersection matrix of the annuli H_i and V_j, that is, each entry of Ω is given by the number of rectangles in which the corresponding annuli overlap. Furthermore, let r be its Perron-Frobenius eigenvalue and let $v > 0$ be the corresponding eigenvector, so we have $\Omega v = rv$. We resize each horizontal and vertical annulus to have width equal to the corresponding entry of the vector v, thus changing also the length of the annuli overlapping it. The length of a horizontal annulus equals the sum of all the widths of the vertical annuli it overlaps, counted with multiplicity. This number equals $(\Omega v)_i$, where the i-th entry corresponds to the horizontal annulus under consideration. Furthermore, the width of a horizontal annulus is simply v_i. Then, the claim follows directly from $\Omega v = rv$, which implies $(\Omega v)_i = rv_i$. The same argument applies to vertical annuli. Finally, v is the unique eigenvector of Ω with strictly positive entries by the theory of Perron-Frobenius eigenvalues, see, for example, [**14**]. From this it follows that $r \geq 1$ is uniquely determined by the matrix Ω. □

THEOREM 2.5 (Thurston's construction [**69**]). *Let α and β be a pair of multicurves that intersect minimally and fill a surface Σ. Let r be the largest eigenvalue of their geometric intersection matrix. There exists a representation $\rho : \langle T_\alpha, T_\beta \rangle \to \mathrm{PSL}(2, \mathbf{R})$, given by*

$$T_\alpha \mapsto \begin{pmatrix} 1 & r \\ 0 & 1 \end{pmatrix}, \quad T_\beta \mapsto \begin{pmatrix} 1 & 0 \\ -r & 1 \end{pmatrix},$$

such that $\phi \in \langle T_\alpha, T_\beta \rangle$ is pseudo-Anosov if $\rho(\phi)$ has an eigenvalue λ outside the unit circle. Furthermore, the dilatation $\lambda(\phi)$ of ϕ equals $|\lambda|$.

Proof of Thurston's construction. The idea of the proof is to associate to the multicurves α and β a singular Euclidean structure, as above, so that the multitwists along α and β are affine homeomorphisms with respect to the associated normal frame. We think of Σ in the following way. The multicurves α and β fill the surface Σ and hence induce a cell decomposition of Σ. The 0-cells are the intersection points of α and β, the 1-cells are the subarcs of α and β connecting the intersection points of α and β, and the 2-cells are the complementary regions of the union $\alpha \cup \beta$. We consider the dual cell decomposition of this cell decomposition. There is one 2-cell (with four 1-cells as boundary) for each intersection point of the multicurves α and β. To obtain a singular Euclidean structure on Σ, we therefore take one rectangle for each 2-cell and identify the sides with translations and rotations by π according to the dual cell decomposition. We can choose the curves α_i to lie horizontally and the curves β_j to lie vertically in the rectangles. Note that the curves α_i and β_j correspond exactly to horizontal and vertical annuli, respectively, in the construction above. Since we suppose α and β to intersect minimally, there are no bigons [**18**], that is, the cell decomposition induced by α and β has no regions with two sides. In particular, the dual cell decomposition has no vertex with only two outgoing edges, so the total angle around every vertex is at least 2π. The claim now follows from Lemmas 2.3 and 2.4, where the representation ρ is given by differentiating. Note that ρ is well-defined on $\langle T_\alpha, T_\beta \rangle$, since the only element of $\langle T_\alpha, T_\beta \rangle$ whose differential is the identity is the identity, as every element of $\langle T_\alpha, T_\beta \rangle$ has at least one fixed point by construction. □

Example 2.6 (Positive arborescent mapping classes). For an explicit example of a pseudo-Anosov mapping class arising from Thurston's construction, see the example discussed in the teaser. In this example, the multicurves α and β intersect each other with the pattern of a plane tree $\Gamma_{\widetilde{X}}$ and both multitwists are positive. More generally, for any plane tree Γ, one can construct such an example arising via Thurston's construction. In order to do so, take one annulus for every vertex of Γ and glue two annuli together along a square exactly if the two corresponding vertices of Γ are connected by an edge, as depicted for the tree $\Gamma_{\widetilde{X}}$ in Figures 0.6 and 0.7. Furthermore, this glueing process should respect the circular order of edges around every vertex of Γ which is given by the embedding of the underlying abstract tree into the plane. By a result of Gerber, there are many examples of different embeddings of a fixed abstract tree yielding different mapping classes [**26**].

1.6. Penner's construction. Another construction of pseudo-Anosov homeomorphisms using Dehn twists is due to Penner [**50**]. It can be seen as a generalisation of a special case of Thurston's construction of pseudo-Anosov homeomorphisms [**69**]. In this case, the transverse, invariant singular measured foliations are no longer given by parallel lines with respect to a singular Euclidean structure. Penner used the machinery of train tracks and their correspondence to measured foliations to prove that his

examples are pseudo-Anosov. For a proof, see Penner's original article [**50**] or Martelli's book [**45**].

THEOREM 2.7 (Penner's construction [**50**]). *Let α and β be two multicurves (without parallel components) which intersect minimally and whose union fills Σ. Let $\mathcal{P}$ be the monoid consisting of products of positive Dehn twists $T^+_{\alpha_i}$ and negative Dehn twists $T^-_{\beta_j}$. Define $\rho : \mathcal{P} \to \mathrm{SL}(n+m, \mathbf{Z})$ by*

$$\rho(\alpha_i) = I + R_{\alpha_i},$$
$$\rho(\beta_j) = I + R_{\beta_j},$$

and extend linearly, where the matrices R_{α_i} and R_{β_j} are obtained from the geometric intersection matrix of the curves $\{\alpha_1, \ldots, \alpha_n, \beta_1, \ldots, \beta_m\}$,

$$\Omega = \begin{pmatrix} 0 & X \\ X^\top & 0 \end{pmatrix} \geq 0,$$

by setting all entries to zero which are not in the row corresponding to α_i or β_j, respectively. Then every $\phi \in \mathcal{P}$ such that every component of α and β gets twisted along at least once is pseudo-Anosov and its dilatation is the Perron-Frobenius eigenvalue of $\rho(\phi)$.

1.7. Coxeter mapping classes. An interesting feature of the pseudo-Anosov mapping classes arising from Thurston's and Penner's construction is the following. The homological actions of specific examples realise, up to a sign, certain Coxeter transformations. This allows for a transfer of ideas and methods.

Let Γ be a finite connected graph without loops or double edges and let $\mathfrak{s}$ be an assignment of a sign $+$ or $-$ to every vertex v_i of Γ. The pair $(\Gamma, \mathfrak{s})$ is called a *mixed-sign Coxeter graph*, see [**29**]. To such a pair, we associate certain products of reflections. Let $\mathbf{R}^{V_\Gamma}$ be the real vector space abstractly generated by the vertices v_i of Γ. We equip $\mathbf{R}^{V_\Gamma}$ with the symmetric bilinear form B, given by $B(v_i, v_i) = -2\mathfrak{s}(v_i)$ and $B(v_i, v_j) = a_{ij}$, where a_{ij} is the ij-th entry of the adjacency matrix $A(\Gamma)$ of Γ. To every vertex v_i, we associate a reflection s_i about the hyperplane in $\mathbf{R}^{V_\Gamma}$ perpendicular to v_i,

$$s_i(v_j) = v_j - 2\frac{B(v_i, v_j)}{B(v_i, v_i)} v_i.$$

A product of the s_i containing every s_i exactly once is called a *Coxeter transformation* associated to the pair $(\Gamma, \mathfrak{s})$. For arbitrary graphs Γ, this product is highly non-unique. If Γ is a tree, however, the Coxeter transformation is uniquely determined up to conjugation [**64**]. This allows us to talk about "the" Coxeter transformation associated to a pair $(\Gamma, \mathfrak{s})$ in case Γ is a tree. For our purposes, the most important examples of trees are the simply laced finite Dynkin diagrams, depicted in Figure 2.4. Two kinds of sign assignments $\mathfrak{s}$ are of interest to us: all signs $\mathfrak{s}$ positive, written $(\Gamma, +)$, which is the case we call *classical*, and signs $\mathfrak{s}$ that give a bipartition of the (necessarily bipartite) graph Γ, written $(\Gamma, \pm)$, which is the case we call *alternating-sign*.

In the case of classical Coxeter trees $(\Gamma, +)$, A'Campo realised the Coxeter transformation, up to a sign, as the homological action of a mapping class given by the product

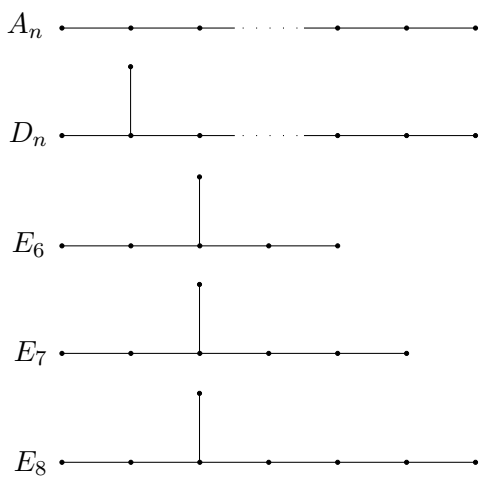

FIGURE 2.4. The Dynkin diagrams A_n, D_n, E_6, E_7 and E_8.

of two positive multitwists along multicurves that intersect each other with the pattern of Γ, see [**2**]. Similarly, in the case of alternating-sign Coxeter trees $(\Gamma, \pm)$, Hironaka and the author realised the Coxeter transformation, up to a sign, as the homological action of a mapping class given by the product of two multitwists of opposite signs along multicurves that intersect each other with the pattern of Γ, see [**31**]. We call these mapping classes *Coxeter mapping classes*. Two observations are of special interest for us. Firstly, the Coxeter mapping classes ϕ built by Hironaka and the author also arise via Penner's construction. Indeed, the union of the constructed multicurves fills the surface and components intersect at most once, hence their intersection is minimal. Secondly, the given matrix describing the homological action of ϕ equals the corresponding matrix product $\rho(\phi)$ of Penner's construction described in Theorem 2.7, compare with [**31**]. We deduce that for such a mapping class ϕ realising the Coxeter transformation associated to $(\Gamma, \pm)$, the dilatation equals the spectral radius of the Coxeter transformation associated to $(\Gamma, \pm)$. This simplifies some of our calculations.

EXAMPLE 2.8. Let $(\Gamma, \pm)$ be the 4-cycle graph with alternating signs, as depicted in Figure 2.5. There are, up to conjugation and inversion, two Coxeter transformations:

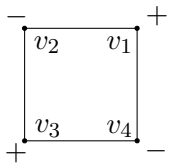

FIGURE 2.5.

the one corresponding to the bipartite order, $s_1 s_3 s_2 s_4$, and the one corresponding to the cyclic order, $s_1 s_2 s_3 s_4$. Two quick calculations confirm that their spectral radii are equal to and greater than $3 + 2\sqrt{2}$, respectively.

2. Fibred links and Murasugi sums

A *link* L in the 3-sphere $\mathbf{S}^3$ is a smooth embedding of a disjoint union of circles $\mathbf{S}^1$ into $\mathbf{S}^3$, up to self-homeomorphisms of $\mathbf{S}^3$ sending one such embedding to another. Let Σ be a *Seifert surface* for the link $L \subset \mathbf{S}^3$, that is, an oriented connected compact surface embedded in $\mathbf{S}^3$ having L as boundary. The *Seifert form*

$$\langle\ ,\ \rangle : H_1(\Sigma;\mathbf{R}) \times H_1(\Sigma;\mathbf{R}) \to \mathbf{Z}$$

corresponding to the Seifert surface Σ is defined as follows. Let $\alpha_1, \ldots, \alpha_n$ be simple closed curves in Σ that represent a basis of $H_1(\Sigma;\mathbf{R})$. Then we set

$$\langle [\alpha_i], [\alpha_j] \rangle = \mathrm{lk}(\alpha_i, \alpha_j^\sharp),$$

where lk denotes the linking number and $\alpha_j^\sharp$ denotes the pushoff of α_j in the positive normal direction of Σ, and extend by imposing bilinearity. Up to normalisation, the *Alexander polynomial* $\Delta_L(t)$ of a link L is defined to be $\Delta_L(t) = \det(tA - A^\top)$, where A is a *Seifert matrix*, that is, a matrix for the Seifert form of a Seifert surface for L. Since the Alexander polynomial of a link L is independent of all our choices, we immediately see that its degree is a lower bound for the first Betti number of any Seifert surface for L. In particular, the degree of the Alexander polynomial is a lower bound for the *first Betti number of* L, that is, the minimal first Betti number among Seifert surfaces for L. Analogously, the *genus* of L is the minimal genus among Seifert surfaces for L. For a knot K, the genus equals half the first Betti number.

2.1. Fibred links. A link is called *fibred* if its complement $\mathbf{S}^3 \setminus L$ fibres over $\mathbf{S}^1$. Furthermore, we require the fibration $f : \mathbf{S}^3 \setminus L \to \mathbf{S}^1$ to be trivial in a tubular neighbourhood of the link components, that is, every link component L_i possesses a neighbourhood V homeomorphic to $\mathbf{S}^1 \times \mathbf{D}^2$ such that $L_i = \mathbf{S}^1 \times \{0\}$ and f restricted to $\mathbf{S}^1 \times \mathbf{D}^2$ is given by the argument of $x \in \mathbf{D}^2$.

The outstanding feature of fibred links is that all their information is contained in a 2-dimensional description. In order to see this, consider the induced surface bundle $\mathbf{S}^3 \setminus \mathrm{int}(V) \to \mathbf{S}^1$ with fibre $\Sigma = f^{-1}(1)$. Removing a point of $\mathbf{S}^1$ yields an open interval, over which every surface bundle is trivial. Hence, there exists a fibre-preserving homeomorphism from $\mathbf{S}^3 \setminus \mathrm{int}(V) \to \mathbf{S}^1$ to the surface bundle

$$[0,1] \times \Sigma \Big/ (0, \phi(x)) \sim (1, x) \longrightarrow [0,1] \big/ 0 \sim 1 \simeq \mathbf{S}^1,$$

for some self-homeomorphism ϕ of Σ that fixes the boundary $\partial\Sigma$ pointwise. The self-homeomorphism $\phi : \Sigma \to \Sigma$ is called the *monodromy* of the fibred link L, and is defined up to isotopy and conjugation. Indeed, one can show directly that if ψ is obtained from ϕ via isotopy and conjugation, then their *mapping tori*

$$[0,1] \times \Sigma \Big/ (0, \phi(x)) \sim (1, x) \quad \text{and} \quad [0,1] \times \Sigma \Big/ (0, \psi(x)) \sim (1, x)\,,$$

respectively, are related by a fibre-preserving homeomorphism, see, for example, [**15**]. Given the mapping torus of the monodromy, one directly obtains the link L inside $\mathbf{S}^3$ by glueing in a solid torus along each boundary component, as dictated by the

fibredness condition. Furthermore, using another representative of the monodromy gives rise to a self-homeomorphism of $\mathbf{S}^3$ sending the links obtained in this way to each other. Summarising, we have the following proposition connecting fibred links to surface homeomorphisms.

PROPOSITION 2.9. *The monodromy uniquely determines the fibred link.*

2.2. The Alexander polynomial of fibred links. In this section, our goal is to describe the Alexander polynomial of a fibred link as the characteristic polynomial of the action induced on the first homology by the monodromy. The proof we give is adapted from [**47**].

PROPOSITION 2.10. *The Alexander polynomial of a fibred link equals the characteristic polynomial of the homological action of the monodromy.*

PROOF. Fix a basis for the first homology of the fibre surface Σ. We show that $M = A^{-\top}A$, where A is a matrix for the Seifert form and M is the matrix of the homological action of the monodromy. From this, the claim follows by the above definition of the Alexander polynomial, since $M = A^{-\top}A$ has the same characteristic polynomial as $M^\top = A^\top A^{-1}$. In order to show $M = A^{-\top}A$, consider two simple closed curves α and β on Σ. By definition, $\langle [\alpha], [\beta] \rangle = \mathrm{lk}(\alpha, \beta^\sharp)$. We now consider Σ as $\Sigma \times \{0\}$ inside the link exterior $[0,1] \times \Sigma \Big/ (0, \phi(x)) \sim (1, (x))$. In these coordinates, $\beta^\sharp$ may be chosen as $(\frac{1}{2}, \beta)$. Furthermore, flowing the positive unit flow in the first coordinate for the time $\frac{1}{2}$ induces an isotopy of the link exterior sending $(\frac{1}{2}, \beta)$ to $(1, \beta) = (0, \phi(\beta))$ and $(0, \alpha)$ to $(\frac{1}{2}, \alpha)$. In particular, we have $\mathrm{lk}(\alpha, \beta^\sharp) = \mathrm{lk}(\phi(\beta), \alpha^\sharp)$ and hence $\langle [\alpha], [\beta] \rangle = \langle \phi_*[\beta], [\alpha] \rangle$. Since α and β are arbitrary simple closed curves on Σ, the last equality translates to $A = A^\top M$, or, equivalently, $M = A^{-\top}A$. Here, we use that the Seifert matrix A associated to a fibre surface is invertible, see, for example, the chapters on fibred knots and Alexander invariants in [**15**]. □

Since the Alexander polynomial is the characteristic polynomial of a map on the first homology of the fibre surface Σ, we get that it is of degree $b_1(\Sigma)$. In particular, since the degree of the Alexander polynomial is a lower bound for the first Betti number of any Seifert surface, we obtain the following result.

REMARK 2.11. *The fibre surface of a fibred link realises the genus of the link.*

EXAMPLE 2.12. The simplest fibre surfaces of fibred links are the *positive* and the *negative Hopf band*. They are obtained by inserting a full positive or negative full twist into an unknotted, untwisted annulus. The monodromy of a positive or negative Hopf band is a positive or negative Dehn twist along its core curve, respectively. A nice explanation of this fact can be found in a recent article by Baader and Graf, in which they interpret fibredness in terms of elastic cords [**8**]. Baader and Graf show that the monodromy is uniquely determined by the images of proper arcs which cut the fibre surface into discs (thought of as a elastic cords fixed at the boundary of the surface and lying on one side of it) after being dragged through 3-space to the other side of the fibre

surface. Using this interpretation, Figure 2.6 suffices to prove that the monodromy of a negative Hopf band is a negative Dehn twist along its core curve.

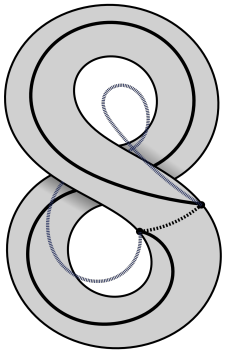

FIGURE 2.6. How to drag an elastic cord fixed at the boundary of a negative Hopf band to the other side of the Hopf band through 3-space. This figure is taken from [**8**].

2.3. Murasugi sum. Given two Seifert surfaces, it is possible to build new Seifert surfaces via the *Murasugi sum*, that is, glueing the surfaces (separated by a plane) together along a disc (contained in the plane), whose boundary circle is divided into $2n$ arcs that alternatingly belong to one surface or the other, see Figure 2.7 for an example. A special case is the *connected sum* of two Seifert surfaces, which is the case

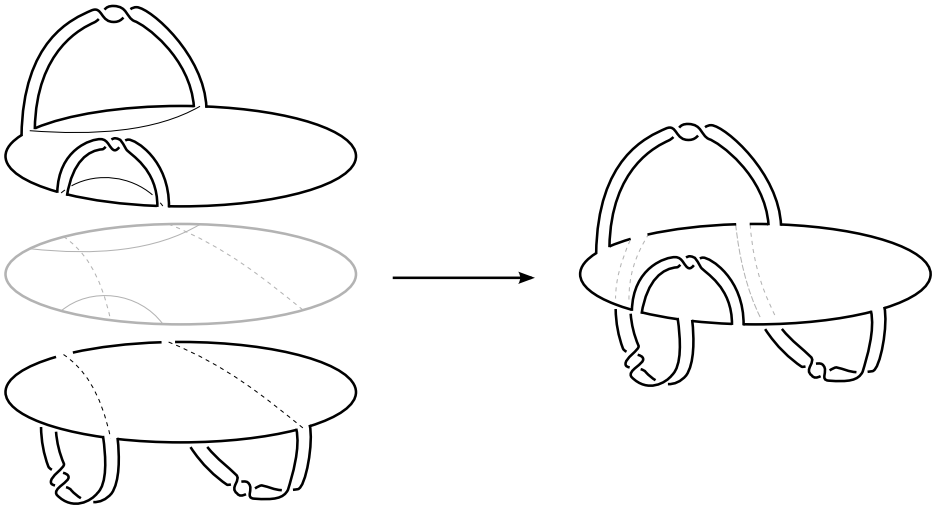

FIGURE 2.7. A Murasugi sum of two surfaces, which are in turn obtained by a connected sum of two Hopf bands. The lines on the disc indicate the core curves of these Hopf bands.

$n = 1$ in the definition of the Murasugi sum. Similarly, the case $n = 2$ is often called *plumbing*. Since the two Seifert surfaces are separated by a plane, a Seifert matrix

for their Murasugi sum is given by an upper diagonal 2×2 block matrix, with Seifert matrices for the original surfaces on the diagonal.

The Murasugi sum is an important operation in the theory of fibred links. By theorems of Stallings and Gabai, a Murasugi sum Σ of two Seifert surfaces Σ_1 and Σ_2 is a fibre surface if and only if both summands are fibre surfaces [**25, 63**]. Furthermore, the monodromy ϕ of Σ is the composition $\phi_1 \circ \phi_2$ of the monodromies ϕ_1 and ϕ_2 of Σ_1 and Σ_2, respectively, extended to Σ by the identity map.

Products of two multitwists, as in Thurston's construction, occur naturally in knot theory: as monodromies of certain fibred links. Many fibre surfaces can be built inductively by taking Murasugi sums of already constructed fibre surfaces, starting from Hopf bands. As we have seen in Example 2.12, the monodromy of a positive or negative Hopf band is a positive or negative Dehn twist along its core curve, respectively. Therefore, the monodromy of a connected sum of several positive or negative Hopf bands is a positive or negative multitwist along its core curves, respectively. So, the Murasugi sum of two such fibre surfaces yields a fibre surface with the monodromy given by a product of two multitwists. Fibred links built in this fashion contain many interesting classes of links.

Example 2.13 (Positive arborescent Hopf plumbings). Given a plane tree Γ, a *positive arborescent Hopf plumbing* corresponding to Γ is obtained as follows. Take a positive Hopf band H_i for every vertex v_i of Γ, and plumb the Hopf bands together in such a way that the core curves α_i and α_j of two such Hopf bands H_i and H_j intersect exactly if the corresponding vertices v_i and v_j are connected by an edge in Γ. Furthermore, this plumbing process should respect the circular order of edges around every vertex of Γ. This information together with the information of how the core curves intersect algebraically in the plumbing uniquely determines a fibred link, since it uniquely determines a monodromy. Indeed, the monodromy is a positive arborescent mapping class, as described in Example 2.6. In other words, the monodromy is a product of positive Dehn twists along the core curves of the Hopf band such that every core curve gets twisted along exactly once. Furthermore, such a product is unique up to conjugation by Steinberg's argument for the uniqueness of the Coxeter transformation associated with a finite tree [**64**].

Example 2.14 (Positive braid links). A *positive braid on $n+1$ strands* is given by a *positive braid word* in n generators, that is, a word in positive powers of the generators $\sigma_1, \dots, \sigma_n$. Actually, a positive braid is given by a word up to braid relations $\sigma_i\sigma_j = \sigma_j\sigma_i$ for $|i-j| \neq 1$ and $\sigma_i\sigma_{i+1}\sigma_i = \sigma_{i+1}\sigma_i\sigma_{i+1}$. As this difference is not crucial for our purposes, we often blur the difference between positive braids and words representing them. A geometric representation of the positive braid word $w = \sigma_1^2\sigma_2^2\sigma_1\sigma_3\sigma_2^2\sigma_3$ can be found on the left in Figure 0.10. On the right in Figure 0.10, the *closure* of w is depicted. This is an operation constructing a link out of the geometric representation of a braid. Consequently, a *positive braid link* is a link which has a representation as the closure of a positive braid word. The *positive braid index* of a positive braid link L is the minimal number of strands of a positive braid having L as its closure. The

canonical Seifert surface associated to a positive braid word is obtained as follows. Take a disc D_i, $i = 1, \dots, n+1$, for every strand of the geometric representation, and for every occurrence of a generator σ_i in the positive braid word, glue a band with a positive half twist at the corresponding location between the discs D_i and D_{i+1}. This is depicted for the word $w = \sigma_1^2\sigma_2^2\sigma_1\sigma_3\sigma_2^2\sigma_3$ in Figure 2.8. By a result of Stallings, the

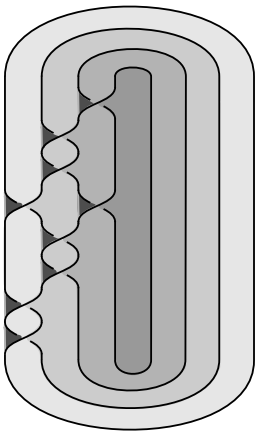

FIGURE 2.8. The canonical Seifert surface corresponding to the positive braid word w. By a result of Stallings, it is the fibre surface of the link [**63**].

canonical Seifert surface associated with a positive braid word is the fibre surface of the link in case it is connected [**63**]. More precisely, it is a plumbing of positive Hopf bands. It is possible to explicitly see the Hopf bands out of which the fibre surface is plumbed. Figure 2.9 exhibits some Hopf bands in the fibre surface of w. In fact, every pair of

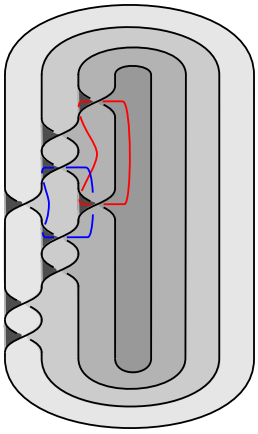

FIGURE 2.9. Taking an annular neighbourhood of the red or the blue curve yields a positive Hopf bands in the fibre surface of w.

consecutive generators σ_i constitutes a Hopf band. Baader introduced *brick diagrams* to study positive braids [**3**]: a brick diagram consists of a rectangle (brick) per Hopf

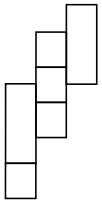

FIGURE 2.10. The brick diagram corresponding to the fibre surface of w.

band in the plumbing construction, see Figure 2.10 for the brick diagram corresponding to w.

EXAMPLE 2.15 (Symmetric, definite Seifert forms). In Chapter 5, we give several results on Murasugi sums of Seifert surfaces with symmetric, definite Seifert form, extending statements we obtain for fibred links which have a product of two multitwists as monodromy. The prototype of a Seifert surface with symmetric, definite Seifert form is the annulus with n full twists, where n is a non-zero integer. A matrix for the corresponding Seifert form is of size 1×1, given by (n). More Seifert surfaces with symmetric, definite Seifert forms can be obtained by taking connected sums. For example, the surface depicted in Figure 2.7 on the top left is a connected sum of two negative Hopf bands. Taking the core curves of the Hopf bands as a basis for the first homology of the surface, the Seifert form is given by minus the identity matrix of size two. Similarly, any connected sum of twisted annuli has symmetric, definite Seifert form if all the annuli are twisted in the same sense. Murasugi summing two such connected sums as depicted in Figure 2.7 yields a special case of *quasi-rational links* studied by Hirasawa and Murasugi [**30**], and more generally a special case of *plumbing baskets* studied by Rudolph [**60**]. Interesting classes of links obtained in this way are, for example, alternating quasi-rational links, alternating-sign Coxeter links and arborescent plumbings of positively twisted annuli, in particular positive arborescent Hopf plumbings, compare with [**30, 31, 60**].

3. The Alexander polynomial and the signature function

Closely related to the Alexander polynomial of a link L is the *signature function* $[0,1] \to \mathbf{Z}$, that is, the function assigning to each number $t \in [0,1]$ the signature $\sigma_\omega(L)$ of the Hermitian matrix

$$S_\omega = (1-\omega)A + (1-\overline{\omega})A^\top,$$

where A is a Seifert matrix for L and $\omega = e^{i\pi t} \in \mathbf{S}^1$. For $\omega = -1$, this equals the definition of the classical signature invariant $\sigma(L)$, introduced by Trotter [**72**], and for the number $\omega = 1$, it is equal to zero.

3.1. Signature jumps. As $\omega \in \mathbf{S}^1$ varies, the eigenvalues $\lambda_i(\omega) \in \mathbf{R}$ of S_ω depend continuously on ω. This is a vague statement, compare, for example, with Theorem 1.4 in Marden's book [**44**] to obtain a precise version. Typically, some eigenvalues $\lambda_i(\omega)$ may pass through zero for some number $\omega_0 \in \mathbf{S}^1$. In this case, $\det(S_{\omega_0}) = 0$ and the

ω-signature $\sigma_\omega(L)$ may have a discontinuity at ω_0. If this is the case, we say that the ω-signature *jumps* at ω_0 and call half the difference of the ω-signatures directly after and directly before ω_0 the *signature jump* j_{ω_0} at ω_0. More precisely, for $\omega_0 = e^{it_0}$, $j_{e^{it_0}} = \frac{1}{2}(\sigma_{e^{i(t_0+\epsilon)}} - \sigma_{e^{i(t_0-\epsilon)}})$, for ϵ small enough.

REMARK 2.16. The signature may only jump at zeroes $\omega_0 \in \mathbf{S}^1$ of the Alexander polynomial. Indeed, for any $\omega \in \mathbf{S}^1$, we have $S_\omega = -(1-\overline{\omega})(\omega A - A^T)$, and consequently, for any discontinuity $\omega_0 \neq 1$,

$$\Delta_L(\omega_0) = \det(\omega_0 A - A^T)) = \det((-(1-\overline{\omega}_0)^{-1} S_{\omega_0}) = 0.$$

LEMMA 2.17. *If the ω-signature $\sigma_\omega(L)$ of a link L jumps at $\omega_0 \neq 1$, then the jump is congruent* mod(2) *to the multiplicity of the zero of the Alexander polynomial at ω_0.*

PROOF. Let $\Delta_L(t) = z_0(t-\mu_1)\cdots(t-\mu_d)$ be the Alexander polynomial of the link L. For any $\omega \in \mathbf{S}^1$, it follows that

$$\det(S_\omega) = (-(1-\overline{\omega}))^n \cdot z_0(\omega-\mu_1)\cdots(\omega-\mu_d) \in \mathbf{R}.$$

We now calculate in two different ways how the sign of $\det(S_\omega)$ changes when ω passes through ω_0. If $\det(S_\omega) \neq 0$, then the sign of $\det(S_\omega)$ equals $(-1)^{\frac{n-\sigma_\omega(K)}{2}}$. There are finitely many zeroes of the Alexander polynomial on the unit circle, so directly before and after ω_0, $\det(S_\omega) \neq 0$. Thus, when passing through ω_0, the sign of $\det(S_\omega)$ changes by $(-1)^{j_{\omega_0}}$. On the other hand, if m denotes the multiplicity of the zero of the Alexander polynomial at ω_0, then the argument of the expression

$$(-(1-\overline{\omega}))^n \cdot z_0(\omega-\mu_1)\cdots(\omega-\mu_d) \in \mathbf{R} \subset \mathbf{C}$$

changes by πm when ω passes through ω_0. Therefore, we also have that when passing through ω_0, the sign of $\det(S_\omega)$ changes by $(-1)^m$. Consequently, we also have $(-1)^{j_{\omega_0}} = (-1)^m$ and thus j_{ω_0} equals m mod(2). □

3.2. Zeroes of the Alexander polynomial on the unit circle. In this subsection, we prove that the absolute value of the signature of a link is a lower bound for the number of zeroes of the Alexander polynomial that lie on the unit circle. Seemingly, this result has been known for quite a while without a complete reference. For example, if the Alexander polynomial has only simple zeroes on the unit circle, it follows from a result of Stoimenow [**65**]. Recently, a complete proof of the result has been provided by Feller and the author in the appendix of [**39**], and independently by Gilmer and Livingston [**27**]. In this subsection, we stay close to the appendix of [**39**].

LEMMA 2.18. *For any zero $\omega_0 \neq 0$ of the Alexander polynomial, the multiplicity is greater or equal to the nullity of $\omega_0 A - A^T$.*

PROOF. Consider the matrix $tA - A^T \in \mathrm{Mat}_{n\times n}(\mathbf{C}[t])$. There exist square matrices $P, Q \in \mathrm{GL}(\mathbf{C}[t])$ such that $P(tA-A^T)Q$ is in Smith normal form, that is, $P(tA-A^T)Q$ is a diagonal matrix with entries $\alpha_i \in \mathbf{C}[t]$ and such that $\alpha_i | \alpha_{i+1}$, see [**62**]. Setting

$c = \det(P)\det(Q) \in \mathbf{C}$, we obtain

$$\begin{aligned} c\Delta_K(t) &= \det(P)\det(tA - A^T)\det(Q) \\ &= \det(P(tA - A^T)Q) \\ &= \alpha_1 \cdots \alpha_n \\ &= (t - \omega_0)^m p(t), \end{aligned}$$

where $p(\omega_0) \neq 0$. The number of α_i that have a (perhaps multiple) zero at ω_0 is exactly equal to the nullity of $\omega_0 A - A^T$. Therefore, we get that m is greater than or equal to the nullity of $\omega_0 A - A^T$. However, m is exactly the multiplicity of the zero of the Alexander polynomial at ω_0. □

REMARK 2.19. The multiplicity of the zero of the Alexander polynomial at ω_0 can be strictly greater than the nullity of $\omega_0 A - A^T$. For example, take any link with nullity $\text{null}(S_{-1}) = 1$. On one hand, the multiplicity of the zero of the Alexander polynomial at -1 is greater than or equal to 1 by Lemma 2.18, on the other hand, the multiplicity is even by Lemma 2.17, and hence greater than or equal to 2.

Since for $\omega_0 \neq 1$, the jump $|j_{\omega_0}|$ is less than or equal to the nullity of S_{ω_0} and the nullity of S_{ω_0} equals the nullity of $\omega_0 A - A^T$, we get the following proposition relating the signature jumps to the multiplicity of the zeroes of the Alexander polynomial as a consequence of Lemma 2.18.

PROPOSITION 2.20. *If the ω-signature $\sigma_\omega(L)$ jumps at $\omega_0 \neq 1$, then the signature jump j_{ω_0} at ω_0 is smaller than or equal to the multiplicity of the zero of the Alexander polynomial at ω_0.*

THEOREM 2.21. *The Alexander polynomial $\Delta_L(t)$ of any link L is either identically zero or has at least $|\sigma(L)|$ zeroes (counted with multiplicity) on the unit circle.*

PROOF. So far, we examined the case $\omega_0 \neq 1$. In order to make a statement about the total number of zeroes of the Alexander polynomial that lie on the unit circle, we also have to study the situation at $\omega_0 = 1$. If ω tends towards 1, the eigenvalues $\lambda_i(\omega)$ of S_ω tend, up to some normalisation constant, to the eigenvalues of $iA - iA^T$. Since $A - A^T$ is skew-symmetric, the signature of $iA - iA^T$ is zero. Therefore, for ω close enough to 1, the modulus $|\sigma_\omega(L)| = |\sigma(M_\omega)|$ is bounded from above by the nullity of $A - A^T$, which in turn is bounded from above by the order of the zero of the Alexander polynomial at 1 by Lemma 2.18. Together with Proposition 2.20, this yields the desired result. □

4. The topological 4-genus

The *topological 4-genus* $g_4^{\text{top}}(K)$ of a knot K is the minimal genus among surfaces which are properly, locally-flatly embedded in the 4-ball $\mathbf{B}^4$ and have the knot $K \subset \mathbf{S}^3$ as boundary. In order to obtain an interesting invariant, it is necessary to ask for the embedding to be locally-flat and not just topological. Indeed, every knot K bounds a properly, topologically embedded disc in $\mathbf{B}^4$: the cone over K.

An important and rather astonishing theorem in the study of the topological 4-genus is due to Freedman and states that the topological 4-genus of a knot with Alexander polynomial 1 equals zero.

THEOREM 2.22 (Freedman's disc theorem [**24**]). *A knot with Alexander polynomial* 1 *bounds a properly, locally-flatly embedded disc in* $\mathbf{B}^4$.

Freedman's disc theorem has recently been generalised by Feller in the following sense. For every knot K, the degree of the Alexander polynomial $\Delta_K(t)$ is an upper bound for twice the topological 4-genus $g_4^{\text{top}}(K)$ [**21**].

Freedman's disc theorem can be used to construct locally-flat surfaces with a given knot K as boundary, but with smaller genus than $g(K)$. One starts with a Seifert surface $\Sigma \subset \mathbf{S}^3$ realising the knot's genus. As we have seen in Remark 2.11, the fibre surface of a fibred link indeed realises the genus of the link. Therefore, in the case where the knot K is fibred, one can start with the fibre surface of K. If it is possible to find a (necessarily incompressible) punctured torus T in Σ such that ∂T has Alexander polynomial 1, then by Freedman's disc theorem (Theorem 2.22), one can cut out the punctured torus T and reglue a disc D locally-flatly embedded in $\mathbf{B}^4$ along its boundary ∂T. This is the strategy used by Rudolph, Baader and Lewark to construct locally-flat surfaces with a given knot K as boundary, but with smaller genus than $g(K)$, see [**58, 4, 9**].

The following proposition is a homological reformulation of this method, given by Baader, Feller, Lewark and the author [**7**]. In Chapter 6, we use this proposition to calculate the topological 4-genus of certain positive arborescent Hopf plumbings, which in turn allows us to bound the topological 4-genus of many positive braids away from the ordinary genus.

PROPOSITION 2.23 (Proposition 3 in [**7**]). *Let K be a knot with a Seifert surface Σ and let $V \subset H_1(\Sigma)$ be a subgroup. If the Seifert form of Σ restricted to V has Alexander polynomial* 1*, then $g_4^{\text{top}}(K)$ is bounded from above by $g(K) - \operatorname{rk}(V)/2$.*

In the context of Proposition 2.23, the *Alexander polynomial* of a bilinear form is $\det(tM - M^\top) \in \mathbf{Z}[t^{\pm 1}]$, where M is a matrix representing the form. It does not depend on the choice of representation and is considered up to multiplication with units in $\mathbf{Z}[t^{\pm 1}]$. We say that a subgroup V as in Proposition 2.23 is *Alexander-trivial*.

While Proposition 2.23 gives an upper bound for the topological 4-genus, there also exist lower bounds for the topological 4-genus coming from the Seifert form. These bounds have been studied in detail by Taylor [**68**]. For our purposes, the following interpretation in terms of ω-signatures suffices: for every $\omega \in \mathbf{S}^1 \setminus \{1\}$ at which the signature function does not jump, we have $|\sigma_\omega(K)| \leq 2g_4^{\text{top}}(K)$, see [**54**]. If the signature function does jump at ω, we have to replace $|\sigma_\omega(K)|$ by the mean of the absolute value directly before and directly after the jump. We mostly use the specialised bound for the classical signature $\omega = -1$, originally due to Kauffman and Taylor [**33**].

CHAPTER 3

Spectra of products of multitwists

In this chapter, we study two kinds of spectra of pseudo-Anosov mapping classes: the *geometric spectrum*, that is, the Galois conjugates of the dilatation, and the *algebraic spectrum*, that is, the eigenvalues of the induced homological action.

We start out by considering a special case of a construction of pseudo-Anosov mapping classes due to Thurston [**69**]: products of two multitwists along multicurves α and β that intersect minimally and fill a surface Σ. Recall that a mapping class ϕ is pseudo-Anosov if it has a representative for which there exists a pair of transverse, invariant singular measured foliations such that one of them gets stretched by some real number $\lambda > 1$ and the other one by λ^{-1}. The number λ is called the dilatation of ϕ and is algebraic [**69**]. If a product of two multitwists in Thurston's construction is pseudo-Anosov, Leininger showed that its dilatation is bounded from below by Lehmer's number, the largest real root of the polynomial $t^{10} + t^9 - t^7 - t^6 - t^5 - t^4 - t^3 + t + 1$, approximately equal to 1.176 [**37**]. Furthermore, all Galois conjugates of its trace $\lambda + \lambda^{-1}$ are real by a theorem of Hubert and Lanneau [**32**]. As a consequence, all Galois conjugates of the dilatation λ are contained in $\mathbf{R} \cup \mathbf{S}^1$. Indeed, all Galois conjugates of λ are among the roots of the polynomial $t^n p(t + t^{-1})$, where $p(t)$ is the minimal polynomial of $\lambda + \lambda^{-1}$ over $\mathbf{Q}$ and n is the degree of p. In particular, since all roots of $p(t)$ are real, every Galois conjugate λ' of λ satisfies $\lambda' + \lambda'^{-1} \in \mathbf{R}$ and thus $\lambda' \in \mathbf{R} \cup \mathbf{S}^1$. Our first result is a sharper version of this fact for the special case of a product of exactly two multitwists.

THEOREM 3.1. *If a product of two multitwists in Thurston's construction is pseudo-Anosov, then all Galois conjugates of its dilatation are contained in*

(a) $\mathbf{R}_{>0}$ *if the two twists are of opposite sign,*
(b) $\mathbf{R}_{>0} \cup \mathbf{S}^1$ *if the two twists are of the same sign.*

If the multicurves α and β used in Thurston's construction do not intersect minimally or are not filling, the mapping classes we consider need not be pseudo-Anosov. However, we can still prove the equivalent of Theorem 3.1 for the eigenvalues of the homological action.

THEOREM 3.2. *Let $\phi : \Sigma \to \Sigma$ be the product of two multitwists. Then all eigenvalues of the homological action ϕ_* are contained in*

(a) $\mathbf{R}_{>0}$ *if the two twists are of opposite sign,*
(b) $\mathbf{R}_{<0} \cup \mathbf{S}^1$ *if the two twists are of the same sign.*

Similar statements for specific pairs of multicurves α and β have been made by several authors: statement (b) for mapping classes associated to classical Coxeter graphs that are finite forests by A'Campo [**1, 2**], and statement (a) for mapping classes associated to alternating-sign Coxeter graphs by Hironaka and the author [**31**]. The proof methods are similar.

1. Key observation

The following proposition contains the key observation to all our results on the location of Galois conjugates of the dilatation and the eigenvalues of the homological action in this chapter, and on the zeroes of the Alexander polynomial in Chapter 5. Specific instances of this proposition applied to the homological action of certain mapping classes or the Alexander polynomial of certain links can be found in [**1, 30, 31, 46**].

PROPOSITION 3.3. *Let X be any real matrix of size $n \times m$.*

(a) *The eigenvalues λ_i of $\begin{pmatrix} I_n & X \\ 0 & \pm I_m \end{pmatrix}\begin{pmatrix} I_n & 0 \\ X^\top & \pm I_m \end{pmatrix}$ are related to the eigenvalues μ_i of $\begin{pmatrix} 0 & X \\ X^\top & 0 \end{pmatrix}$ by the equation $\mu_i^2 = -2 + \lambda_i + \lambda_i^{-1}$.*

(b) *The eigenvalues λ_i of $\begin{pmatrix} I_n & X \\ 0 & I_m \end{pmatrix}\begin{pmatrix} I_n & 0 \\ -X^\top & I_m \end{pmatrix}$ are related to the eigenvalues μ_i of $\begin{pmatrix} 0 & X \\ X^\top & 0 \end{pmatrix}$ by the equation $\mu_i^2 = 2 - \lambda_i - \lambda_i^{-1}$.*

PROOF. The inverse of the matrix product

$$\begin{pmatrix} I_n & X \\ 0 & \pm I_m \end{pmatrix}\begin{pmatrix} I_n & 0 \\ X^\top & \pm I_m \end{pmatrix} = \begin{pmatrix} I_n + XX^\top & \pm X \\ \pm X^\top & I_m \end{pmatrix} = A$$

is given by the matrix

$$\begin{pmatrix} I_n & \mp X \\ \mp X^\top & I_m + X^\top X \end{pmatrix} = A^{-1}.$$

Adding these two matrices reveals

$$\begin{pmatrix} 0 & X \\ X^\top & 0 \end{pmatrix}^2 = -2I_{n+m} + A + A^{-1}.$$

The corresponding equation for the eigenvalues, as claimed in (a), follows from the fact that A and A^{-1} are simultaneously diagonalisable. To establish (b), we follow the same scheme, except that the inverse of the matrix product

$$\begin{pmatrix} I_n & X \\ 0 & I_m \end{pmatrix}\begin{pmatrix} I_n & 0 \\ -X^\top & I_m \end{pmatrix} = \begin{pmatrix} I_n - XX^\top & X \\ -X^\top & I_m \end{pmatrix}$$

is given by the matrix

$$\begin{pmatrix} I_n & -X \\ X^\top & I_m - X^\top X \end{pmatrix}.$$

The rest of the proof is again a direct verification. □

2. The geometric spectrum

In this section, we consider the Galois conjugates of the dilatation of a product of two multitwists in Thurston's construction. In particular, we assume the multicurves α and β to intersect minimally and fill the surface Σ.

PROOF OF THEOREM 3.1. Let ϕ be a product of two multitwists that is pseudo-Anosov, given by Thurston's construction with multicurves α and β on a surface Σ of finite type. Furthermore, let

$$\Omega = \begin{pmatrix} 0 & X \\ X^\top & 0 \end{pmatrix} \geq 0$$

be the geometric intersection matrix of the multicurves α and β, and let r be its largest eigenvalue.

Case (a): the twists are of opposite sign. By Thurston's construction (Theorem 2.5), the dilatation λ of ϕ is given by the larger root of the quadratic polynomial

$$t^2 - (2 + r^2)t + 1.$$

Equivalently, λ equals the larger solution of the equation

$$r^2 = -2 + t + t^{-1}.$$

By Proposition 3.3 (a), λ is an eigenvalue (in fact, the largest one) of the matrix product

$$M = \begin{pmatrix} I_n & X \\ 0 & I_m \end{pmatrix} \begin{pmatrix} I_n & 0 \\ X^\top & I_m \end{pmatrix}$$

and thus, all Galois conjugates of λ are among the eigenvalues λ_i of M. On the other hand, the eigenvalues λ_i of M are all real and positive, since $-2 + \lambda_i + \lambda_i^{-1}$ is a non-negative real number by Proposition 3.3 (a).

Case (b): the twists are of the same sign. By Thurston's construction (Theorem 2.5), the dilatation λ of ϕ is given by the largest modulus among the roots of the quadratic polynomial

$$t^2 - (2 - r^2)t + 1.$$

Both roots of this polynomial are negative. Hence, λ equals the largest root of the quadratic polynomial

$$(-t)^2 - (2 - r^2)(-t) + 1 = t^2 + (2 - r^2)t + 1.$$

Equivalently, λ equals the larger solution of the equation

$$r^2 = 2 + t + t^{-1}.$$

By Proposition 3.3 (b), λ is an eigenvalue (in fact, the largest one) of the matrix product

$$M = -\begin{pmatrix} I_n & X \\ 0 & I_m \end{pmatrix} \begin{pmatrix} I_n & 0 \\ -X^\top & I_m \end{pmatrix}.$$

Again, all Galois conjugates of λ are among the eigenvalues λ_i of M. These are all contained in $\mathbf{R}_{>0} \cup \mathbf{S}^1$, since $2 + \lambda_i + \lambda_i^{-1}$ is a non-negative real number by Proposition 3.3 (b). □

3. The homological spectrum

In this section, we drop our previous assumptions on the pair of multicurves α and β. More precisely, we no longer suppose that they intersect minimally or fill the surface Σ. The resulting product of two multitwists along α and β need no longer be pseudo-Anosov and we restrict our attention to the study of its homological action. Let $\gamma \subset \Sigma$ be a simple closed curve in Σ. The action of a Dehn twist along γ on the first homology of Σ is described by

$$(T_\gamma^+)_*([\delta]) = [\delta] + \mathrm{i}(\gamma, \delta)[\gamma],$$
$$(T_\gamma^-)_*([\delta]) = [\delta] - \mathrm{i}(\gamma, \delta)[\gamma],$$

where δ is a curve representing the homology class $[\delta]$ and $\mathrm{i}(\gamma, \delta)$ is the *algebraic intersection number* of the curves γ and δ, that is, intersections counted with signs, depending on the orientation of the intersection point, see, for example, [**18**].

Example 3.4. Let Σ be the torus, and let α and β be representatives of standard generators of the first homology of Σ, as in Figure 3.1. Then, the induced action

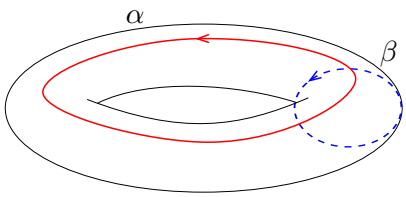

Figure 3.1.

$(T_\alpha^+ T_\beta^-)_*$ on homology is given by the matrix product

$$\begin{pmatrix} 1 & 1 \\ 0 & 1 \end{pmatrix} \begin{pmatrix} 1 & 0 \\ 1 & 1 \end{pmatrix} = \begin{pmatrix} 2 & 1 \\ 1 & 1 \end{pmatrix}.$$

The homological action of a multitwist is given similarly to what is described in Example 3.4. If the multicurves α and β represent a basis of the first homology of the surface Σ, as in Example 3.4, then the homological action is given by block matrices of size 2×2 with identity blocks on the diagonal, a zero off-diagonal block and the other off-diagonal block given by a block of the algebraic intersection matrix of the multicurves α and β, with a sign depending on the twist:

$$(T_\alpha^\pm)_* = \begin{pmatrix} I & \pm X \\ 0 & I \end{pmatrix},$$
$$(T_\beta^\pm)_* = \begin{pmatrix} I & 0 \\ \mp X^\top & I \end{pmatrix},$$

where $\left(\begin{smallmatrix} 0 & X \\ X^\top & 0 \end{smallmatrix}\right)$ is the algebraic intersection matrix of the multicurves α and β. In fact, due to the symmetry of the situation, we only have to consider the products of multitwists $T_\alpha^+ T_\beta^-$ and $T_\alpha^+ T_\beta^+$. In this case, the location result for the eigenvalues claimed in Theorem 3.2 is directly proved using Proposition 3.3 (a) or (b), respectively,

depending on whether the multitwists are of opposite or the same sign. The main technicality we have to deal with for the general case is the fact that the multicurves α and β need not represent a basis of the first homology of the surface Σ.

Proof of Theorem 3.2. Let Σ be an oriented surface of finite type. Furthermore, let $\alpha = \alpha_1 \dot\cup \cdots \dot\cup \alpha_n \subset \Sigma$ and $\beta = \beta_1 \dot\cup \cdots \dot\cup \beta_m \subset \Sigma$ be two multicurves in the surface Σ, and let ϕ be the product of a multitwist along α and a multitwist along β.

By definition, ϕ is supported in a neighbourhood of $\alpha \cup \beta$. In particular, there is an induced map $\phi|_{\Sigma'} : \Sigma' \to \Sigma'$, where Σ' is obtained from Σ by puncturing every connected component of $\Sigma \setminus (\alpha \cup \beta)$ that does not yet have a puncture. The diagram

$$\begin{array}{ccc} \Sigma' & \xhookrightarrow{\iota} & \Sigma \\ {\scriptstyle \phi|_{\Sigma'}}\downarrow & & \downarrow{\scriptstyle \phi} \\ \Sigma' & \xhookrightarrow{\iota} & \Sigma \end{array}$$

commutes, since the horizontal arrows are given by the inclusion of Σ' into Σ. Hence, the induced diagram

$$\begin{array}{ccc} H_1(\Sigma';\mathbf{R}) & \xrightarrow{\iota_*} & H_1(\Sigma;\mathbf{R}) \\ {\scriptstyle (\phi|_{\Sigma'})_*}\downarrow & & \downarrow{\scriptstyle \phi_*} \\ H_1(\Sigma';\mathbf{R}) & \xrightarrow{\iota_*} & H_1(\Sigma;\mathbf{R}) \end{array}$$

on the first homology commutes as well. We consider the subspaces V and V' of $H_1(\Sigma;\mathbf{R})$ and $H_1(\Sigma';\mathbf{R})$, respectively, generated by all the homology classes corresponding to simple closed curves α_i and β_j,

$$V = \langle [\alpha_1], \dots, [\alpha_n], [\beta_1], \dots, [\beta_m] \rangle \subset H_1(\Sigma;\mathbf{R}),$$
$$V' = \langle [\alpha_1], \dots, [\alpha_n], [\beta_1], \dots, [\beta_m] \rangle \subset H_1(\Sigma';\mathbf{R}).$$

For the homological action ϕ_*, the image of $\phi_* - \mathrm{id}_{H_1(\Sigma;\mathbf{R})}$ is contained in V. It follows that the only possible eigenvalue of ϕ_* that is not an eigenvalue of $\phi_*|_V$ is 1. Therefore, we may assume $V = H_1(\Sigma;\mathbf{R})$. We claim that in this case, ι_* is surjective. Actually, we argue that already $\iota_*|_{V'}$ is surjective. Indeed, the subspace $V' \simeq \mathbf{R}^{n+m}$ is freely generated by the homology classes $[\alpha_i]$ and $[\beta_j]$, since all the simple closed curves α_i and β_j are different loops in a graph to which Σ' retracts, and intersect only at vertices of this graph. By definition (and slightly abusing notation), we have $\iota(\alpha_i) = \alpha_i$ and $\iota(\beta_j) = \beta_j$, and therefore $\iota_*(V') = V = H_1(\Sigma;\mathbf{R})$. Furthermore, $(\phi|_{\Sigma'})_*(V') \subset (V')$, and the diagram

$$\begin{array}{ccc} V' & \xrightarrow{\iota_*|_{V'}} & H_1(\Sigma;\mathbf{R}) \\ {\scriptstyle (\phi|_{\Sigma'})_*|_{V'}}\downarrow & & \downarrow{\scriptstyle \phi_*} \\ V' & \xrightarrow{\iota_*|_{V'}} & H_1(\Sigma;\mathbf{R}) \end{array}$$

commutes, where the horizontal arrows are surjective. By Lemma 3.5 below, the spectrum of ϕ_* is contained in the spectrum of $(\phi|_{\Sigma'})_*|_{V'}$. In particular, we are done if we

can show that the spectrum of $(\phi|_{\Sigma'})_*|_{V'}$ is contained in $\mathbf{R}_{>0}$ or $\mathbf{R}_{<0} \cup \mathbf{S}^1$, depending on whether ϕ is a product of two multitwists of opposite or of the same sign, respectively. In order to prove this last claim, we note that in the basis

$$\{[\alpha_1], \ldots, [\alpha_n], [\beta_1], \ldots, [\beta_m]\}$$

of V', the map $(\phi|_{\Sigma'})_*|_{V'}$ is given by the matrix product

$$\begin{pmatrix} I_n & X \\ 0 & I_m \end{pmatrix} \begin{pmatrix} I_n & 0 \\ X^\top & I_m \end{pmatrix}$$

if ϕ is the product of two multitwists of opposite sign and by the matrix product

$$\begin{pmatrix} I_n & X \\ 0 & I_m \end{pmatrix} \begin{pmatrix} I_n & 0 \\ -X^\top & I_m \end{pmatrix}$$

if ϕ is the product of two multitwists of the same sign. Here,

$$\begin{pmatrix} 0 & X \\ X^\top & 0 \end{pmatrix}$$

is the algebraic intersection matrix of the multicurves α and β. The inclusions claimed for the spectrum of $(\phi|_{\Sigma'})_*|_{V'}$ now follow directly from Proposition 3.3 (a) or (b), respectively, which states that for each eigenvalue λ of $(\phi|_{\Sigma'})_*|_{V'}$, $-2 + \lambda + \lambda^{-1}$ or $2 - \lambda - \lambda^{-1}$, respectively, is a non-negative real number. This completes the proof of Theorem 3.2. □

LEMMA 3.5. *Let V and W be finite dimensional vector spaces. Furthermore, let π, f and g be linear maps such that the diagram*

$$\begin{array}{ccc} V & \xrightarrow{\pi} & W \\ {\scriptstyle f}\downarrow & & \downarrow{\scriptstyle g} \\ V & \xrightarrow{\pi} & W \end{array}$$

commutes and π is surjective. Then the spectrum of g is contained in the spectrum of f.

PROOF. We write V as the direct sum $V = U \oplus \ker(\pi)$, where $\pi|_U : U \to W$ is an isomorphism. Restricting to U, we have

$$g \circ \pi|_U = \pi \circ f|_U = \pi|_U \circ \mathrm{proj}_U \circ f|_U,$$

or, equivalently,

$$(\pi|_U)^{-1} \circ g \circ \pi|_U = \mathrm{proj}_U \circ f|_U,$$

where $\mathrm{proj}_U : V \to U$ is the projection to the direct summand U. In particular, the spectrum of g agrees with the spectrum of $\mathrm{proj}_U \circ f|_U$. Thus, it suffices to prove that the spectrum of $\mathrm{proj}_U \circ f|_U$ is contained in the spectrum of f. We have $f(\ker(\pi)) \subset \ker(\pi)$. Therefore, according to the direct sum decomposition $V = U \oplus \ker(\pi)$, f is of lower triangular block form

$$\begin{pmatrix} \mathrm{proj}_U \circ f|_U & 0 \\ * & f|_{\ker(\pi)} \end{pmatrix}.$$

It follows that the spectrum of $\mathrm{proj}_U \circ f|_U$ is indeed contained in the spectrum of f. □

4. The spectrum on the unit circle

In the case of a product of two multitwists of the same sign, it is a natural question to ask how much of the spectrum is contained in the unit circle. For the geometric spectrum, this seems rather difficult to answer, since one has to determine which eigenvalues λ_i of the matrix products studied in Proposition 3.3 have the same minimal polynomial as the dilatation λ.

For the homological spectrum, this difficulty does not arise. For example, in the case where the two multicurves α and β represent a basis of the first homology of Σ, we obtain the following result.

PROPOSITION 3.6. *Let $\phi : \Sigma \to \Sigma$ be a product of two multitwists of the same sign defined by multicurves α and β that represent a basis of the first homology of Σ. Then the induced action ϕ_* on homology has $\sigma(\Omega_a + 2I) + \mathrm{null}(\Omega_a + 2I)$ eigenvalues (counted with multiplicity) on $\mathbf{S}^1$, where Ω_a is the algebraic intersection matrix of α and β.*

PROOF. By Lemma 3.7 below, the number of eigenvalues of Ω_a that lie in the interval $[-2, 2]$ equals $\sigma(\Omega_a + 2I) + \mathrm{null}(\Omega_a + 2I)$. But since the eigenvalues μ_i of Ω_a and λ_i of ϕ_* are related by the equation

$$\mu_i^2 = 2 - \lambda_i - \lambda_i^{-1}$$

by Proposition 3.3 (b), the number of eigenvalues of ϕ_* on $\mathbf{S}^1$ equals the number of eigenvalues of Ω_a that lie in the interval $[-2, 2]$. □

LEMMA 3.7. *Let X be any real matrix of size $n \times m$. The number of eigenvalues (counted with multiplicity) of $\Omega = \left(\begin{smallmatrix} 0 & X \\ X^\top & 0 \end{smallmatrix}\right)$ in the interval $[-2, 2]$ equals $\sigma(\Omega + 2I) + \mathrm{null}(\Omega + 2I)$.*

PROOF. We study the signature of the symmetric matrix $\Omega + 2I$. It equals the number of positive eigenvalues minus the number of negative eigenvalues of $\Omega + 2I$. Equivalently, thinking in terms of eigenvalues of Ω, it is equal to the number of eigenvalues of Ω strictly greater than -2 minus the number of eigenvalues of Ω strictly smaller than -2. Since the spectrum of Ω is symmetric with respect to the origin, we have that the number of eigenvalues of Ω strictly smaller than -2 equals the number of eigenvalues of Ω strictly larger than 2. Thus, the signature of $\Omega + 2I$ equals the number of eigenvalues of Ω that lie in the interval $(-2, 2]$. Furthermore, the multiplicity of the eigenvalues of Ω at -2 equals the nullity of $\Omega + 2I$. In particular, we have that the number of eigenvalues of Ω that lie in the interval $[-2, 2]$ equals $\sigma(\Omega + 2I) + \mathrm{null}(\Omega + 2I)$. □

We come back to considerations of this kind in Chapter 5. There, we relate this discussion to certain examples of links and their signature invariant. For example, we show that if α and β intersect with the pattern of a tree, then at least two thirds of the eigenvalues lie on $\mathbf{S}^1$. In other words, we show that at least two thirds of the eigenvalues of the adjacency matrix of a tree lie in the interval $[-2, 2]$. However, we first study

the dilatation of pseudo-Anosov homeomorphisms arising from Penner's construction in the next chapter.

CHAPTER 4

Minimal dilatation in Penner's construction

In this chapter, we determine the minimal dilatations arising from Penner's construction of pseudo-Anosov mapping classes [**50**]. We stay close to the author's original exposition in [**41**].

By a result of Leininger, the dilatation of any pseudo-Anosov mapping class arising from Penner's construction is bounded from below by $\sqrt{5}$, see the appendix of [**37**]. However, Leininger states that this bound is not sharp. For every orientable closed surface, we give the optimal lower bound and determine a pseudo-Anosov mapping class arising via Penner's construction realising it.

THEOREM 4.1. *On an orientable closed surface Σ_g of genus $g \geq 1$, the minimal dilatation λ_g among mapping classes arising from Penner's construction is*

$$1 + 2\cos^2\left(\frac{\pi}{2g+1}\right) + 2\sqrt{\cos^2\left(\frac{\pi}{2g+1}\right) + \cos^4\left(\frac{\pi}{2g+1}\right)}.$$

Furthermore, the dilatation λ_g is realised by the Coxeter mapping class associated to the Coxeter graph $(A_{2g}, \pm)$ with alternating signs.

Recent results deal with Galois conjugates of dilatations arising from Penner's construction. For example, they lie dense in the complex plane by a theorem of Strenner [**67**]. On the other hand, Shin and Strenner showed that they cannot lie on the unit circle and used their result to disprove Penner's conjecture that every pseudo-Anosov mapping class has a power arising via his construction [**61**].

REMARK 4.2. The sequence λ_g of minimal dilatations among mapping classes arising via Penner's construction for $g \geq 1$ is monotonically increasing in g. This follows directly from the formula given in Theorem 4.1, since $\cos(\frac{\pi}{2g+1})$ is monotonically increasing in $g \geq 1$. Thus, the minimum among all dilatations arising from Penner's construction is

$$\lambda_1 = \frac{3+\sqrt{5}}{2},$$

the square of the golden ratio, and is geometrically realised by the monodromy of the figure eight knot. Furthermore, since $\cos(\frac{\pi}{2g+1})$ converges to 1 as $g \to +\infty$, the sequence λ_g converges to the limit

$$\lim_{g\to\infty} \lambda_g = 3 + 2\sqrt{2},$$

the square of the silver ratio.

REMARK 4.3. In our original article [**41**], the minimal dilatation λ_g among mapping classes arising from Penner's construction is given as

$$2 - \cos\left(\frac{2g-1}{2g+1}\pi\right) + \sqrt{3 - 4\cos\left(\frac{2g-1}{2g+1}\pi\right) + \cos^2\left(\frac{2g-1}{2g+1}\pi\right)}.$$

The different look of the formula stems from the slightly different calculation of the dilatation of the Coxeter mapping class associated to the Coxeter graph $(A_{2g}, \pm)$ with alternating signs.

Outline. As a first step in the proof of Theorem 4.1, we calculate the dilatation of the Coxeter mapping class corresponding to the alternating-sign Coxeter graph $(A_{2g}, \pm)$ in Proposition 4.4. Having calculated these dilatations allows us to neglect all mapping classes for which we can deduce larger dilatation. Section 2 is devoted to this task: in Proposition 4.5, we show that we can disregard the case where two components of the multicurves used in Penner's construction intersect more than once, essentially reducing the problem to a question about alternating-sign Coxeter mapping classes. Using monotonicity of the spectral radius under Coxeter graph inclusion in Proposition 4.6, we are able to exclude almost all Coxeter graphs that do not correspond to a finite Dynkin diagram. For pairs of multicurves that intersect with the pattern of a graph that we did not rule out, we study in Section 3 which surfaces their union can fill. This finally allows us to finish the proof of Theorem 4.1 by calculating the dilatations of very few small genus examples. We round off in Section 4, where we hint at generalisations to surfaces with punctures, discuss difficulties and ask about asymptotic behaviour.

1. The Coxeter mapping class associated to $(A_{2g}, \pm)$

Recall from Chapter 2 that one way to describe the Coxeter mapping class ϕ_g with alternating-sign Coxeter graph $(A_{2g}, \pm)$ is the following: let Σ_g be a closed surface of genus g. Let α and β be two multicurves in Σ_g, with g components each, that intersect with the pattern of the Dynkin tree A_{2g}. For $g = 3$, this is depicted in Figure 4.1. Then, ϕ_g is the mapping class given by a negative Dehn twist along all components of β, followed by a positive Dehn twist along all components of α. Manifestly, the mapping classes ϕ_g also arise via Thurston's construction [**69**], which is described in Chapter 2.

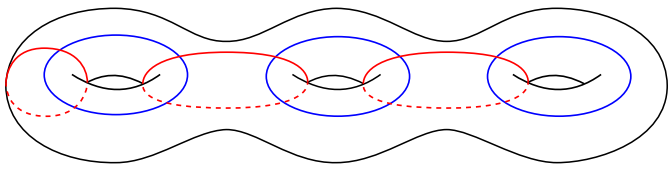

FIGURE 4.1.

PROPOSITION 4.4. *The Coxeter mapping class ϕ_g associated to the Coxeter tree $(A_{2g}, \pm)$ with alternating signs has dilatation*

$$1 + 2\cos^2\left(\frac{\pi}{2g+1}\right) + 2\sqrt{\cos^2\left(\frac{\pi}{2g+1}\right) + \cos^4\left(\frac{\pi}{2g+1}\right)} < 3 + 2\sqrt{2}.$$

PROOF. By Thurston's construction (Theorem 2.5), the dilatation of ϕ_g equals the larger root of the quadratic polynomial

$$t^2 - (2 + r^2)t + 1, \tag{1}$$

where r is the spectral radius of the adjacency matrix of the underlying graph, which in our case is the path A_{2g}. This spectral radius equals $2\cos(\frac{\pi}{2g+1})$, see, for example, [**14**]. Solving for the larger root of equation (1) yields

$$1 + 2\cos^2\left(\frac{\pi}{2g+1}\right) + 2\sqrt{\cos^2\left(\frac{\pi}{2g+1}\right) + \cos^4\left(\frac{\pi}{2g+1}\right)}.$$

Furthermore, since $\cos(\frac{\pi}{2g+1}) < 1$ for any $g \geq 1$, this number is smaller than $3+2\sqrt{2}$. □

2. Two dilatation bounds for Penner's construction

Being a product of non-negative matrices $\rho(\alpha_i) = I + R_{\alpha_i}$ and $\rho(\beta_j) = I + R_{\beta_j}$, the matrix product $\rho(\phi)$ of Penner's construction (Theorem 2.7) described in Chapter 2 is non-negative as well. This allows us to use Perron-Frobenius theory. The one standard fact we repeatedly use is the following. If a non-negative matrix M is entrywise greater than or equal to another non-negative matrix N, written $M \geq N$, then the spectral radius of M is greater than or equal to the spectral radius of N, see, for example, [**14**]. We directly observe that the dilatation among mapping classes arising from Penner's construction is minimised by products of Dehn twists such that every component of the multicurves α and β gets twisted along exactly once. Propositions 4.5 and 4.6 give lower bounds for the dilatation of mapping classes arising from Penner's construction using certain pairs of multicurves α and β.

PROPOSITION 4.5. *In Penner's construction, if two components α_i and β_j of the multicurves α and β intersect at least twice, then any resulting pseudo-Anosov mapping class has dilatation greater than or equal to $3 + 2\sqrt{2}$.*

PROOF. Let ϕ be a pseudo-Anosov mapping class arising from Penner's construction using the multicurves α and β. We consider the matrix product $\rho(\phi)$ associated to ϕ in Penner's construction (Theorem 2.7). Furthermore, we suppose that two components α_i and β_j of α and β intersect $x \geq 2$ times. Without loss of generality, we assume that $T_{\alpha_i}^+$ appears in the product ϕ before $T_{\beta_j}^-$. From the definition, we directly obtain

$$\rho(\phi) \geq (I + R_{\alpha_i})(I + R_{\beta_j}).$$

Up to a change of basis (permuting the basis elements such that the first two basis elements correspond to α_i and β_j), we have

$$(I + R_{\alpha_i})(I + R_{\beta_j}) = \begin{pmatrix} 1 & x & * \\ 0 & 1 & 0 \\ 0 & 0 & I_{n+m-2} \end{pmatrix} \begin{pmatrix} 1 & 0 & 0 \\ x & 1 & * \\ 0 & 0 & I_{n+m-2} \end{pmatrix}$$
$$\geq \begin{pmatrix} 1+x^2 & x & 0 \\ x & 1 & 0 \\ 0 & 0 & I_{n+m-2} \end{pmatrix} = M(x).$$

For $x = 2$, the largest eigenvalue of $M(x)$ is exactly $3+2\sqrt{2}$. The statement now follows from monotonicity of the spectral radius of non-negative matrices under "$\geq$". □

PROPOSITION 4.6. *In Penner's construction, if the multicurves α and β intersect with the pattern of a graph that contains an affine Dynkin diagram $\widetilde{D}_n$, $\widetilde{E}_6$, $\widetilde{E}_7$ or $\widetilde{E}_8$ as a subgraph, then any resulting pseudo-Anosov mapping class ϕ has dilatation greater than or equal to $3 + 2\sqrt{2}$.*

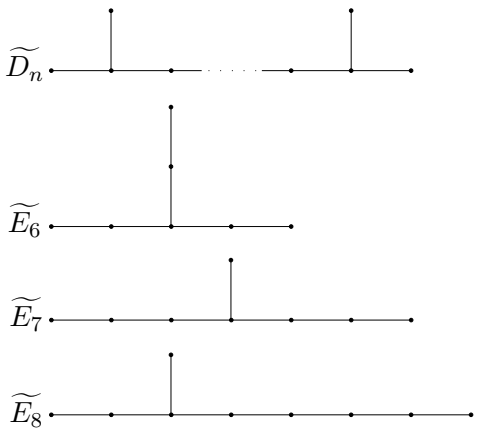

FIGURE 4.2. The affine Dynkin diagrams $\widetilde{D}_n$, $\widetilde{E}_6$, $\widetilde{E}_7$ and $\widetilde{E}_8$.

PROOF. Let ϕ be a pseudo-Anosov mapping class arising from Penner's construction using multicurves α and β that intersect with the pattern of a graph that contains an affine Dynkin diagram $\Gamma = \widetilde{D}_n, \widetilde{E}_6, \widetilde{E}_7$ or $\widetilde{E}_8$ as a subgraph. As observed at the beginning of this section, we can assume every component of the multicurves α and β to be twisted along exactly once. Let $\rho(\phi)$ be the corresponding matrix product described in Penner's construction (Theorem 2.7). Furthermore, let $\rho(\phi_\Gamma)$ be the subproduct associated to the curve components corresponding to the vertices of Γ. We have $\rho(\phi) \geq \rho(\phi_\Gamma)$. The spectral radius of $\rho(\phi_\Gamma)$ is in turn an upper bound for the dilatation λ of the alternating-sign Coxeter mapping class associated to $(\Gamma, \pm)$. We calculate this dilatation λ knowing that it equals the larger root of the quadratic polynomial

$$t^2 - (2 + r^2)t + 1,$$

as in the proof of Proposition 4.4, where r is the spectral radius of the adjacency matrix of the underlying graph. In our case, the underlying graphs are affine Dynkin diagrams, and hence the spectral radius of their adjacency matrices equals 2, see, for example, [**14**]. Solving for the larger root of the quadratic equation above, we obtain $\lambda = 3 + 2\sqrt{2}$. □

3. Filling pairs of multicurves

Let Σ_g be an orientable closed surface of genus g. A pair of multicurves α and β whose union fills Σ_g induces a cell decomposition of Σ_g: the 0-cells are the intersection points of α and β, the 1-cells are the connected components of $\alpha \cup \beta$ without the intersection points and the 2-cells are the connected components of the complement of $\alpha \cup \beta$. In particular, the contribution of the 0-cells and 1-cells to the Euler characteristic can be directly deduced from the intersection graph of α and β. In order to know the number of 2-cells, additional information on the framing of the curves might be necessary. For a pair of multicurves that intersect with the pattern of a tree, however, the number of 2-cells does not depend on the framing and can thus be calculated directly from the tree. For the Dynkin diagram A_n, the number of 2-cells of the induced cell decomposition is two if n is odd and one if n is even. We directly deduce which closed surfaces can be filled by a pair of multicurves that intersect with the pattern of the Dynkin diagram A_n.

LEMMA 4.7. *The union of two multicurves α and β that intersect with pattern A_{2g} or A_{2g+1} can only fill a closed surface of genus g.*

We proceed similarly for the Dynkin diagram D_n: the number of 2-cells of the induced cell decomposition is two if n is odd and three if n is even. This yields the following result.

LEMMA 4.8. *The union of two multicurves α and β that intersect with pattern D_{2g+1} or D_{2g+2} can only fill a closed surface of genus g.*

If the intersection graph of two multicurves α and β contains a cycle, the number of 2-cells may well depend on the framing of the curves. Since the Euler characteristic of an orientable closed surface is even, we can still deduce the parity of the number of 2-cells directly from the graph. For example, we obtain that the number of 2-cells of a cell decomposition induced by a pair of multicurves α and β that intersect like a $2n$-cycle is even and hence at least two. Again, we directly deduce information about the genus of a surface filled that way.

LEMMA 4.9. *The union of two multicurves α and β that intersect with the pattern of a $2g$-cycle can only fill closed surfaces of genus at most g.*

3.1. Proof of Theorem 4.1. Let Σ_g be an orientable closed surface of genus g. As we have seen in Proposition 4.4, there exists a mapping class ϕ_g on Σ_g that arises via Penner's construction and has dilatation $\lambda_g < 3 + 2\sqrt{2}$. Hence, if we want to find the minimal dilatation of mapping classes on Σ_g arising from Penner's construction, we

can discard all pairs of multicurves α and β that always yield dilatations greater than or equal to $3+2\sqrt{2}$. By Proposition 4.5, this excludes pairs of multicurves α and β with components α_i and β_j that intersect more than once. Furthermore, by Proposition 4.6, this rules out pairs of multicurves α and β that intersect with the pattern of a graph that contains an affine Dynkin diagram $\widetilde{D}_n, \widetilde{E}_6, \widetilde{E}_7$ or $\widetilde{E}_8$ as a subgraph. In Example 2.8, we have seen that the spectral radius of any Coxeter transformation associated to the 4-cycle with alternating signs is greater than or equal to $3 + 2\sqrt{2}$. With the same reasoning as in the proof of Proposition 4.6, pairs of multicurves α and β that intersect with the pattern of a graph that contains a 4-cycle as a subgraph can be disregarded.

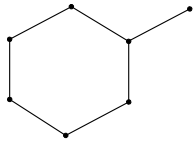

FIGURE 4.3. The enriched 6-cycle.

The only intersection patterns of a pair of multicurves α and β we still have to consider are the Dynkin diagrams A_n, D_n, E_6, E_7, E_8, the $2n$-cycle and the enriched 6-cycle, depicted in Figure 4.3. By Lemma 4.7, Lemma 4.8 and Lemma 4.9, every A_n, D_n and $2n$-cycle encoding the intersections of a pair of multicurves α and β that fills Σ_g contains A_{2g} as a subgraph. In particular, the dilatations arising via Penner's construction using these multicurves are greater than or equal to the dilatation of the Coxeter mapping class ϕ_g associated to the Coxeter tree $(A_{2g}, \pm)$ with alternating signs. This proves Theorem 4.1 for $g \geq 5$, since the union of two multicurves α and β intersecting with the pattern of E_6, E_7, E_8 or the enriched 6-cycle can only fill a surface of genus $g \leq 4$. The only thing left to deal with are these exceptional four graphs. We note that the enriched 6-cycle contains E_7 as a subgraph. Thus, the dilatation of any Coxeter mapping class associated to the enriched 6-cycle with alternating signs is greater than or equal to the dilatation of the Coxeter mapping class associated to $(E_7, \pm)$. For these remaining four graphs, we simply calculate the dilatation of their associated alternating-sign Coxeter mapping classes and compare them to the dilatation of the Coxeter mapping classes ϕ_g associated to $(A_{2g}, \pm)$. Table 4.1 sums up the situation. It is apparent that the Coxeter mapping classes associated to the

graph	genus of surface filled	dilatation
A_6	3	≈ 5.049
A_8	4	≈ 5.345
E_6	3	≈ 5.552
E_7	3	≈ 5.704
E_8	4	≈ 5.783
enriched 6-cycle	≤ 4	> 5.7

TABLE 4.1.

Coxeter graphs $(A_{2g}, \pm)$ with alternating signs minimise the dilatation also for closed surfaces of genus $g \leq 4$. This completes the proof of Theorem 4.1.

4. Surfaces with punctures

Let $\lambda_{g,p}$ be the minimal dilatation among mapping classes arising from Penner's construction for an orientable surface $\Sigma_{g,p}$ of genus g with p punctures. Up to now, we have determined $\lambda_{g,0}$. We remark that our proof works exactly the same for $\lambda_{g,1}$. This yields $\lambda_{g,0} = \lambda_{g,1}$. If the number of punctures is small, say $p \leq 4$, it is conceivable that adjustments to our argument could be made, revealing alternating-sign Coxeter mapping classes associated to A_n, D_n or the $2n$-cycle to minimise dilatation among mapping classes arising from Penner's construction. However, if the number of punctures increases, our examples cannot fill $\Sigma_{g,p}$ any longer and it seems that dilatations should become greater than $3 + 2\sqrt{2}$. In particular, our simplifications in the form of Propositions 4.5 and 4.6 fail and many more cases would have to be considered: intersection patterns with affine subgraphs, loops, multiple edges and additional information on the framing of the corresponding curves.

Remark 4.10. The numbers $\lambda_{g,p}$ are bounded from above by a constant that does not depend on g and p. Figure 4.4 depicts two multicurves α and β that intersect minimally and fill a sphere with eight punctures. Analogous examples can be constructed for any number of punctures. Furthermore, we can combine this example with

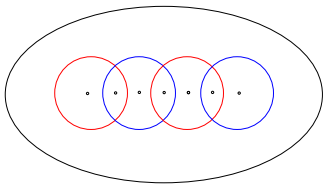

Figure 4.4.

our minimising examples for closed surfaces, as depicted in Figure 4.1, such that the components of the multicurves still intersect along a path. Let ϕ be the product of Dehn twists along the components of the multicurves given by the bipartite order, with alternating signs. Since the multicurves intersect with the pattern of a path and each pair of components intersects at most twice, it is a direct observation that there exists a constant c such that every row sum of the matrix product $\rho(\phi)$ of Penner's construction (Theorem 2.7) is bounded from above by c. In particular, the Perron-Frobenius eigenvalue of $\rho(\phi)$ and thus also the dilatation of ϕ is bounded from above by c.

If g is large compared to p, filling multicurves α and β as in Remark 4.10, but with different properties can be found. For example, multicurves α and β with only single intersections among components. Furthermore, α and β can be chosen to intersect with the pattern of a tree with vertices of degree at most three. This results in a smaller constant than c from Remark 4.10 bounding the row sums of the matrix product $\rho(\phi)$ corresponding to the associated alternating-sign Coxeter mapping class ϕ.

REMARK 4.11. In general, for a fixed p, the function $\lambda_{g,p}$ is not increasing in g. Indeed, we have

$$\lambda_{0,3} = 3 + 2\sqrt{2} > \lambda_{1,3}.$$

The equality on the left follows from the following observation. If two simple closed curves on the sphere with three punctures intersect, then they intersect at least twice by the Jordan curve theorem. In particular, on the sphere with three punctures, pseudo-Anosov mapping classes arising from Penner's construction have $\lambda \geq 3+2\sqrt{2}$ by Proposition 4.5. On the other hand, it is possible to fill the sphere with three punctures by two simple closed curves intersecting exactly twice. The product of two Dehn twists along these curves realises $\lambda_{0,3} = 3 + 2\sqrt{2}$. The inequality on the right follows from the fact that the torus with three punctures can be filled by a pair of multicurves that intersect with the pattern of the Dynkin diagram D_4, whose associated alternating-sign Coxeter transformation has spectral radius strictly smaller than $3 + 2\sqrt{2}$.

Even though $\lambda_{g,p}$ is not always increasing in g, it might be so for g large enough compared to p. In this case, one could ask about the limit of $\lambda_{g,p}$ for a fixed p, as $g \to +\infty$. These are two specific instances of the following, more broadly formulated question.

QUESTION 4.12. *For a fixed $p > 1$, what is the asymptotic behaviour of $\lambda_{g,p}$?*

CHAPTER 5

The signature function of positive Murasugi sums

In this chapter, we study Murasugi sums of two Seifert surfaces with symmetric, definite Seifert form. In particular, we consider their signature function and the location of the zeroes of their Alexander polynomial. Recall from Chapter 2 that the signature function is closely related to the Alexander polynomial: the signature function of a link L is a function $[0,1] \to \mathbf{Z}$, and is locally constant except at some $t \in [0,1]$ for which $\omega = e^{i\pi t}$ is a zero of the Alexander polynomial. Furthermore, its value at 1 equals the classical signature invariant σ.

One reason for our interest in the signature function is its close connection to the topological 4-genus of knots. More precisely, its values at t for which $\omega = e^{i\pi t}$ is not a zero of the Alexander polynomial yield lower bounds for twice the topological 4-genus of the knot [**54**]. Therefore, we would like to know the maximal value of the signature function. Our main theorem of this chapter establishes monotonicity of the signature function for Murasugi sums of two Seifert surfaces with symmetric, definite Seifert form. This implies that the maximum of the signature function is attained at $t = 1$, and is equal to the classical signature invariant. Recall from Chapter 2 that important examples include arborescent plumbings of bands with any number of positive full twists, in particular positive arborescent Hopf plumbings.

THEOREM 5.1. *The signature function of a Murasugi sum of two Seifert surfaces with symmetric, positive definite Seifert form is monotonic.*

Monotonicity of the signature function seems to be a rather uncommon phenomenon. As an example, we consider torus knots $T(p,q)$: the signature function has the first negative jump at the point $2/p + 2/q$. This can be seen using Litherland's formula for the signature function of torus knots [**42**]. In particular, if $2/p + 2/q < 1$, the signature function of the torus knot $T(p,q)$ is not monotonic. On the other hand, by checking the few examples for which $2/p + 2/q \geq 1$, one can see that the few torus knots with monotonic signature function are actually positive arborescent Hopf plumbings.

Our proof of Theorem 5.1 uses the ideas developed in Chapter 3, in particular Proposition 3.3. Along the way, we also prove an analogue of Theorems 3.1 and 3.2 (on the geometric and homological spectrum of a product of two multitwists) for the zeroes of the Alexander polynomial of a Murasugi sum of two Seifert surfaces with symmetric, definite Seifert form (Theorem 5.4). Furthermore, this allows us to deduce log-concavity of the Conway polynomial of a Murasugi sum of two Seifert surfaces with symmetric, positive definite Seifert form (Corollary 5.5). Our ideas were also applied by Misev, who showed that in a positive arborescent Hopf plumbing corresponding to

a tree which is not a spherical or affine Dynkin diagram, there exist infinitely many unknotted annuli with framing ± 1, even up to the action of the monodromy [**48**].

In the last part of this chapter, we consider the signature of positive arborescent Hopf plumbings and give a sharp lower bound in terms of the first Betti number.

THEOREM 5.2. *The signature of a positive arborescent Hopf plumbing is greater than or equal to two thirds of the first Betti number.*

There are several views on Theorem 5.2. For example, from the fact that the signature invariant of a link is a lower bound for the number of zeroes of the Alexander polynomial on the unit circle, it follows that at least two thirds of the eigenvalues of the Coxeter transformation corresponding to a finite forest lie on the unit circle. This application was mentioned in the author's original article [**39**], where also Theorem 5.2 is proved. Here, we choose to highlight the following equivalent reformulation for the adjacency matrix of a finite forest. It results directly from Lemma 3.7 and the correspondence stated in Proposition 3.3 (b).

COROLLARY 5.3. *At least two thirds of the eigenvalues of the adjacency matrix of a finite forest lie in the interval* $[-2, 2]$.

We give examples of positive arborescent Hopf plumbings with arbitrarily large first Betti number for which the bound in Theorem 5.2 (and hence the bound in Corollary 5.3) is sharp. These examples are also interesting in the context of Chapters 6 and 7, since their topological 4-genus equals exactly two times their signature invariant [**7**].

1. Zeroes of the Alexander polynomial

In this section, we consider the location of the zeroes of the Alexander polynomial of a Murasugi sum of two Seifert surfaces with symmetric, definite Seifert form.

Let us start by quickly considering the fibred case. Recall from Chapter 2 that the Murasugi sum of two fibre surfaces with symmetric, definite Seifert form yields a fibre surface whose monodromy is given by the product of two multitwists. In this case, Theorem 3.2 directly translates to the zeroes of the Alexander polynomial $\Delta_L(t)$, since it equals the characteristic polynomial of the homological action of the monodromy by Proposition 2.10. However, our method actually extends to Murasugi sums of certain non-fibred surfaces, the crucial feature being that the Seifert form of both summands is symmetric and definite.

THEOREM 5.4. *Let L be the boundary of a Murasugi sum of two Seifert surfaces Σ_1 and $\Sigma_2 \subset \mathbf{S}^3$ with symmetric, definite Seifert forms. Then all zeroes of the Alexander polynomial $\Delta_L(t)$ are contained in*

(a) $\mathbf{R}_{>0}$ *if the two Seifert forms are definite of opposite sign,*
(b) $\mathbf{R}_{<0} \cup \mathbf{S}^1$ *if the two Seifert forms are definite of the same sign.*

For specific subclasses of the links we consider in Theorem 5.4, the corresponding result has been obtained by several authors: statement (b) for positive arborescent Hopf plumbings by A'Campo [**1, 2**] and statement (a) for alternating quasi-rational links by Hirasawa and Murasugi [**30**], and for the even more restrictive class of alternating-sign Coxeter links by Hironaka and the author [**31**].

PROOF OF THEOREM 5.4. Let L be the boundary of a Murasugi sum of two Seifert surfaces Σ_1 and $\Sigma_2 \subset \mathbf{S}^3$ with symmetric, definite Seifert forms, given by Seifert matrices B and C, respectively. Then, a Seifert matrix A for L is given by a block matrix

$$A = \begin{pmatrix} B & Y \\ 0 & C \end{pmatrix}.$$

Since B and C are symmetric, definite matrices, there exist invertible matrices D_B and D_C such that $D_B B D_B^\top = \pm I_n$ and $D_C C D_C^\top = \pm I_m$, respectively, where the sign depends on whether the Seifert matrices are positive or negative definite. Define the matrix D to be

$$D = \begin{pmatrix} D_B & 0 \\ 0 & D_C \end{pmatrix}$$

and let X be the matrix $D_B Y D_C^T$. The Alexander polynomial $\Delta_L(t)$ of L is defined to be $\det(tA - A^\top)$. Since A is invertible, the zeroes of $\Delta_L(t)$ are exactly the eigenvalues of $A^\top A^{-1}$, which in turn are equal to the eigenvalues of $A^\top (A^\top A^{-1})^\top A^{-\top} = AA^{-\top}$. Furthermore, the eigenvalues of $AA^{-\top}$ are equal to the eigenvalues of

$$DAA^{-\top}D^{-1} = DAD^\top D^{-\top} A^{-\top} D^{-1} = DAD^\top (DA^\top D^\top)^{-1}.$$

Case (a): the Seifert matrices are definite of opposite sign. By symmetry, we may assume B is positive definite. It is directly checked that

$$DAD^\top (DA^\top D^\top)^{-1} = \begin{pmatrix} I_n & X \\ 0 & -I_m \end{pmatrix} \begin{pmatrix} I_n & 0 \\ X^\top & -I_m \end{pmatrix}.$$

It suffices to show that the spectrum of $DAD^\top (DA^\top D^\top)^{-1}$ is contained in $\mathbf{R}_{>0}$. Therefore, the result follows from Proposition 3.3 (a), since for any eigenvalue λ of the matrix product $DAD^\top (DA^\top D^\top)^{-1}$, $-2 + \lambda + \lambda^{-1}$ is a non-negative real number.

Case (b): the Seifert matrices are definite of the same sign. As before, we assume positivity. It is directly checked that

$$DAD^\top (DA^\top D^\top)^{-1} = \begin{pmatrix} I_n & X \\ 0 & I_m \end{pmatrix} \begin{pmatrix} I_n & 0 \\ -X^\top & I_m \end{pmatrix}.$$

It suffices to show that the spectrum of $DAD^\top (DA^\top D^\top)^{-1}$ is contained in $\mathbf{R}_{<0} \cup \mathbf{S}^1$. This follows directly from Proposition 3.3 (b), since for any eigenvalue λ of the matrix product $DAD^\top (DA^\top D^\top)^{-1}$, $2 - \lambda - \lambda^{-1}$ is a non-negative real number. □

2. Log-concavity of the Conway polynomial

Newton's inequalities state that for the elementary symmetric functions s_k in the n real numbers $a_1, \ldots, a_n$,

$$\frac{s_k^2}{\binom{n}{k}^2} \geq \frac{s_{k-1}}{\binom{n}{k-1}} \frac{s_{k+1}}{\binom{n}{k+1}}$$

holds, see, for example, [**73**]. In particular, for the coefficients s_k of a polynomial with only real roots $a_1, \ldots, a_n \in \mathbf{R}$, we have

$$s_k^2 > s_{k-1} s_{k+1},$$

for $k = 1, \ldots, n-1$. We say the coefficient sequence of the polynomial is *strictly log-concave*. As is done in [**30, 31**] for the subclasses considered, Theorem 5.4 and Newton's inequalities allow us to directly deduce that the Alexander polynomial of a boundary link of a Murasugi sum of two Seifert surfaces with symmetric, definite Seifert forms of opposite sign has strictly log-concave coefficient sequence. However, Theorem 5.4 also allows us to deduce strict log-concavity of the coefficient sequence for the Conway polynomial $\nabla_L(t)$ in the case of positive Seifert forms.

Corollary 5.5. *Let L be the boundary of a Murasugi sum of two Seifert surfaces Σ_1 and $\Sigma_2 \subset \mathbf{S}^3$ with symmetric, positive definite Seifert forms. Then $\nabla_L(t) = t^k q(t^2)$, where $q(t)$ is a polynomial with positive and strictly log-concave coefficient sequence.*

Proof of Corollary 5.5. Let L be the boundary of a Murasugi sum of two Seifert surfaces with symmetric, positive definite Seifert forms. The Conway polynomial $\nabla_L(t)$ of a link L is related to the Alexander polynomial $\Delta_L(t)$ by

$$\Delta_L(t^2) = \nabla_L(t - t^{-1}),$$

see, for example, [**15**]. Thus, the Conway polynomial of L has only purely imaginary roots, since the roots of the Alexander polynomial are contained in $\mathbf{R}_{<0} \cup \mathbf{S}^1$. As a polynomial with only imaginary roots, the Conway polynomial of L is of the form

$$\nabla_L(t) = t^k(t^2 + a_1) \cdots (t^2 + a_l) = t^k q(t^2),$$

with all numbers a_i real and strictly positive. In particular, the coefficient sequence of the polynomial $q(t)$ is positive and furthermore strictly log-concave by Newton's inequalities. □

3. Monotonicity of the signature function

Recall from Chapter 2 that the signature function of a link assigns to each number $t \in [0, 1]$ the signature $\sigma_\omega(L)$ of the hermitian matrix

$$S_\omega = (1 - \omega)A + (1 - \overline{\omega})A^\top,$$

where A is a Seifert matrix for L and $\omega = e^{i\pi t} \in \mathbf{S}^1$. Gilmer and Livingston show that the Alexander polynomial of L has at least $\sigma_{-1}(L) + \mathrm{null}_{-1}(L)$ zeroes on the unit circle [**27**], where $\mathrm{null}_\omega(L)$ is the nullity of S_ω. For the Murasugi sum of two Seifert

surfaces with symmetric, positive definite Seifert form, Proposition 5.6 shows that this is in fact a sharp result.

PROPOSITION 5.6. *Let L be the boundary of a Murasugi sum of two Seifert surfaces Σ_1 and $\Sigma_2 \subset \mathbf{S}^3$ with symmetric, positive definite Seifert forms. For $\omega \neq 1 \in \mathbf{S}^1$, the number of zeroes of $\Delta_L(t)$ on $\mathbf{S}^1$ with real part at least $Re(\omega)$ equals $\sigma_\omega(L) + \mathrm{null}_\omega(L)$.*

The proof of Proposition 5.6 is similar to the proof of Proposition 3.6 and implicitly contains a slight refinement of Lemma 3.7.

PROOF. Let L be the boundary of a Murasugi sum of two Seifert surfaces Σ_1 and $\Sigma_2 \subset \mathbf{S}^3$ with symmetric, positive definite Seifert matrices B and C, respectively. Define the Seifert matrix A and the matrices D and X as in the proof of Theorem 5.4. For $\omega \neq 1 \in \mathbf{S}^1$, we now calculate $\sigma_\omega(L)$, that is, the signature of the Hermitian matrix $S_\omega = (1-\omega)A + (1-\overline{\omega})A^\top$. It is equal to the signature of the matrix

$$DS_\omega D^\top = \begin{pmatrix} c(\omega)I_n & (1-\omega)X \\ (1-\overline{\omega})X^\top & c(\omega)I_m \end{pmatrix},$$

where $c(\omega) = 2 - 2\mathrm{Re}(\omega)$ is a positive real number. The signature of $DS_\omega D^\top$ is the number of positive eigenvalues of $DS_\omega D^\top$ minus the number of negative eigenvalues of $DS_\omega D^\top$. Equivalently, thinking in terms of eigenvalues of

$$M_\omega = \begin{pmatrix} 0 & (1-\omega)X \\ (1-\overline{\omega})X^\top & 0 \end{pmatrix},$$

it is equal to the number of eigenvalues of M_ω strictly greater than $-c(\omega)$ minus the number of eigenvalues of M_ω strictly smaller than $-c(\omega)$. The matrix M_ω is hermitian, and if (v, w) is an eigenvector of M_ω with eigenvalue μ, then $(v, -w)$ is an eigenvector of M_ω with eigenvalue $-\mu$. Hence, the spectrum of M_ω is symmetric with respect to the origin. Therefore, the number of eigenvalues of M_ω strictly smaller than $-c(\omega)$ equals the number of eigenvalues of M_ω strictly larger than $c(\omega)$. Thus, the signature of $DS_\omega D^\top$ equals the number of eigenvalues of M_ω that lie in the interval $(-c(\omega), c(\omega)]$. Furthermore, the multiplicity of the eigenvalue of M_ω at $-c(\omega)$ equals the nullity of $DS_\omega D^\top$. In particular, the number of eigenvalues of M_ω that lie in the interval $[-c(\omega), c(\omega)]$ equals $\sigma_\omega(L) + \mathrm{null}_\omega(L)$.

It remains to show that the zeroes of $\Delta_L(t)$ on $\mathbf{S}^1$ with real part at least $\mathrm{Re}(\omega)$ are in one-to-one correspondence with the eigenvalues of M_ω that lie in the interval $[-c(\omega), c(\omega)]$. From the proof of Theorem 5.4 and Proposition 3.3 (b), we know that the zeroes λ_i of $\Delta_L(t)$ are related to the eigenvalues μ_i of the matrix

$$M_0 = \begin{pmatrix} 0 & X \\ X^\top & 0 \end{pmatrix}$$

by the equation $\mu_i^2 = 2 - \lambda_i - \lambda_i^{-1}$. On the other hand, a direct calculation yields $M_\omega^2 = c(\omega)M_0^2$. It follows that the zeroes λ_i of $\Delta_L(t)$ are related to the eigenvalues ρ_i of M_ω by the equation

$$\rho_i^2 = c(\omega)(2 - \lambda_i - \lambda_i^{-1}).$$

Thus, the eigenvalues ρ_i of M_ω that lie in the interval $[-c(\omega), c(\omega)]$ are in one-to-one correspondence with zeroes λ_i of $\Delta_L(t)$ such that $2-\lambda_i-\lambda_i^{-1} \leq c(\omega) = 2-2\mathrm{Re}(\omega) > 0$. This is exactly the case for the zeroes of $\Delta_L(t)$ on $\mathbf{S}^1$ with real part at least $\mathrm{Re}(\omega)$. □

With Proposition 5.6 established, we are ready to prove monotonicity of the signature function for the Murasugi sum of two Seifert surfaces with symmetric, positive definite Seifert form.

Proof of Theorem 5.1. If we restrict the signature function to the $\omega \in \mathbf{S}^1$ for which

$$\mathrm{null}_\omega(L) = 0,$$

the statement follows directly from Proposition 5.6, since the number of zeroes of $\Delta_L(t)$ on $\mathbf{S}^1$ of real part at least $\mathrm{Re}(\omega)$ can only increase when decreasing $\mathrm{Re}(\omega)$. In order to extend the result to the whole signature function, including the (finitely many) $\omega \in \mathbf{S}^1$ for which

$$\mathrm{null}_\omega(L) > 0,$$

we again use Proposition 5.6 and obtain that the jump of the signature function at ω equals the number of zeroes of $\Delta_L(t)$ on $\mathbf{S}^1$ with real part exactly $\mathrm{Re}(\omega)$. By Lemma 2.18, the number of zeroes of $\Delta_L(t)$ on $\mathbf{S}^1$ with real part exactly $\mathrm{Re}(\omega)$ is greater than or equal to two times the nullity $\mathrm{null}_\omega(L)$. On the other hand, two times the nullity $\mathrm{null}_\omega(L)$ is clearly an upper bound for the signature jump at ω, which we know to equal the the number zeroes of $\Delta_L(t)$ on $\mathbf{S}^1$ with real part exactly $\mathrm{Re}(\omega)$. Using Proposition 5.6 again, we obtain that at its (finitely many) jumping points, the signature function evaluates to the mean of the values before and after the jump. □

Remark 5.7. A slightly different way to prove monotonicity of the signature function is the following. First, show that the number of zeroes of the Alexander polynomial on the unit circle equals the signature plus the nullity of the link, as for the special case $\omega = -1$ in Proposition 5.6. Then, using that the signature function can only jump at zeroes of the Alexander polynomial and only by at most twice the order of the zero, one can show that every signature jump is positive.

4. The signature of positive arborescent Hopf plumbings

The goal of this section is to prove that the signature of a positive arborescent Hopf plumbing is greater than or equal to two thirds of the first Betti number.

Let Γ be a finite plane tree. Recall from Chapter 2 that a matrix S for the symmetrised Seifert form of the corresponding positive Hopf plumbing with core curves α_i is given by $S_{ii} = 2$ for all i and $S_{ij} = 1$ if and only if α_i and α_j intersect, otherwise $S_{ij} = 0$. In other words, $S = 2I + A(\Gamma)$, where $A(\Gamma)$ is the adjacency matrix of Γ. In order to prove Theorem 5.2, we use Lemma 5.8, which, roughly speaking, gives a way of decomposing any tree into pieces on which the Seifert form is positive definite. We always identify the plane tree Γ with its associated positive Hopf plumbing. When we write $\sigma(\Gamma)$ or $b_1(\Gamma)$, we mean the signature or the first Betti number, respectively, of

the associated positive Hopf plumbing. For example, $b_1(\Gamma)$ is equal to the number of vertices of Γ.

LEMMA 5.8. *Any tree Γ with at least six vertices has a subtree $\Gamma_0 \subset \Gamma$ with at least six vertices such that*

$$\sigma(\Gamma) \geq \sigma(\Gamma - \Gamma_0) + b_1(\Gamma_0) - 2.$$

PROOF OF THEOREM 5.2. Let Γ be a finite plane tree. The idea is to apply Lemma 5.8 first to Γ, then to some tree of the forest $\Gamma - \Gamma_0$, and so on. We apply Lemma 5.8 as often as possible, say r times, until the remaining forest does not have a tree with six or more vertices. Let $\Gamma_{0,i}$ be the subtree we obtain by the i-th use of Lemma 5.8 and define the forest $\Gamma_{1,i} = \Gamma_{1,i-1} - \Gamma_{0,i}$ recursively, where $\Gamma_{0,1} = \Gamma_0$ and $\Gamma_{1,0} = \Gamma$. By Lemma 5.8, we get

$$\sigma(\Gamma) \geq \sigma(\Gamma_{1,1}) + (b_1(\Gamma_{0,1}) - 2) \geq ... \geq \sigma(\Gamma_{1,r}) + \sum_{i=1}^{r}(b_1(\Gamma_{0,i}) - 2).$$

It is directly checked that for any tree Γ with at most five vertices, either $\sigma(\Gamma) = b_1(\Gamma)$ or $\sigma(\Gamma) = 4$. Since $\Gamma_{1,r}$ is a forest consisting only of trees with at most five vertices, we get that $\sigma(\Gamma_{1,r}) \geq \frac{4}{5}b_1(\Gamma_{1,r}) \geq \frac{2}{3}b_1(\Gamma_{1,r})$. Furthermore, since $b_1(\Gamma_{0,i}) \geq 6$, we have that $b_1(\Gamma_{0,i}) - 2 \geq \frac{2}{3}b_1(\Gamma_{0,i})$. This yields

$$\sigma(\Gamma_{1,r}) + \sum_{i=1}^{r}(b_1(\Gamma_{0,i}) - 2) \geq \frac{2}{3}\left(b_1(\Gamma_{1,r}) + \sum_{i=1}^{r} b_1(\Gamma_{0,i})\right) = \frac{2}{3}b_1(\Gamma).$$

Piecing all the inequalities together, we get that the signature $\sigma(\Gamma)$ is at least two thirds of the first Betti number $b_1(\Gamma)$, as desired. □

PROOF OF LEMMA 5.8. Let Γ be a tree with at least six vertices. We choose a root for Γ and orient all the edges away from the root. Let v be a vertex that is outermost among the vertices of degree at least three. Every edge pointing away from v defines a subtree of Γ with only vertices of degree at most two: the maximal subtree containing the edge and v but no other edge adjacent to v. Let $n = \deg(v) - 1$ denote the number of such subtrees. Furthermore, let k be the number of vertices outside (that is, further away from the root) of v, let v' be the vertex which is adjacent to v but closer to the root and define v'' and v''' analogously to v', see Figure 5.1.

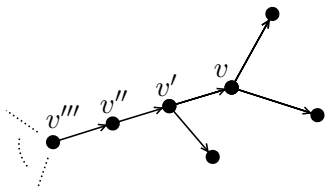

FIGURE 5.1.

Case 1: $k \geq 5$. Let Γ_0 be the union of the n subtrees specified above. Since on $\Gamma_0 - v$, the Seifert form is positive definite, the statement holds.

Case 2: $k = 4, n \leq 3$. Let Γ_0 be as in Case 1, but add the vertex v' and the corresponding edge. Since on $\Gamma_0 - v'$, the Seifert form is positive definite, the statement holds. Note that in this case, $\Gamma - \Gamma_0$ need not be connected.

Case 3: $k = n = 4$. Let Γ_0 be as in Case 2. Since the Seifert form is not positive definite on $\Gamma_0 - v'$, we cannot proceed as in Case 2. The Seifert form of Γ is given by the matrix

$$\left(\begin{array}{ccc|cccccc} \ddots & \vdots & \vdots & \vdots & \vdots & \vdots & \vdots & \vdots & \vdots \\ \cdots & * & * & * & 0 & 0 & 0 & 0 & 0 \\ \cdots & * & 2 & * & 0 & 0 & 0 & 0 & 0 \\ \hline \cdots & * & * & 2 & 1 & 0 & 0 & 0 & 0 \\ \cdots & 0 & 0 & 1 & 2 & 1 & 1 & 1 & 1 \\ \cdots & 0 & 0 & 0 & 1 & 2 & 0 & 0 & 0 \\ \cdots & 0 & 0 & 0 & 1 & 0 & 2 & 0 & 0 \\ \cdots & 0 & 0 & 0 & 1 & 0 & 0 & 2 & 0 \\ \cdots & 0 & 0 & 0 & 1 & 0 & 0 & 0 & 2 \end{array}\right) \sim \left(\begin{array}{ccc|cccccc} \ddots & \vdots & \vdots & \vdots & \vdots & \vdots & \vdots & \vdots & \vdots \\ \cdots & * & * & * & 0 & 0 & 0 & 0 & 0 \\ \cdots & * & 2 & * & 0 & 0 & 0 & 0 & 0 \\ \hline \cdots & * & * & 2 & 1 & 0 & 0 & 0 & 0 \\ \cdots & 0 & 0 & 1 & 0 & 0 & 0 & 0 & 0 \\ \cdots & 0 & 0 & 0 & 0 & 2 & 0 & 0 & 0 \\ \cdots & 0 & 0 & 0 & 0 & 0 & 2 & 0 & 0 \\ \cdots & 0 & 0 & 0 & 0 & 0 & 0 & 2 & 0 \\ \cdots & 0 & 0 & 0 & 0 & 0 & 0 & 0 & 2 \end{array}\right),$$

where the bottom-right block corresponds to the restriction of the Seifert form to Γ_0, the top-left block to the restriction of the the Seifert form to $\Gamma - \Gamma_0$ and $\sim$ denotes a change of basis. By changing basis again, we get that the Seifert form can be expressed by the matrix

$$\left(\begin{array}{ccc|cccccc} \ddots & \vdots & \vdots & \vdots & \vdots & \vdots & \vdots & \vdots & \vdots \\ \cdots & * & * & 0 & 0 & 0 & 0 & 0 & 0 \\ \cdots & * & 2 & 0 & 0 & 0 & 0 & 0 & 0 \\ \hline \cdots & 0 & 0 & 2 & 1 & 0 & 0 & 0 & 0 \\ \cdots & 0 & 0 & 1 & 0 & 0 & 0 & 0 & 0 \\ \cdots & 0 & 0 & 0 & 0 & 2 & 0 & 0 & 0 \\ \cdots & 0 & 0 & 0 & 0 & 0 & 2 & 0 & 0 \\ \cdots & 0 & 0 & 0 & 0 & 0 & 0 & 2 & 0 \\ \cdots & 0 & 0 & 0 & 0 & 0 & 0 & 0 & 2 \end{array}\right) \sim \left(\begin{array}{ccc|cccccc} \ddots & \vdots & \vdots & \vdots & \vdots & \vdots & \vdots & \vdots & \vdots \\ \cdots & * & * & 0 & 0 & 0 & 0 & 0 & 0 \\ \cdots & * & 2 & 0 & 0 & 0 & 0 & 0 & 0 \\ \hline \cdots & 0 & 0 & 2 & 0 & 0 & 0 & 0 & 0 \\ \cdots & 0 & 0 & 0 & -\frac{1}{2} & 0 & 0 & 0 & 0 \\ \cdots & 0 & 0 & 0 & 0 & 2 & 0 & 0 & 0 \\ \cdots & 0 & 0 & 0 & 0 & 0 & 2 & 0 & 0 \\ \cdots & 0 & 0 & 0 & 0 & 0 & 0 & 2 & 0 \\ \cdots & 0 & 0 & 0 & 0 & 0 & 0 & 0 & 2 \end{array}\right).$$

Since the changes of basis we applied never changed the top-left block, we get that $\sigma(\Gamma) = \sigma(\Gamma - \Gamma_0) + 4$.

Case 4: $k = 3$, $n = 2$, $\deg(v') = 2$. Let Γ_0 be as in Case 2 but add the vertex v'' and the corresponding edge. Since on $\Gamma_0 - v''$, the Seifert form is positive definite, the statement holds. Again, $\Gamma - \Gamma_0$ need not be connected.

Case 5: $k = n = 3$, $\deg(v') = 2$. Let Γ_0 be as in Case 4. This works very similar to Case 3. Writing down a matrix for the Seifert form of Γ with the Seifert form restricted to Γ_0 in the bottom-right block and applying a change of basis, we get that $\sigma(\Gamma) = \sigma(\Gamma - \Gamma_0) + 4$.

Case 6: $k = n = 2$, $\deg(v') = \deg(v'') = 2$. Let Γ_0 be as in Case 4 but add the vertex v''' and the corresponding edge. Since on $\Gamma_0 - v'''$, the Seifert form is positive definite, the statement holds. Again, $\Gamma - \Gamma_0$ need not be connected.

Case 7: none of the other cases apply. If three or four vertices lie outside of v', then let Γ_0 be as in Case 4. Since Case 6 does not apply, at least five vertices lie outside of v''. Since none of the other cases apply, it is easily checked that on $\Gamma_0 - v''$, the Seifert form is positive definite and the statement holds. If at least five vertices lie outside of v', then let Γ_0 be as in Case 2. Again none of the other cases apply, the Seifert form is positive definite on $\Gamma_0 - v'$ and the statement holds. Once more, $\Gamma - \Gamma_0$ need not be connected. □

REMARK 5.9. The optimality of Theorem 5.2 follows directly from Case 5 in the proof of Lemma 5.8. The signature of the link corresponding to the tree dealt with in this case is 4, while its first Betti number is 6. By the reasoning in the proof, glueing such a tree to another tree always adds 4 to the signature and 6 to the first Betti number. Like this, as is depicted in Figure 5.2 for three copies, one always obtains a tree with signature equal to exactly two thirds of the first Betti number. By a result of Baader, Feller, Lewark and the author, $2g_4^{\mathrm{top}} = |\sigma|$ holds for these examples [**7**]. Furthermore, they maximise the ratio of genus defect and first Betti number among positive arborescent Hopf plumbings [**7**].

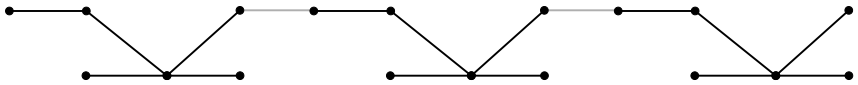

FIGURE 5.2. A positive arborescent Hopf plumbing with $2g_4^{\mathrm{top}} = |\sigma|$. This figure is taken from [**7**].

CHAPTER 6

Positive braid knots of maximal topological 4-genus

In this and the following chapter, we turn our focus to positive braid knots. More specifically, we study their *topological 4-genus* g_4^{top}, that is, the minimal genus among surfaces which are properly, locally-flatly embedded in the 4-ball and have a given knot K as boundary. We contrast the topological 4-genus both to the smooth 4-genus (where the embedding is required to be smooth) and the ordinary Seifert genus g. For a knot, we call the difference $g - g_4^{\text{top}}$ of ordinary genus and topological 4-genus the *genus defect*. The rest of this chapter stays very close to the author's original article [**40**].

The smooth 4-genus of a torus knot equals the ordinary genus g by a theorem of Kronheimer and Mrowka [**35**]. By work of Rudolph, this equality extends to the more general class of links bounding quasipositive surfaces, in particular to positive braid knots [**59**]. However, the story is very different for the topological 4-genus g_4^{top}. A first example is due to Rudolph [**58**]: for the torus knot $T(5,6)$, the inequality $g_4^{\text{top}} < g$ holds. More recently, a large proportional difference $g - g_4^{\text{top}}$ with respect to g was found for all torus knots with non-maximal signature σ by Baader, Feller, Lewark and the author [**7**]. On the other hand, there exists a lower bound, due to Kauffman and Taylor, for the topological 4-genus of knots: $2g_4^{\text{top}}(K) \geq |\sigma(K)|$ holds for any knot K [**33**]. We show that for positive braid knots, this bound is in fact the only obstruction to non-maximal topological 4-genus, that is, $g_4^{\text{top}} < g$.

THEOREM 6.1. *For a positive braid knot K, the equality $g_4^{\text{top}}(K) = g(K)$ holds exactly if $|\sigma(K)| = 2g(K)$.*

Combining this result with Baader's classification of prime positive braid links of maximal signature [**3**], we immediately get a full description of all prime positive braid knots of maximal topological 4-genus: they are exactly the torus knots of maximal signature.

COROLLARY 6.2. *The torus knots $T(2,n)$, $T(3,4)$ and $T(3,5)$ are the only prime positive braid knots K with $g_4^{\text{top}}(K) = g(K)$.*

Our proof of Theorem 6.1 uses two main ingredients. The first one is a homological criterion from [**7**] using Freedman's disc theorem [**24**], allowing us to conclude $g_4^{\text{top}} < g$ for certain positive braids. The second one is that genus defect $g - g_4^{\text{top}}$ is inherited from *surface minors*, that is, incompressible subsurfaces. Similar to Baader's four surface minors T, E, X and Y obstructing maximal signature for positive braid links, we use enriched versions $\widetilde{T}$, $\widetilde{E}$, $\widetilde{X}$ and $\widetilde{Y}$ to obstruct maximal topological 4-genus for positive braid knots.

Theorem 6.1 also allows us to compute the topological 4-genus for positive braid knots K with $|\sigma(K)| = 2g(K) - 2$. Combining the lower bound of Kauffman and Taylor with $g_4^{\text{top}}(K) < g(K)$ yields the exact result $g_4^{\text{top}}(K) = g(K) - 1$. This suffices to compute the topological 4-genus for prime positive braids knots with up to 12 crossings. Table 6.1 lists all these knots, except for the torus knots $T(2, n)$, $T(3, 4)$ and $T(3, 5)$, which have maximal topological 4-genus.

knot	braid notation	g	$\lvert\sigma\rvert$	g_4^{top}
10_{139}	$\sigma_1^4\sigma_2\sigma_1^3\sigma_2^2$	4	6	3
10_{152}	$\sigma_1^3\sigma_2^2\sigma_1^2\sigma_2^3$	4	6	3
$11n77$	$\sigma_1^2\sigma_2^2\sigma_1\sigma_3\sigma_2^3\sigma_3^2$	4	6	3
$12n242$	$\sigma_1\sigma_2^2\sigma_1^2\sigma_2^7$	5	8	4
$12n472$	$\sigma_1\sigma_2^4\sigma_1^2\sigma_2^5$	5	8	4
$12n574$	$\sigma_1\sigma_2^6\sigma_1^2\sigma_2^3$	5	8	4
$12n679$	$\sigma_1^3\sigma_2^2\sigma_1^2\sigma_2^5$	5	8	4
$12n688$	$\sigma_1^3\sigma_2^4\sigma_1^2\sigma_2^3$	5	8	4
$12n725$	$\sigma_1\sigma_2^2\sigma_1^4\sigma_2^5$	5	8	4
$12n888$	$\sigma_1^3\sigma_2^3\sigma_1^3\sigma_2^3$	5	8	4

TABLE 6.1. Small positive braid knots.

This list is created with the help of the software Knotinfo [**34**]. Previously, the values of the topological 4-genus for all these examples except 10_{152} were marked as unknown. However, these values can also be deduced from work of Borodzik and Friedl on the algebraic unknotting number [**13**].

1. Positive braid knots

We start by recalling the important concepts around positive braid knots, some of them already introduced in Chapter 2. A *positive braid knot* is a knot that can be obtained from a positive braid via the closure operation, an important example being torus knots. A *positive braid on* $n + 1$ *strands* is a finite word in positive powers of the braid generators $\sigma_1, \dots, \sigma_n$. By a theorem of Stallings, positive braid knots are fibred with the standard Seifert surface as fibre [**63**]. As Baader did in [**3**], we use *brick diagrams* to visualise the fibre surface of positive braid knots: each horizontal bar corresponds to a braid generator σ_i and each *brick*, that is, each rectangle, corresponds to a positive Hopf band in the plumbing construction of the fibre surface. If two bricks link, it means that the core curves of the corresponding positive Hopf bands intersect once, see Figure 6.1. Let the *linking pattern* be the plane graph obtained by putting a vertex into every brick and an edge between two vertices exactly if the corresponding bricks link. It can be easily seen that if the linking pattern of a positive braid β is not connected, then the positive braid link $\widehat{\beta}$ is not prime. In fact, the converse is also true since positive braids are visually prime by a theorem of Cromwell [**16**].

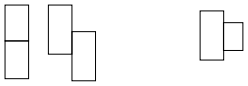

FIGURE 6.1. Bricks that link (on the left) and bricks that do not link (on the right).The two examples on the left yield the trefoil knot, while the example on the right yields a connected sum of two Hopf bands.

2. Trees

Let us for a moment consider the case where the linking pattern is a tree. There are many brick diagrams that yield the same tree as linking pattern. Since closures of positive braids corresponding to different brick diagrams might be equivalent as links in $\mathbf{R}^3$, it is natural to ask whether the plane tree of the linking pattern uniquely determines the positive braid link up to ambient isotopy. As we see in the following remark, this is almost the case.

REMARK 6.3. The fibre surface $\Sigma(\beta)$ of a positive braid β retracts to its brick diagram. Since for a successive plumbing of positive Hopf bands, the monodromy is conjugate to the product (in the succession of plumbing) of positive Dehn twists along the core curves of the Hopf bands [**63**], the conjugacy class of the monodromy is completely determined by the plane tree given by the linking pattern of the brick diagram, together with the algebraic intersections of the core curves. Therefore, also the corresponding fibred link $\widehat{\beta}$ is determined by this data. Indeed, the conjugacy class of the monodromy determines a fibration of the link exterior up to homeomorphism. Furthermore, it fixes the boundary of the fibre $\Sigma(\beta)$ pointwise and the fibredness condition for links dictates how to glue solid tori along the boundary of the fibred mapping torus to obtain $\mathbf{S}^3$ containing a copy of the link $\widehat{\beta}$, see also Proposition 2.9. Note that in general, the information on the algebraic intersection of the core curves is necessary to determine the positive braid link, see [**10**].

Furthermore, if the linking pattern is a tree, a matrix for the Seifert form of the corresponding fibre surface $\Sigma = \Sigma(\beta)$ is, up to a change of basis, independent of the algebraic intersection of the core curves, and hence particularly easy to describe: as a basis of $H_1(\Sigma; \mathbf{Z})$ take the core curves $[\alpha_i]$ of the positive Hopf bands corresponding to the bricks. A matrix A for the Seifert form is then given by $A_{ii} = 1$ and $A_{ij} = 1$ if $i < j$ and the curves α_i and α_j intersect (that is, if the corresponding vertices of the linking pattern are connected by an edge). All other entries are equal to zero.

EXAMPLE 6.4. Let $\widetilde{T}$, $\widetilde{E}$, $\widetilde{X}$ and $\widetilde{Y}$ be the canonical fibre surfaces

$$\begin{aligned}
\widetilde{T} &= \Sigma(\sigma_1^5\sigma_2\sigma_1^4\sigma_2),\\
\widetilde{E} &= \Sigma(\sigma_1^7\sigma_2\sigma_1^3\sigma_2),\\
\widetilde{X} &= \Sigma(\sigma_1^2\sigma_2^2\sigma_1\sigma_3\sigma_2^2\sigma_3),\\
\widetilde{Y} &= \Sigma(\sigma_1^4\sigma_2^2\sigma_1^3\sigma_2),
\end{aligned}$$

see Figure 6.2 for the corresponding brick diagrams and the linking patterns. By exhibiting a two-dimensional subspace B of $H_1(\widetilde{X};\mathbf{Z})$ which is *Alexander-trivial*, that is,

$$\det(A|_{B\times B} - t(A|_{B\times B})^\top) \in \mathbf{Z}[t^{\pm 1}]$$

is a unit for some matrix A of the Seifert form, it is shown in [**7**] that the three-component link $\partial\widetilde{X}$ does not have maximal topological 4-genus, compare with Proposition 2.23. More precisely, it is shown that the topological 4-genus equals one while the ordinary genus equals two. In this example, we carry out the same computation for $\partial\widetilde{T}$, $\partial\widetilde{E}$ and $\partial\widetilde{Y}$. For reasons of self-containedness, we also repeat the computation for $\partial\widetilde{X}$. Number the vertices of the linking patterns in Figure 6.2 from top to bottom (and from left to right if several vertices are on the same level, as indicated for $\widetilde{T}$ in Figure 6.2). As a basis for the first homology, take the core curves of the corresponding

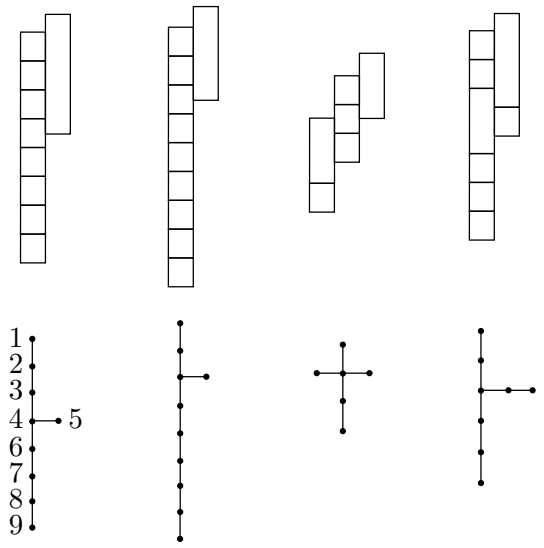

FIGURE 6.2. Brick diagrams for $\widetilde{T}$, $\widetilde{E}$, $\widetilde{X}$ and $\widetilde{Y}$ and the corresponding linking patterns. The versions for T, E, X and Y are obtained by deleting the lowest brick or vertex, respectively.

Hopf bands with the chosen numbering. In this basis, consider the subspaces

$$\begin{aligned}
B_{\widetilde{T}} &= \langle(-1,2,-3,4,-2,-3,2,-1,1)^\top,\ e_8\rangle,\\
B_{\widetilde{E}} &= \langle(2,-4,6,-3,-5,4,-3,2,-1,1)^\top,\ e_9\rangle,\\
B_{\widetilde{X}} &= \langle(-1,-1,2,-1,-1,0)^\top,\ e_6\rangle,\\
B_{\widetilde{Y}} &= \langle(1,-2,3,-2,1,-2,1,-1)^\top,\ e_7\rangle
\end{aligned}$$

of $H_1(\widetilde{T};\mathbf{Z})$, $H_1(\widetilde{E};\mathbf{Z})$, $H_1(\widetilde{X};\mathbf{Z})$ and $H_1(\widetilde{Y};\mathbf{Z})$, respectively. Using the matrix A of the Seifert form described above, it is a straightforward computation to see that in all four cases, the given subspaces are Alexander-trivial. For example, writing v for the first basis vector of $B_{\widetilde{T}}$ and $A_{\widetilde{T}}$ for the matrix of the Seifert form corresponding to $\widetilde{T}$

described above, one obtains

$$v^\top A_{\widetilde{T}} v = 0,\ v^\top A_{\widetilde{T}} e_8 = 1,$$
$$e_8^\top A_{\widetilde{T}} v = 0,\ e_8^\top A_{\widetilde{T}} e_8 = 1,$$

or, equivalently,

$$A_{\widetilde{T}}|_{B_{\widetilde{T}}\times B_{\widetilde{T}}} = \begin{pmatrix} 0 & 1 \\ 0 & 1 \end{pmatrix}.$$

Consequently, $\det(A_{\widetilde{T}}|_{B_{\widetilde{T}}\times B_{\widetilde{T}}} - t(A_{\widetilde{T}}|_{B_{\widetilde{T}}\times B})^\top) = t$ is a unit in $\mathbf{Z}[t^{\pm 1}]$. The computation for the other cases works analogously. Proposition 2.23 now implies non-maximality of the topological 4-genus. Since the signature does not allow for a genus defect $g - g_4^{\text{top}}$ greater than one, we conclude

$$g_4^{\text{top}}(\partial\widetilde{T}) = g(\partial\widetilde{T}) - 1 = 3,$$
$$g_4^{\text{top}}(\partial\widetilde{E}) = g(\partial\widetilde{E}) - 1 = 4,$$
$$g_4^{\text{top}}(\partial\widetilde{X}) = g(\partial\widetilde{X}) - 1 = 1,$$
$$g_4^{\text{top}}(\partial\widetilde{Y}) = g(\partial\widetilde{Y}) - 1 = 3.$$

In order to detect genus defect for a positive braid knot $\widehat{\beta}$, we search for minors $\widetilde{T}, \widetilde{E}, \widetilde{X}$ or $\widetilde{Y}$ in the fibre surface $\Sigma(\beta)$. This is always based on the fact that the linking pattern of β contains the tree corresponding to $\widetilde{T}, \widetilde{E}, \widetilde{X}$ or $\widetilde{Y}$ via deleting vertices and contracting edges. One can then see that also $\Sigma(\beta)$ contains $\widetilde{T}, \widetilde{E}, \widetilde{X}$ or $\widetilde{Y}$, respectively, as a surface minor, implying $g_4^{\text{top}}(\widehat{\beta}) < g(\widehat{\beta})$. For example, Figure 6.3 shows how the tree corresponding to $\widetilde{X}$ is contained in the linking pattern of the positive braid $\sigma_1^2\sigma_2^3\sigma_1^2\sigma_2^2$.

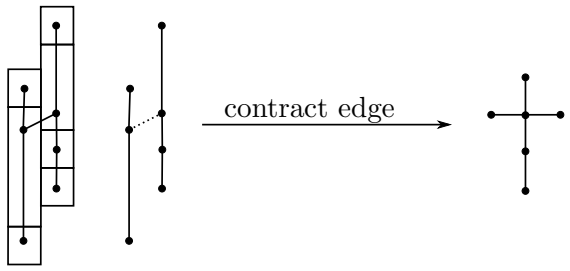

FIGURE 6.3. Contracting an edge of the linking pattern of $\sigma_1^2\sigma_2^3\sigma_1^2\sigma_2^2$ yields the tree corresponding to $\widetilde{X}$.

3. Maximal topological 4-genus for trees

Before we prove it for the case of positive braid knots, we show an analogue of Theorem 6.1 for knots obtained as *positive arborescent Hopf plumbing*. This notion generalises knots corresponding to brick diagrams having some plane tree as linking pattern. Starting from any finite plane tree Γ, we plumb positive Hopf bands (which are in one-to-one correspondence with the vertices of the tree) such that their core

curves intersect once exactly if the corresponding vertices of Γ are connected by an edge. Otherwise, they do not intersect. Furthermore, they respect the circular ordering of the vertices given by the plane tree structure of Γ. This construction is strictly more general than positive braid knots with a plane tree as linking pattern: vertices of a tree can have arbitrary valency, while for linking patterns associated with positive braid knots, this valency is bounded from above by 6.

PROPOSITION 6.5. *For a knot K obtained by positive arborescent Hopf plumbing, the equality $g_4^{\mathrm{top}}(K) = g(K)$ holds exactly if $|\sigma(K)| = 2g(K)$.*

PROOF. If $|\sigma(K)| = 2g(K)$, then $g_4^{\mathrm{top}}(K) = g(K)$ follows from the signature bound of Kauffman and Taylor [**33**]. If $|\sigma(K)| < 2g(K)$, we distinguish three different cases. If Γ has at least three vertices of degree at least three, then the corresponding fibre surface contains $\widetilde{X}$ as a minor and thus $g_4^{\mathrm{top}}(K) < g(K)$. If Γ has two vertices of degree at least three, then at least one of the leaves has distance at least two from the closest vertex of degree at least three, since otherwise K cannot be a knot. Again the corresponding fibre surface contains $\widetilde{X}$ as a minor, since Γ contains the tree corresponding to $\widetilde{X}$ via deleting vertices and contracting edges. If Γ has only one vertex of degree at least three, then $|\sigma(K)| < 2g(K)$ holds if and only if Γ contains the linking pattern of T, E, X or Y as an induced subgraph. This can be calculated directly from the associated Seifert forms. Alternatively, it also follows from Baader's classification of positive braid links of maximal signature [**3**]. Again, for K to be a knot, Γ cannot be equal to T, E, X or Y. It follows that Γ in fact contains the linking pattern of $\widetilde{T}, \widetilde{E}, \widetilde{X}$ or $\widetilde{Y}$ as an induced subgraph. Hence, the corresponding fibre surface contains $\widetilde{T}, \widetilde{E}, \widetilde{X}$ or $\widetilde{Y}$ as a surface minor. □

4. Maximal topological 4-genus for positive braid knots

The proof of Theorem 6.1 for positive braid knots K is divided into two parts, depending on the *positive braid index* of K, that is, the minimal number of strands of a positive braid β representing the knot K. For K of positive braid index at most three, we can essentially reduce the problem to Proposition 6.5. For K of positive braid index at least four, we show that the strict inequality $g_4^{\mathrm{top}}(K) < g(K)$ always holds.

PROPOSITION 6.6. *For a knot K obtained as the closure of a positive braid β on three strands, $g_4^{\mathrm{top}}(K) = g(K)$ holds exactly if $|\sigma(K)| = 2g(K)$.*

PROOF. We assume to have applied all possible braid relations $\sigma_1\sigma_2\sigma_1 \to \sigma_2\sigma_1\sigma_2$ to the braid β, so, up to cyclic permutation, β can be assumed to be of the form $\sigma_1^{a_1}\sigma_2^{b_1}\cdots\sigma_1^{a_m}\sigma_2^{b_m}$, where $a_i > 0$ and $b_i \geq 2$. If $m \leq 2$, the linking pattern of the braid is a plane tree and we are done by Proposition 6.5. We now show that in the other cases we already have $g_4^{\mathrm{top}}(\widehat{\beta}) < g(\widehat{\beta})$. For this, let $m > 2$ and remark that at least one of the b_i has to be odd and hence at least three, otherwise the permutation given by the braid leaves the third strand invariant and $\widehat{\beta}$ is not a knot.

Case 1: $m \geq 4$. Up to cyclic permutation, the braid β contains the word $\sigma_1^2\sigma_2^3\sigma_1^2\sigma_2^2$ as a *subword*, that is, via reducing powers of occurrences of generators, and thus the fibre surface of $\widehat{\beta}$ contains $\widetilde{X}$ as a minor, implying $g_4^{\text{top}}(\widehat{\beta}) < g(\widehat{\beta})$.

Case 2: $m = 3$, $a_i = 1$. If, up to cyclic permutation, (b_1, b_2, b_3) equals $(2, 2, 3)$, the Seifert form of $\widehat{\beta}$ is positive definite. If (b_1, b_2, b_3) equals $(2, 3, 3)$ or $(3, 3, 3)$, the second strand is left invariant by the permutation given by the braid, so we can assume that one of the b_i is at least four. Furthermore, since one of the b_i has to be odd, (b_1, b_2, b_3) can be assumed to be at least $(2, 3, 4)$ or $(5, 2, 2)$ with respect to the product order. In both cases, β contains the word $\sigma_1\sigma_2^5\sigma_1\sigma_2^4$ as a subword and thus the fibre surface of $\widehat{\beta}$ contains $\widetilde{T}$ as a minor, implying $g_4^{\text{top}}(\widehat{\beta}) < g(\widehat{\beta})$.

Case 3: $m = 3$, at least one $a_i \geq 2$. As before, one of the b_i has to be at least three, say b_1. If a_1 or a_2 is at least two, then β contains, up to cyclic permutation, $\sigma_1^2\sigma_2^3\sigma_1^2\sigma_2^2$ as a subword and thus the fibre surface of $\widehat{\beta}$ contains $\widetilde{X}$ as a minor. Now assume $a_1 = a_2 = 1$ and $a_3 \geq 2$. We also assume $b_2 = b_3 = 2$, otherwise we are, up to cyclic permutation, in the case we already dealt with. Note that the permutation given by a braid of the form $\sigma_1\sigma_2^{b_1}\sigma_1\sigma_2^2\sigma_1^2\sigma_2^2$ leaves the second strand invariant, so a_3 needs to be at least three in order for $\widehat{\beta}$ to be a knot. Now, up to cyclic permutation, β must contain the word $\sigma_2^5\sigma_1\sigma_2^2\sigma_1^3$ and the fibre surface of $\widehat{\beta}$ contains $\widetilde{T}$ as a minor, implying $g_4^{\text{top}}(\widehat{\beta}) < g(\widehat{\beta})$. □

The following lemma gives a condition under which a positive braid β cannot be of *minimal positive braid index*, that is, does not realise the positive braid index of its closure $\widehat{\beta}$.

LEMMA 6.7. *Let β be a positive braid on at least three strands. If for some i the linking pattern of the subword of β induced by the generators σ_i and σ_{i+1} is a path, then β is not of minimal positive braid index.*

PROOF. We can assume the subword of β induced by the generators σ_i and σ_{i+1} to be $\sigma_i^k\sigma_{i+1}\sigma_i\sigma_{i+1}^l$, for some positive numbers k and l. This can be achieved by cyclic permutation and possibly reversing the order of the word β, operations that do not change the associated unoriented fibre surface. Similarly, we can assume that all occurrences of generators with index smaller than i take place before the last occurrence of σ_i and, likewise, all occurrences of generators with index greater than $i+1$ take place after the first occurrence of σ_{i+1}. The situation is schematically depicted in Figure 6.4 on the left. The strand depicted in thick red passes below the two strands it crosses. Thus, the closure of β is isotopic to the closure of the braid depicted schematically in Figure 6.4 on the right. However, this braid has one strand less than β. □

PROPOSITION 6.8. *If K is a prime knot obtained as the closure of a positive braid β of minimal positive braid index ≥ 4, then $g_4^{\text{top}}(K) < g(K)$.*

PROOF. Let β be a positive braid of minimal positive braid index ≥ 4 whose closure $\widehat{\beta}$ is a prime knot. We assume to have applied all possible braid relations $\sigma_i\sigma_{i+1}\sigma_i \to \sigma_{i+1}\sigma_i\sigma_{i+1}$ to β. This process terminates: it increases the sum of all

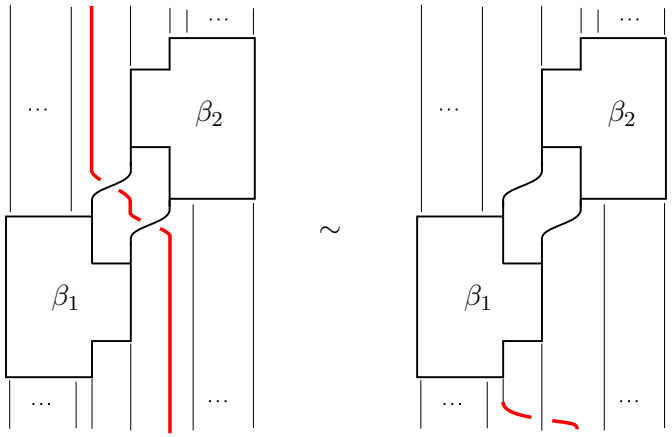

FIGURE 6.4.

indices of generators (counted with multiplicity) while not changing the number of generators. In other words, the crossings of β are as far to the right as possible. We can furthermore assume that β still contains, up to cyclic permutation, the subword $\sigma_1\sigma_2^2\sigma_1\sigma_2^2$, since otherwise β would not be of minimal positive braid index.

We first delete, without disconnecting the linking pattern, a minimal amount of occurrences of σ_2 so that the induced subword of β in the first two generators is, after a possible cyclic permutation, of the form $\sigma_1^{a_1}\sigma_2^{b_1}\sigma_1^{a_2}\sigma_2^{b_2}$, where b_1 and b_2 are greater than or equal to two. For example, if the induced subword of β in the first two generators is $\sigma_1\sigma_2^2\sigma_1\sigma_2^2\sigma_1\sigma_2^2$, we delete one occurrence of σ_2 (to the power two), yielding, after a possible cyclic permutation, $\sigma_1\sigma_2^2\sigma_1^2\sigma_2^2$. Note that in case $a_1 = a_2 = 1$, no generators σ_2 have to be deleted to achieve the desired form.

Case 1: $a_1 = a_2 = 1$, $b_1 = b_2 = 2$. In this case, we did not have to delete any occurrence of σ_2 and the induced subword of β in the first two generators is exactly $\sigma_1\sigma_2^2\sigma_1\sigma_2^2$. Both occurrences of σ_2 have to be split by an occurrence of σ_3, since otherwise the permutation given by β would leave the first or second strand invariant, see Figure 6.5. Furthermore, these occurrences have to be to the power at least two, since we ruled out the possibility of a braid relation $\sigma_2\sigma_3\sigma_2 \to \sigma_3\sigma_2\sigma_3$. If one of the occurrences of σ_3 is to some power at least three, β contains, up to cyclic permutation, the subword $\sigma_2^2\sigma_3^3\sigma_2^2\sigma_3^2$ and thus the fibre surface of $\widehat{\beta}$ contains the minor $\widetilde{X}$, implying $g_4^{\text{top}}(\widehat{\beta}) < g(\widehat{\beta})$. If the power of both occurrences of σ_3 is equal to two, we repeat the same argument, increasing the index by one: both occurrences of σ_3 have to be split by an occurrence of σ_4, otherwise the permutation given by β would leave the first or second strand invariant. As before, we distinguish cases depending on the powers of the occurrences of σ_4. We repeat this argument and case distinction with increasing index as long as necessary. Eventually, some splitting occurrence has to be of power at least three and β contains, up to cyclic permutation, the subword $\sigma_i^2\sigma_{i+1}^3\sigma_i^2\sigma_{i+1}^2$.

Case 2: $a_1 = a_2 = 1$, $b_1 \geq 3$, $b_2 = 2$. In this case, we did not have to delete any occurrence of σ_2 and the induced subword of β in the first two generators is exactly

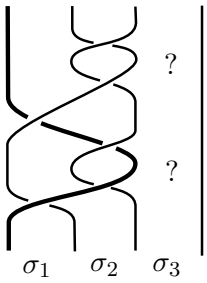

FIGURE 6.5. If no occurrence of σ_3 splits the first (second) occurrence of σ_2, the first (second) strand is left invariant by the permutation defined by β.

$\sigma_1\sigma_2^{b_1}\sigma_1\sigma_2^2$. As in Case 1, the second occurrence of σ_2 has to be split by an occurrence of σ_3 (otherwise the permutation given by β would leave the second strand invariant), so β must contain a subword of the form $\sigma_1\sigma_2^{b_1}\sigma_1\sigma_2\sigma_3^{c_1}\sigma_2$. Note that c_1 must be greater than or equal to two, since we applied all possible braid relations $\sigma_2\sigma_3\sigma_2 \to \sigma_3\sigma_2\sigma_3$. Figure 6.6 depicts the brick diagram and linking pattern of this subword for $b_1 = 3$ and $c_1 = 2$. Since the linking pattern is not connected, there has to be another occurrence

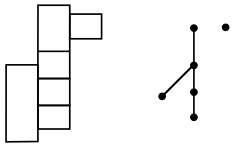

FIGURE 6.6.

of σ_3 in β, otherwise the closure $\widehat{\beta}$ would not be prime. What are the possibilities for the other occurrences of σ_3? If the first occurrence of σ_2 is split by an occurrence of σ_3, again the occurrence of σ_3 has to be to the power at least two. Hence, β contains, up to reversing order and cyclic permutation, the subword $\sigma_2^3\sigma_3^2\sigma_2^2\sigma_3^2$ and the fibre surface of $\widehat{\beta}$ contains the minor $\widetilde{X}$, implying $g_4^{\text{top}}(\widehat{\beta}) < g(\widehat{\beta})$. Similarly, if β contains, up to reversing order and cyclic permutation, the subword $\sigma_1\sigma_2^3\sigma_1\sigma_3\sigma_2^2\sigma_3$, again the fibre surface of $\widehat{\beta}$ contains the minor $\widetilde{X}$, implying $g_4^{\text{top}}(\widehat{\beta}) < g(\widehat{\beta})$. If we exclude these cases, the only two possibilities for the induced subword of β in the first three generators are $\sigma_1\sigma_2^{b_1}\sigma_1\sigma_2\sigma_3^{c_1}\sigma_2\sigma_3^{c_2}$ and $\sigma_1\sigma_2^{b_1}\sigma_1\sigma_3^{c_2}\sigma_2\sigma_3^{c_1}\sigma_2$, which are, up to cyclic permutation, reverse to each other. If c_2 is greater or equal to two, the fibre surface of $\widehat{\beta}$ again contains the minor $\widetilde{X}$, implying $g_4^{\text{top}}(\widehat{\beta}) < g(\widehat{\beta})$, so we assume the induced subword of β in the first three generators to be, up to reversing order and cyclic permutation, $\sigma_1\sigma_2^{b_1}\sigma_1\sigma_2\sigma_3^{c_1}\sigma_2\sigma_3$. But in this case, β restricted to the second and third generator has a path as linking pattern and is not minimal by Lemma 6.7.

Case 3: $a_1 = a_2 = 1$, $b_1, b_2 \geq 3$. The only possibility not considered in Case 2 is the following: β contains, up to cyclic permutation, the subword $\sigma_1\sigma_2^3\sigma_1\sigma_2\sigma_3^2\sigma_2\sigma_3^2\sigma_2$, thus also $\sigma_1\sigma_2^3\sigma_1\sigma_2\sigma_3^2\sigma_2\sigma_3^2$ and the fibre surface of $\widehat{\beta}$ contains $\widetilde{X}$ as a minor, implying $g_4^{\text{top}}(\widehat{\beta}) < g(\widehat{\beta})$. However, when reconsidering our discussion of Case 2, the powers of

σ_2 appearing could be greater, so we get $\sigma_1\sigma_2^{b_1}\sigma_1\sigma_2^{b_2'}\sigma_3^{c_1}\sigma_2^{b_2''}\sigma_3^{c_2}$ as possibilities for the induced subword of β in the first three generators, where $b_2 = b_2' + b_2''$. Again, note that if c_2 or b_2'' is greater than or equal to two, the fibre surface of $\widehat{\beta}$ contains the minor $\widetilde{X}$, implying $g_4^{\text{top}}(\widehat{\beta}) < g(\widehat{\beta})$, so we assume the induced subword of β in the first three generators to be, up to reversing order and cyclic permutation, $\sigma_1\sigma_2^{b_1}\sigma_1\sigma_2^{b_2'}\sigma_3^{c_1}\sigma_2\sigma_3$. Again, β restricted to the second and third generator has a path as linking pattern and is not minimal.

Case 4: $a_1 + a_2 \geq 3$, $b_1 + b_2 \geq 5$. We can apply the same arguments as in the cases above. From this it follows that if the fibre surface of $\widehat{\beta}$ contains no minor $\widetilde{X}$, then the induced subword in the first three generators is, after the described process of deleting some generators σ_2, either $\delta = \sigma_1^{a_1}\sigma_2^{b_1}\sigma_1^{a_2}\sigma_2^{b_2'}\sigma_3^{c_1}\sigma_2^{b_2''}\sigma_3^{c_2}$ or $\mu = \sigma_1^{a_1}\sigma_2^{b_1}\sigma_1^{a_2}\sigma_3^{c_2}\sigma_2^{b_2'}\sigma_3^{c_1}\sigma_2^{b_2''}$. As before, these two words are, up to cyclic permutation, reverse to each other. But since we might have deleted some generators σ_2 to obtain them, we should consider them separately. Again as before, if c_2 or b_2'' is greater than or equal to two, the fibre surface of $\widehat{\beta}$ contains the minor $\widetilde{X}$, implying $g_4^{\text{top}}(\widehat{\beta}) < g(\widehat{\beta})$. If we restrict the subword $\delta = \sigma_1^{a_1}\sigma_2^{b_1}\sigma_1^{a_2}\sigma_2^{b_2'}\sigma_3^{c_1}\sigma_2\sigma_3$ to the second and third generator, the linking pattern is a path. Note that reinserting the deleted generators σ_2 would split $\sigma_1^{a_1}$ or $\sigma_1^{a_2}$. In any case, the linking pattern of β restricted to the second and third generator is still a path and β is not minimal. This does not necessarily hold for the other possible subword $\mu = \sigma_1^{a_1}\sigma_2^{b_1}\sigma_1^{a_2}\sigma_3\sigma_2^{b_2'}\sigma_3^{c_1}\sigma_2$. However, note that if b_2' is greater than or equal to two, then μ contains the subword $\sigma_1\sigma_2^2\sigma_1\sigma_3\sigma_2^2\sigma_3^2$ and the fibre surface of $\widehat{\beta}$ contains the minor $\widetilde{X}$, implying $g_4^{\text{top}}(\widehat{\beta}) < g(\widehat{\beta})$. So we are left with the possibility $\mu = \sigma_1^{a_1}\sigma_2^{b_1}\sigma_1^{a_2}\sigma_3\sigma_2\sigma_3^{c_1}\sigma_2$. If all the deleted occurrences of σ_2 appeared before the first occurrence of σ_3 in μ, after a cyclic permutation the linking pattern of β restricted to the second and third generator again is a path and β is not minimal. If some deleted occurrence of σ_2 appeared after the first occurrence of σ_3 in μ, then β contains the word $\sigma_1\sigma_2^2\sigma_1\sigma_3\sigma_2^2\sigma_3^2$ as a subword and, as before, $g_4^{\text{top}}(\widehat{\beta}) < g(\widehat{\beta})$.

Case 5: $a_1 + a_2 \geq 3$, $b_1 = b_2 = 2$. In this case, there is one last new possibility: as in Case 1, the word $\sigma_2\sigma_3^{c_1}\sigma_2^2\sigma_3^{c_2}\sigma_2$ could be a subword of β (without directly yielding $\sigma_2^3\sigma_3^2\sigma_2^2\sigma_3^2$ as a subword). Since we applied all possible braid relations $\sigma_2\sigma_3\sigma_2 \to \sigma_3\sigma_2\sigma_3$, c_1 and c_2 are greater than or equal to two. If β should, up to cyclic permutation, neither contain $\sigma_2^3\sigma_3^2\sigma_2^2\sigma_3^2$ nor $\sigma_2^2\sigma_3^3\sigma_2^2\sigma_3^2$ as subword, then c_1 and c_2 are both equal to two and the induced subword of β in the first two generators is exactly $\sigma_1^{a_1}\sigma_2^2\sigma_1^{a_2}\sigma_2^2$. In particular, we again did not have to delete any occurrence of σ_2 in the deletion process described above. If the induced subword of β in the first three generators was $\sigma_1^{a_1}\sigma_2\sigma_3^2\sigma_2\sigma_1^{a_2}\sigma_2\sigma_3^2\sigma_2$, the permutation given by β would leave the third strand invariant and $\widehat{\beta}$ would not be a knot. Thus, there has to be at least one more occurrence of a generator σ_3. This gives the last two possibilities of induced subwords of β in the first three generators: $\gamma = \sigma_1^{a_1}\sigma_2\sigma_3^2\sigma_2\sigma_1^{a_2}\sigma_3^{c_3}\sigma_2\sigma_3^2\sigma_2$ and $\sigma_1^{a_1}\sigma_2\sigma_3^2\sigma_2\sigma_1^{a_2}\sigma_2\sigma_3^2\sigma_2\sigma_3^{c_3}$, which are, up to cyclic permutation, reverse to each other. If β has four strands, then actually β would have to equal γ. But the closure $\widehat{\gamma}$ can never be a knot, since the last two strands get permuted among themselves independently of a_1, a_2 and c_3. Now let β have

at least five strands. If γ is the induced subword of β in the first three generators, one of the occurrences of σ_3^2 has to be separated by an occurrence of σ_4 to the power at least two (recall that we ruled out the possibility of a braid relation $\sigma_3\sigma_4\sigma_3 \to \sigma_4\sigma_3\sigma_4$), since otherwise the first two strands would get permuted among themselves by β and $\widehat{\beta}$ would not be a knot. One can then see that β contains, up to reversing order and cyclic permutation, one of the subwords $\sigma_3^3\sigma_4^2\sigma_3^2\sigma_4^2$ or $\sigma_2\sigma_3\sigma_4^2\sigma_3\sigma_4\sigma_2^2\sigma_3^2\sigma_2$, each of which guarantees the existence of a minor $\widetilde{X}$ in the fibre surface of $\widehat{\beta}$, implying $g_4^{\text{top}}(\widehat{\beta}) < g(\widehat{\beta})$. □

CHAPTER 7

Genus defect of positive braid knots

In this chapter, we further pursue the idea of characterising genus defect $g - g_4^{\text{top}}$ of positive braid knots by forbidden surface minors. In Chapter 6, we have already shown that $g - g_4^{\text{top}} = 0$ is completely obstructed by the four forbidden surface minors $\widetilde{T}$, $\widetilde{E}$, $\widetilde{X}$ and $\widetilde{Y}$. In this chapter, we show that there exists a finite number of forbidden surface minors characterising genus defect $g - g_4^{\text{top}} \leq c$ of positive braid knots for any fixed number c. The key to the proof is our result that the genus defect of a positive braid knot grows linearly with the positive braid index.

Higman's Lemma states that finite words in a finite alphabet with the subword relation are *well-quasi-ordered*, that is, there exists no infinite antichain [**28**]. For well-quasi-ordered sets, properties that are inherited from minors are of special interest, since they can be characterised by finitely many forbidden minors. Indeed, if infinitely many minors were necessary to characterise such a property, then they would constitute an infinite antichain. Baader and Dehornoy noted that restricting to the positive braid monoid on a certain number of strands, Higman's Lemma states that the subword order is a well-quasi-order and it directly follows that their fibre surfaces are well-quasi-ordered by the surface minor relation [**5**]. However, the subword order on the positive braid monoid is not a well-quasi-order if we do not restrict to a certain number of strands: for example, $\sigma_1, \sigma_2, \sigma_3 \dots$ is an infinite antichain. However, Baader and Dehornoy ask whether fibre surfaces of positive braids with the surface minor relation are well-quasi-ordered [**5**].

We do not answer the question of Baader and Dehornoy. Instead, we directly prove the following two applications a positive answer would yield for the genus defect $g - g_4^{\text{top}}$ and the signature defect $2g - |\sigma|$ of positive braid knots.

THEOREM 7.1. *Among prime positive braid knots, $g - g_4^{\text{top}} \leq c$ is characterised by finitely many forbidden surface minors for any $c \geq 0$.*

THEOREM 7.2. *Among prime positive braid knots, $2g - |\sigma| \leq c$ is characterised by finitely many forbidden surface minors for any $c \geq 0$.*

The key idea for the proof is a reduction to the case of restricted braid index, so we can apply Higman's Lemma. This is achieved by Theorem 7.3, which states that the genus defect of positive braid knots grows linearly with the positive braid index. Theorem 7.3 is interesting in its own right, since it highlights the discrepancy between the smooth and the locally-flat category in 4-dimensional topology, a phenomenon we already encountered in Chapter 6.

THEOREM 7.3. *For a prime positive braid knot of positive braid index b,*

$$g - g_4^{\text{top}} \geq \frac{1}{16}b - 1.$$

The proof of Theorem 7.3 uses the same techniques as the proof of Theorem 6.1 in Chapter 6. Briefly, we give a series of lemmas to find the linking patterns corresponding to $\widetilde{T}$, $\widetilde{E}$ or $\widetilde{X}$ as induced subgraphs of the linking pattern of any prime positive braid knot of sufficiently large positive braid index. This implies that also the fibre surface contains surface minors $\widetilde{T}$, $\widetilde{E}$ or $\widetilde{X}$, for which we have established genus defect in Chapter 6. Then we use that genus defect is inherited from surface minors.

1. Induced paths in the linking pattern

We start by quickly mentioning the important concepts from Chapters 2 and 6, and introducing our notation for the rest of this chapter.

Let β be a positive braid on b strands. We denote by $\mathcal{P}(\beta)$ and $\Sigma(\beta)$ the linking pattern and canonical Seifert surface of β and $\widehat{\beta}$, respectively. We refer to Chapters 2 and 6 for the definitions. Also, recall from Chapter 2 that if $\mathcal{P}(\beta)$ is connected, then $\Sigma(\beta)$ is the fibre surface of $\widehat{\beta}$ and, in particular, realises the genus of $\widehat{\beta}$. Furthermore, we denote by $\mathcal{P}_I(\beta)$ the subgraph of the linking pattern induced by the generators with indices in $I \subset \{1, \dots, b-1\}$. Similarly, let $\Sigma_I(\beta)$ be the canonical Seifert surface of the subword of β induced by the generators with indices in I. For example, Lemma 6.7 then states that for a positive braid β on $b \geq 3$ strands, if $\mathcal{P}_{\{i,i+1\}}(\beta)$ is a path for some $1 \leq i < b-1$, then β is not of minimal positive braid index.

Our proof method requires us to find the linking patterns corresponding to $\widetilde{T}$, $\widetilde{E}$ or $\widetilde{X}$ as induced subgraphs of the linking pattern of prime positive braid knots. An important way for us to achieve this is the following. Sometimes, it is possible to find an induced subgraph of the linking pattern with a vertex of degree three. In some cases, it is even possible to prolong the arms of this graph (while staying an induced subgraph of the linking pattern) until it is a linking pattern corresponding to $\widetilde{T}$, $\widetilde{E}$ or $\widetilde{X}$. In this context, the following observation is of relevance.

REMARK 7.4. There are many induced paths in the linking pattern of any prime positive braid knot. For example, below is a recipe for finding induced paths starting at a given vertex of the linking pattern (thought of as a brick in the brick diagram) and going in a chosen direction (right or left) in the standard visualisation of the brick diagram.

(1) Fix your chosen brick v. Depending on whether the brick v is linked with a brick in the column on the right (left) or not, proceed with (3) or (2), respectively.
(2) If the brick v is not linked with a brick in the column on the right (left), add a brick w to the path. Here, w is the brick either above or below v, depending on which one is closer to a brick in the same column linking with a brick in the column on the right (left). Then go back to (1) with $v = w$.

(3) If the brick v is linked with at least one brick on the right (left), add a linked brick w on the right (left) to the path. Here, the brick w is chosen to be as close as possible to a brick in its column that is linked with a brick in the column to its right (left). Then go back to (1) with $v = w$.

Choosing the brick closest to a linking brick in step (3) ensures that there is no linking with the former column when adding bricks as in step (2) until again arriving at step (3). Figure 7.1 illustrates the induced path starting at the endpoint on the left chosen by this recipe for a sample brick diagram.

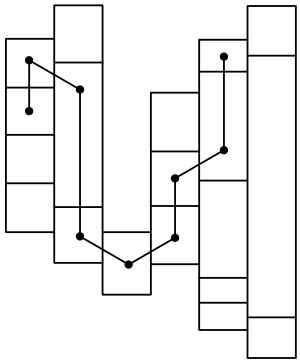

FIGURE 7.1.

The following lemma shows how we can use Remark 7.4 in order to find surface minors $\widetilde{T}$, $\widetilde{E}$ or $\widetilde{X}$. We prove several similar statements in Section 2.

LEMMA 7.5. *Let K be a prime knot obtained as the closure of a positive braid β of minimal positive braid index b. Furthermore, let i be a natural number such that $5 < i < b - 6$. If $\mathcal{P}_i(\beta)$ and $\mathcal{P}_{i+1}(\beta)$ are connected by exactly one edge in $\mathcal{P}(\beta)$, then $\Sigma_{\{i-5,\dots,i+6\}}(\beta)$ contains $\widetilde{T}, \widetilde{E}$ or $\widetilde{X}$ as a surface minor.*

PROOF. Up to conjugation, $\beta_{\{i,i+1\}}$ equals $\sigma_i^a \sigma_{i+1}^b \sigma_i^c \sigma_{i+1}^d$. Either $a, c \geq 2$ or $b, d \geq 2$. Otherwise, $\mathcal{P}_{\{i,i+1\}}(\beta)$ is a path and β is not of minimal positive braid index by Lemma 6.7. By symmetry, we may assume $a, c \geq 2$. Assume $a \geq 3$ for a moment. Then β contains the subword $\sigma_i^3 \sigma_{i+1} \sigma_i^2 \sigma_{i+1}$. In particular, $\mathcal{P}_{\{i,i+1\}}(\beta)$ contains the graph D_5 as an induced subgraph, as indicated in Figure 7.2. Furthermore, since the depicted diagonal edge is the only edge connecting $\mathcal{P}_{\{i\}}(\beta)$ and $\mathcal{P}_{\{i+1\}}(\beta)$ in $\mathcal{P}(\beta)$, we can find an induced subgraph E_{10} of $\mathcal{P}_{\{i,\dots,i+6\}}(\beta)$ by adding a path at the vertex v, as explained in Remark 7.4. In the worst case, this path extends five columns to the right, since the longest arm of E_{10} is of length 6. In particular, $\Sigma_{\{i,\dots,i+6\}}(\beta)$ contains a surface minor $\widetilde{E}$. Therefore, we can assume $a = c = 2$. By symmetry, if in the beginning we assumed $b, d \geq 2$, then this long arm would extend to the left and we would find a surface minor $\widetilde{E}$ of $\Sigma_{\{i-5,\dots,i+1\}}(\beta)$. From now on, we often do not mention this symmetry anymore.

Now we consider the generator σ_{i-1}. Assume that the first occurrence of σ_{i-1} happens before the first occurrence of σ_i in β. There has to be another occurrence of

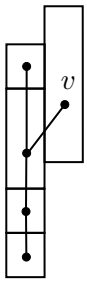

FIGURE 7.2.

σ_{i-1} before the last occurrence of σ_i in β, otherwise $\mathcal{P}_{\{i-1,i\}}(\beta)$ is disconnected and $\widehat{\beta}$ is not prime. Independently of where this occurrence takes place, we can find a surface minor $\widetilde{E}$ or $\widetilde{X}$ of $\Sigma_{\{i-1,\dots,i+6\}}(\beta)$ by adding a path at the vertex v, see Figure 7.3.

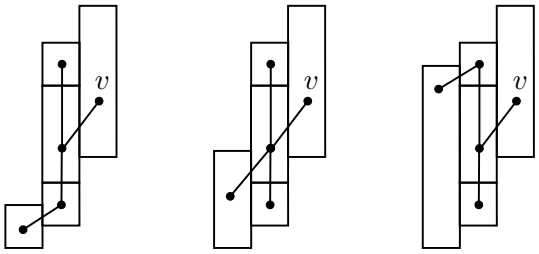

FIGURE 7.3.

Now consider Figure 7.4. We have just shown that there are no crossings in the two regions marked with "X". Hence, there must be at least one crossing in the region

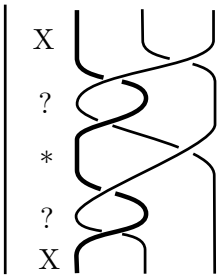

FIGURE 7.4.

marked with "$*$". Otherwise the i-th strand is left invariant by the permutation given by β and $\widehat{\beta}$ is not a knot. Furthermore, in at least one of the two regions marked with "?", there must be at least one crossing. Otherwise, $\widehat{\beta}$ is not prime. If there is no crossing in the upper of the two regions marked with "?", we find a surface minor $\widetilde{T}$ in $\Sigma_{\{i-4,\dots,i+4\}}(\beta)$ by adding a path at the vertices w (to the left) and v (to the right), see Figure 7.5. Similarly, we find a surface minor $\widetilde{T}$ in $\Sigma_{\{i-4,\dots,i+4\}}(\beta)$ if there is no crossing in the lower of the two regions marked with "?".

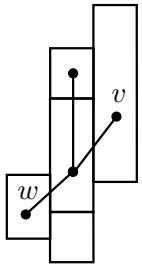

FIGURE 7.5.

We have shown that, up to possibly deleting some generators σ_{i-1}, $\beta_{\{i-1,i,i+1\}}$ equals $\sigma_i\sigma_{i-1}\sigma_i\sigma_{i+1}^b\sigma_{i-1}\sigma_i\sigma_{i-1}\sigma_i\sigma_{i+1}^d$. Using two braid relations $\sigma_i\sigma_{i-1}\sigma_i \to \sigma_{i-1}\sigma_i\sigma_{i-1}$ yields $\sigma_{i-1}\sigma_i\sigma_{i-1}\sigma_{i+1}^b\sigma_{i-1}^2\sigma_i\sigma_{i-1}\sigma_{i+1}^d$, whose intersection pattern contains D_5 as an induced subgraph, as shown in Figure 7.6. Note that by the manipulations we just described, we never change an occurrence of σ_{i+1}. In particular, $\Sigma_{\{i,\dots,i+6\}}(\beta)$ contains a surface minor $\widetilde{E}$ by adding a path at the vertex v in Figure 7.6. □

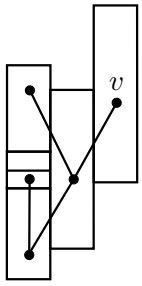

FIGURE 7.6.

REMARK 7.6. Note that if $\mathcal{P}_i(\beta)$ and $\mathcal{P}_{i+1}(\beta)$ are connected by exactly two edges in $\mathcal{P}(\beta)$, then one can find a conjugation of β such that $\mathcal{P}_i(\beta)$ and $\mathcal{P}_{i+1}(\beta)$ are connected by exactly one edge in $\mathcal{P}(\beta)$. Thus, in the following we are often able to assume that $\mathcal{P}_i(\beta)$ and $\mathcal{P}_{i+1}(\beta)$ are connected by at least three edges in $\mathcal{P}(\beta)$.

2. Finding minors $\widetilde{T}$, $\widetilde{E}$ and $\widetilde{X}$

The goal of this section is to give the means for detecting surface minors $\widetilde{T}$, $\widetilde{E}$ and $\widetilde{X}$ of fibre surfaces of prime positive braid knots. We establish a series of lemmas in the spirit of Lemma 7.5 with changing assumptions on the braid β, providing such surface minors. These lemmas basically constitute a case distinction which allows us to prove Proposition 7.10 in Section 3, from which we deduce Theorem 7.3.

LEMMA 7.7. *Let K be a prime knot obtained as the closure of a positive braid β of minimal positive braid index b. Furthermore, let i be a natural number such that $6 < i < b-6$. If $\beta_{\{i,i+1\}}$ ends, up to cyclic permutation, with $\sigma_{i+1}^c\sigma_i^b\sigma_{i+1}^a$ for $a, b, c \geq 2$, then $\Sigma_{\{i-6,\dots,i+6\}}(\beta)$ contains $\widetilde{T}, \widetilde{E}$ or $\widetilde{X}$ as a surface minor.*

PROOF. There have to be at least two additional occurrences of σ_i in $\beta_{\{i,i+1\}}$. Otherwise, there cannot be three or more edges between $\mathcal{P}_i(\beta)$ and $\mathcal{P}_{i+1}(\beta)$ in $\mathcal{P}(\beta)$ and we are done by Lemma 7.5 and Remark 7.6. In particular, $\beta_{\{i,i+1\}}$ contains $\sigma_i^d\sigma_{i+1}^c\sigma_i^b\sigma_{i+1}^a$ as a subword, where $a, b, c, d \geq 2$. If one out of a, b, c or d is strictly greater than 2, then $\Sigma_{i,i+1}(\beta)$ contains $\widetilde{X}$ as a surface minor, compare with the situation in Figure 7.13 (which is obtained by a conjugation). So, we are left with the case where, up to cyclic permutation, $\beta_{\{i,i+1\}} = \sigma_i\sigma_{i+1}^e\sigma_i\sigma_{i+1}^2\sigma_i^2\sigma_{i+1}^2$, for $e \geq 1$.

Now we consider how the occurrences of the generator σ_{i-1} fit into the fixed subword $\beta_{\{i,i+1\}} = \sigma_i\sigma_{i+1}^e\sigma_i\sigma_{i+1}^2\sigma_i^2\sigma_{i+1}^2$. Assume that the first occurrence of σ_{i-1} happens before the first occurrence of σ_i in $\beta_{\{i-1,i,i+1\}}$. There has to be another occurrence of σ_{i-1} before the last occurrence of σ_i in $\beta_{\{i-1,i,i+1\}}$, otherwise $\mathcal{P}_{\{i-1,i\}}$ is disconnected and β is not prime. In each case, we can find a surface minor $\widetilde{X}$ of $\Sigma_{\{i-1,i,i+1\}}$ (by contracting the dotted edge if necessary) as shown in Figure 7.7. By conjugation, an occurrence of

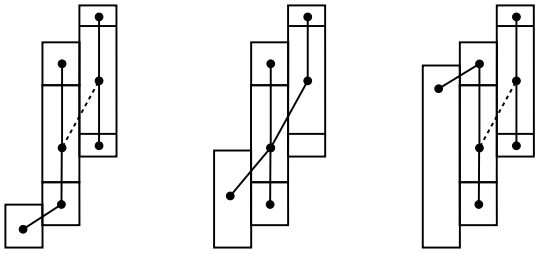

FIGURE 7.7.

σ_{i-1} in $\beta_{\{i-1,i,i+1\}}$ after the last occurrence of σ_i also yields a surface minor $\widetilde{X}$. So, let σ_{i-1} occur only after the first occurrence of σ_i, but before the last one. Since σ_i occurs (counted with multiplicity) exactly four times in $\beta_{\{i-1,i,i+1\}}$, the only way for $\mathcal{P}_{i-1(\beta)}$ and $\mathcal{P}_i(\beta)$ to be connected by at least three edges in $\mathcal{P}(\beta)$ is for σ_{i-1} to split every pair of occurrences of σ_i in $\beta_{\{i-1,i,i+1\}}$. Otherwise, we are again done by Lemma 7.5 and Remark 7.6. In this case, $\beta_{\{i-1,i,i+1\}}$ surely contains $\sigma_i^2\sigma_{i+1}^2\sigma_{i-1}\sigma_i\sigma_{i-1}\sigma_i\sigma_{i+1}^2$ as a subword. Applying the braid relation $\sigma_i\sigma_{i-1}\sigma_i \to \sigma_{i-1}\sigma_i\sigma_{i-1}$ yields the braid word $\sigma_i^2\sigma_{i+1}^2\sigma_{i-1}^2\sigma_i\sigma_{i-1}\sigma_{i+1}^2$, whose canonical fibre surface contains $\widetilde{X}$ as a surface minor. This can be seen by contracting the dotted edge in Figure 7.8. □

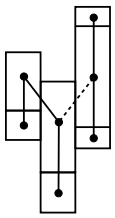

FIGURE 7.8.

LEMMA 7.8. *Let K be a prime knot obtained as the closure of a positive braid β of minimal positive braid index b. Let i be a natural number such that $6 < i < b - 6$.*

Assume furthermore that, up to conjugation, $\beta_{\{i-1,i,i+1\}}$ ends with σ_i^2 and no braid moves

$$\sigma_i\sigma_{i-1}\sigma_i \to \sigma_{i-1}\sigma_i\sigma_{i-1},$$
$$\sigma_i\sigma_{i+1}\sigma_i \to \sigma_{i+1}\sigma_i\sigma_{i+1}$$

can be applied to β. Then $\Sigma_{\{i-6,\dots,i+6\}}(\beta)$ contains $\widetilde{T}, \widetilde{E}$ or $\widetilde{X}$ as a surface minor.

PROOF. We first arrange by conjugation that $\beta_{\{i-1,i,i+1\}}$ does not end with σ_i^3 (but still ends with σ_i^2). Now, if $\beta_{\{i-1,i,i+1\}}$ actually ends with $\sigma_{i-1}\sigma_{i+1}\sigma_i^2$, then one can find a surface minor $\widetilde{T}$ by adding a path at the vertices w (to the left) and v (to the right), see Figure 7.9. So we can assume without loss of generality (using the symmetry of the

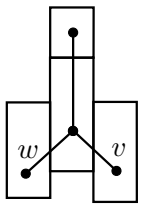

FIGURE 7.9.

situation) that only σ_{i-1} splits the last two occurrences of σ_i, that is, the end σ_i^3 of $\beta_{\{i\}}$ gets split into $\sigma_i\sigma_{i-1}^a\sigma_i^2$ in $\beta_{\{i-1,i,i+1\}}$ for some $a \geq 1$. Actually, this occurrence of σ_{i-1} must be to a power $a \geq 2$, otherwise a braid move $\sigma_i\sigma_{i-1}\sigma_i \to \sigma_{i-1}\sigma_i\sigma_{i-1}$ is possible. So we have to consider the case where both $\beta_{\{i-1,i,i+1\}}$ and $\beta_{\{i-1,i\}}$ end with $\sigma_i^b\sigma_{i-1}^a\sigma_i^2$. If $b \geq 2$, then we are done by Lemma 7.7, so we assume $b = 1$ and consider the case where $\beta_{\{i-1,i\}}$ ends with $\sigma_{i-1}\sigma_i\sigma_{i-1}^a\sigma_i^2$, for some $a \geq 2$.

We now again consider the generator σ_{i+1}. If $\beta_{\{i-1,i,i+1\}}$ ends with $\sigma_{i+1}\sigma_{i-1}\sigma_i\sigma_{i-1}^a\sigma_i^2$, we find a surface minor $\widetilde{E}$ by adding a path at the vertex v, see Figure 7.10. Recall for this that we can assume at least one more occurrence of σ_{i+1} and σ_i earlier in β, because this is the only way for $\mathcal{P}_{i+1}(\beta)$ and $\mathcal{P}_i(\beta)$ to be connected by at least three edges in $\mathcal{P}(\beta)$ (otherwise, we are done by Lemma 7.5 and Remark 7.6). With the same argument, we can also assume another occurrence of σ_{i-1} before the additional occurrence of σ_i. So, we can assume that $\beta_{\{i-1,i,i+1\}}$ ends with $\sigma_i\sigma_{i-1}^b\sigma_i\sigma_{i-1}^a\sigma_i^2$, where

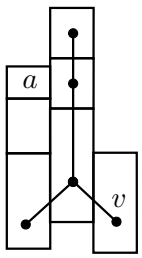

FIGURE 7.10.

$a, b \geq 2$, since otherwise a braid move $\sigma_i\sigma_{i-1}\sigma_i \to \sigma_{i-1}\sigma_i\sigma_{i-1}$ is possible.

Let us once again consider just $\beta_{\{i-1,i\}}$ for a moment. We have reduced the proof to the case where $\beta_{\{i-1,i\}}$ ends with $\sigma_{i-1}^d\sigma_i^c\sigma_{i-1}^b\sigma_i\sigma_{i-1}^a\sigma_i^2$, where $a, b \geq 2$ and $c, d \geq 1$. Now, let us go back to $\beta_{\{i-1,i,i+1\}}$ and distinguish cases depending on where the last occurrence of σ_{i+1} happens.

Case 1: $c \geq 2$ and the last occurrence of σ_{i+1} splits σ_i^c. Similarly to what we did in Figure 7.10, we can find a surface minor $\widetilde{E}$ by adding a path at the vertex v, see Figure 7.11.

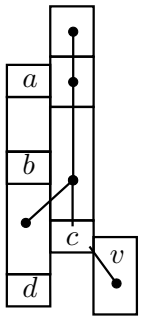

FIGURE 7.11.

Case 2: The last occurrence of σ_{i+1} happens before σ_i^c. Again, we can find a surface minor $\widetilde{E}$ by adding a path at the vertex v, see Figure 7.12. □

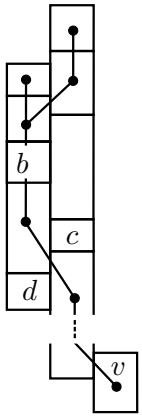

FIGURE 7.12.

LEMMA 7.9. *Let K be a prime knot obtained as the closure of a positive braid β of minimal positive braid index b. Let i be a natural number such that $7 < i < b - 7$. Assume furthermore that no braid moves*

$$\sigma_{i-1}\sigma_{i-2}\sigma_{i-1} \to \sigma_{i-2}\sigma_{i-1}\sigma_{i-2},$$
$$\sigma_i\sigma_{i-1}\sigma_i \to \sigma_{i-1}\sigma_i\sigma_{i-1},$$
$$\sigma_i\sigma_{i+1}\sigma_i \to \sigma_{i+1}\sigma_i\sigma_{i+1},$$
$$\sigma_{i+1}\sigma_{i+2}\sigma_{i+1} \to \sigma_{i+2}\sigma_{i+1}\sigma_{i+2}$$

can be applied to β. If $\beta_{\{i,i+1\}}$ has at least two occurrences of σ_{i+1} to a power ≥ 2, then $\Sigma_{\{i-7,\dots,i+7\}}(\beta)$ contains $\widetilde{T}, \widetilde{E}$ or $\widetilde{X}$ as a surface minor.

By symmetry, Lemma 7.9 also holds if $\beta_{\{i-1,i\}}$ has at least two occurrences of σ_{i-1} to a power ≥ 2.

PROOF. Suppose first that at least two occurrences of σ_{i+1} to a power ≥ 2 in $\beta_{\{i,i+1\}}$ get split by occurrences of σ_{i+2}. Then, these occurrences of σ_{i+2} must be to a power ≥ 2, otherwise, a braid move $\sigma_{i+1}\sigma_{i+2}\sigma_{i+1} \to \sigma_{i+2}\sigma_{i+1}\sigma_{i+2}$ is possible. In particular, $\beta_{\{i,i+1,i+2\}}$ contains the subword $\sigma_{i+1}\sigma_{i+2}^2\sigma_{i+1}^2\sigma_{1+2}^2\sigma_{i+1}$. For $\mathcal{P}_{i+1}(\beta)$ and $\mathcal{P}_{i+2}(\beta)$ to be connected by at least three edges in $\mathcal{P}(\beta)$, there must be at least one more occurrence of σ_{i+1}. It follows that, up to cyclic permutation, $\beta_{\{i,i+1,i+2\}}$ contains the subword $\sigma_{i+1}\sigma_{i+2}^2\sigma_{i+1}^2\sigma_{1+2}^2\sigma_{i+1}^2$, and hence, $\Sigma_{\{i,i+1,i+2\}}(\beta)$ contains $\widetilde{X}$ as a surface minor, compare with Figure 7.13.

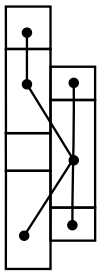

FIGURE 7.13.

Now we suppose at most one occurrence of σ_{i+1} to a power ≥ 2 in $\beta_{\{i,i+1\}}$ gets split by an occurrence of σ_{i+2}. We think of $\beta_{\{i,i+1,i+2\}}$ as a product of factors $(\sigma_i^x\sigma_{i+2}^y\sigma_{i+1})$, where $x, y \geq 0$. There are at least two factors with $x = 0$, since $\beta_{\{i,i+1\}}$ has at least two occurrences of σ_{i+1} to a power ≥ 2. Furthermore, there is at most one factor with $x = 0$ but $y \geq 1$, since we suppose at most one occurrence of σ_{i+1} to a power ≥ 2 in $\beta_{\{i,i+1\}}$ gets split by an occurrence of σ_{i+2}. In particular, there is at least one factor (σ_{i+1}). For $\mathcal{P}_{i+1}(\beta)$ and $\mathcal{P}_{i+2}(\beta)$ to be connected by at least three edges in $\mathcal{P}(\beta)$, there must be at least three factors with $y \geq 1$. Hence, there must be at least two factors with $x, y \geq 1$. We now delete every occurrence of σ_{i+1}, except the ones from the factor (σ_{i+1}), the one from the factor right in front of the factor (σ_{i+1}), and either one of the factors with $x, y \geq 1$. After this deletion we obtain, up to conjugation, $\beta_{\{i,i+1,i+2\}} = \sigma_i^d\sigma_{i+2}^c\sigma_{i+1}\sigma_i^b\sigma_{i+2}^a\sigma_{i+1}^2$, for $a, b, c, d \geq 1$. Note that even though we have an occurrence of σ_{i+1}^2 in $\beta_{\{i,i+1,i+2\}}$, Lemma 7.8 does not apply directly, since the condition on the braid moves is not satisfied. However, we can use the argument at the beginning of its proof and find a surface minor $\widetilde{T}$ by adding paths at vertices w (to the left) and v (to the right), as in Figure 7.14. □

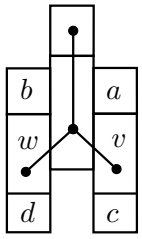

FIGURE 7.14.

3. Linear growth of the genus defect

We are ready to show that for prime positive braid knots, the genus defect $g - g_4^{\text{top}}$ grows linearly with the positive braid index. The following proposition directly implies Theorem 7.3.

PROPOSITION 7.10. *Let K be a prime knot obtained as the closure of a positive braid β of minimal positive braid index b. Let i be a natural number such that $7 < i < b - 7$. Then $\Sigma_{\{i-7,\dots,i+7\}}(\beta)$ contains $\widetilde{T}, \widetilde{E}$ or $\widetilde{X}$ as a surface minor.*

PROOF OF THEOREM 7.3. Let $\Sigma_j = \Sigma_{\{1+16j,\dots,15+16j\}}(\beta)$. By Proposition 7.10, Σ_j contains $\widetilde{T}, \widetilde{E}$ or $\widetilde{X}$ as a surface minor for each integer j such that $0 \leq 16j \leq b - 16$. Since the disjoint union of all surfaces Σ_j is an incompressible subsurfaces of $\Sigma(\beta)$, we get that $\Sigma(\beta)$ contains a disjoint union at least $\frac{b-16}{16}$ copies of $\widetilde{T}, \widetilde{E}$ or $\widetilde{X}$ as a surface minor. Hence, $g - g_4^{\text{top}} \geq \frac{1}{16}b - 1$ holds for $\widehat{\beta}$. □

PROOF OF PROPOSITION 7.10. We start by applying the following braid moves repeatedly until there is no possible braid move

$$\begin{aligned}
\sigma_{i-1}\sigma_{i-2}\sigma_{i-1} &\to \sigma_{i-2}\sigma_{i-1}\sigma_{i-2},\\
\sigma_i\sigma_{i-1}\sigma_i &\to \sigma_{i-1}\sigma_i\sigma_{i-1},\\
\sigma_i\sigma_{i+1}\sigma_i &\to \sigma_{i+1}\sigma_i\sigma_{i+1},\\
\sigma_{i+1}\sigma_{i+2}\sigma_{i+1} &\to \sigma_{i+2}\sigma_{i+1}\sigma_{i+2}
\end{aligned}$$

anymore. This process terminates within a finite number of steps, since each of these braid moves either reduces the sum of powers of generators σ_i or the sum of powers of generators σ_{i-1}, σ_i and σ_{i+1}.

If there is an occurrence of σ_i to a power ≥ 2 in $\beta_{\{i-1,i,i+1\}}$, we are done by Lemma 7.8. So we assume this is not the case, and think of $\beta_{\{i-1,i,i+1\}}$ as a product of factors $(\sigma_{i-1}^x\sigma_{i+1}^y\sigma_i)$, where either $x > 0$ or $y > 0$. If there is more than one occurrence of σ_{i-1} or σ_{i+1} to a power ≥ 2 in $\beta_{\{i-1,i,i+1\}}$, we are done by Lemma 7.9. So we may assume there is at most one factor $(\sigma_{i-1}^x\sigma_{i+1}^y\sigma_i)$ with $x \geq 2$ and at most one such factor with $y \geq 2$. Furthermore, we may assume $\mathcal{P}_i(\beta)$ and $\mathcal{P}_{i+1}(\beta)$ to be connected by at least three edges in $\mathcal{P}(\beta)$, and likewise for $\mathcal{P}_{i-1}(\beta)$ and $\mathcal{P}_i(\beta)$, since otherwise, we are done by Lemma 7.5 and Remark 7.6. It follows that $\beta_{\{i-1,i,i+1\}}$ consists of at least three factors $(\sigma_{i-1}^x\sigma_{i+1}^y\sigma_i)$. Note that factors $(\sigma_{i-1}\sigma_i)$ and $(\sigma_{i+1}\sigma_i)$ are ruled out by the

braid relations we performed at the beginning of the proof. From these observations, it follows that there is at least one factor $(\sigma_{i-1}\sigma_{i+1}\sigma_i)$ in $\beta_{\{i-1,i,i+1\}}$.

In case $\beta_{\{i-1,i,i+1\}}$ ends, up to conjugation, with $(\sigma_{i-1}^x\sigma_{i+1}^y\sigma_i)(\sigma_{i-1}\sigma_{i+1}\sigma_i)$, for numbers $x, y \geq 1$, we find a surface minor $\widetilde{T}$ by adding a path at the vertices w (to the left) and v (to the right), as indicated in Figure 7.15. Note that in order to obtain

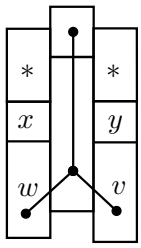

FIGURE 7.15.

the surface minor $\widetilde{T}$, we need to add a path to w and v not passing through the bricks marked by "$*$". However, if we assume $\mathcal{P}_{i+1}(\beta)$ and $\mathcal{P}_{i+2}(\beta)$ are connected by at least three edges in $\mathcal{P}(\beta)$, this can be done for v and similarly for w if $\mathcal{P}_{i-2}(\beta)$ and $\mathcal{P}_{i-1}(\beta)$ are connected by at least three edges in $\mathcal{P}(\beta)$. If this is not the case, we are done by Lemma 7.5 and Remark 7.6.

So far we have shown that we can assume the factors before and after (in the cyclic order) the factor $(\sigma_{i-1}\sigma_{i+1}\sigma_i)$ to be $(\sigma_{i-1}^a\sigma_i)$ and $(\sigma_{i+1}^b\sigma_i)$, respectively, for $a, b \geq 2$. In this case, there must be at least one other factor $(\sigma_{i-1}^x\sigma_{i+1}^y\sigma_i)$. Otherwise, $\mathcal{P}_i(\beta)$ and $\mathcal{P}_{i+1}(\beta)$ are connected by only two edges in $\mathcal{P}(\beta)$. For this factor, only $x = y = 1$ is possible. Furthermore, if there is more than one additional factor, we find that $\beta_{\{i-1,i,i+1\}}$ contains subsequent factors $(\sigma_{i-1}^x\sigma_{i+1}^y\sigma_i)(\sigma_{i-1}\sigma_{i+1}\sigma_i)$, for $x, y \geq 1$, a case we already dealt with. Altogether it follows that, up to conjugation, $\beta_{\{i-1,i,i+1\}}$ is given by $(\sigma_{i+1}^b\sigma_i)(\sigma_{i-1}\sigma_{i+1}\sigma_i)(\sigma_{i-1}^a\sigma_i)(\sigma_{i-1}\sigma_{i+1}\sigma_i)$, for $a, b \geq 2$. The corresponding brick diagram is depicted in Figure 7.16.

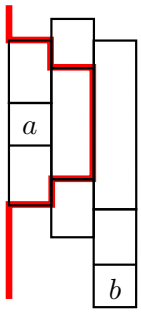

FIGURE 7.16.

We now consider the generator σ_{i-2}. We first note that in $\beta_{\{i-2,i-1,i,i+1\}}$, there must be an occurrence of σ_{i-2} either before the first occurrence of σ_{i-1} or after the last occurrence of σ_{i-1}. Otherwise, the $i-1$-st strand (depicted in thick red in Figure 7.16)

is left invariant by the permutation given by β, and $\widehat{\beta}$ is not a knot. Up to conjugation, we can assume that there is an occurrence of σ_{i-2} after the last occurrence of σ_{i-1}.

There must be other occurrences of σ_{i-2} splitting occurrences of σ_{i-1}. Otherwise, $\mathcal{P}(\beta)$ is disconnected and $\widehat{\beta}$ is not prime. We now distinguish cases depending on where occurrences of σ_{i-2} happen.

Case 1: the occurrence of σ_{i-1}^a in $\beta_{\{i-1,i,i+1\}}$ is split by σ_{i-2}. The occurrence of σ_{i-2} must be to a power ≥ 2, since otherwise a braid move $\sigma_{i-1}\sigma_{i-2}\sigma_{i-1} \to \sigma_{i-2}\sigma_{i-1}\sigma_{i-2}$ is possible. In particular, $\beta_{\{i-2,i-1\}}$ contains $\sigma_{i-1}^2\sigma_{i-2}^2\sigma_{i-1}^2\sigma_{i-2}$ as a subword and we can find a surface minor $\widetilde{E}$ of $\Sigma_{\{i-2,\dots,i+4\}}(\beta)$ by adding a path at the vertex v, as indicated in Figure 7.17.

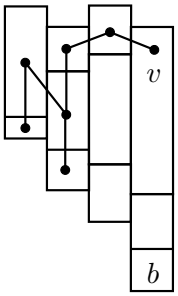

FIGURE 7.17.

Case 2: the occurrence of σ_{i-1}^a in $\beta_{\{i-1,i,i+1\}}$ is not split by σ_{i-2}. In this case, for $\mathcal{P}_{i-2}(\beta)$ and $\mathcal{P}_{i-1}(\beta)$ to be connected by at least three edges in $\mathcal{P}(\beta)$, $\beta_{\{i-2,i-1\}}$ contains $\sigma_{i-1}\sigma_{i-2}\sigma_{i-1}^2\sigma_{i-2}\sigma_{i-1}\sigma_{i-2}$ as a subword. Thus, we can find a surface minor $\widetilde{E}$ of $\Sigma_{\{i-2,\dots,i+5\}}(\beta)$ by adding a path at the vertex v, as indicated in Figure 7.18. □

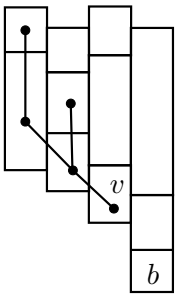

FIGURE 7.18.

REMARK 7.11. Theorem 7.3 does not hold for prime positive braid links. For example, consider the positive braid

$$\beta = (\sigma_1 \dots \sigma_{16}\sigma_{16} \dots \sigma_1)^2$$

on 17 strands. The positive braid β is visually prime and hence prime by a theorem of Cromwell [**16**]. Furthermore, $\widehat{\beta}$ is a link with 17 components. Therefore, the positive

braid β is of minimal positive index. However, a computer calculation yields $|\sigma(\widehat{\beta})| = 33$ and $\text{null}(\widehat{\beta}) = 15$. In particular, we have $b_1(\widehat{\beta}) = \sigma(\widehat{\beta}) + \text{null}(\widehat{\beta})$ and $\widehat{\beta}$ is of maximal topological 4-genus by the lower bound of Kauffman and Taylor [**33**]. Notably, $\Sigma(\beta)$ cannot contain any surface minor $\widetilde{T}$, $\widetilde{E}$ or $\widetilde{X}$.

4. Surface minor theory for the genus defect

In this section, we deduce the surface minor theoretic applications of Theorem 7.3. More precisely, we show that among prime positive braid knots, having at most a certain genus defect $g - g_4^{\text{top}}$ can be characterised by finitely many forbidden surface minors. Our proof also yields the same result for the signature defect $2g - |\sigma|$.

LEMMA 7.12. *Let K be a prime knot obtained as the closure of a positive braid β of minimal positive index b. Then $g - g_4^{\text{top}} \leq c$ holds for $K = \widehat{\beta}$ if and only if it holds for $\widehat{\beta}_{\{1,\dots,16c+32\}}$.*

PROOF. If $b \leq 16c+33$, then $\beta = \beta_{\{1,\dots,16c+32\}}$ and the statement is obviously true. Now let $b > 16c + 33$. As in the proof of Theorem 7.3, both $\Sigma(\beta)$ and $\Sigma_{\{1,\dots,16c+32\}}(\beta)$ contain a disjoint union of at least $c + 1$ copies of $\widetilde{T}$, $\widetilde{E}$ or $\widetilde{X}$ as a surface minor by Proposition 7.10. Hence, $g - g_4^{\text{top}} > c$ holds for both K and $\widehat{\beta}_{\{1,\dots,16c+32\}}$. □

PROOF OF THEOREM 7.1. We show that among positive braids of minimal positive braid index whose closure is a prime knot, $g - g_4^{\text{top}} \leq c$ can be characterised by finitely many forbidden subwords for any $c \geq 0$. This implies the result on the level of surfaces, since every prime positive braid knot can be written as the closure of a positive braid of minimal positive braid index, while the associated fibre surface does not change its isotopy type. Furthermore, the forbidden surface minors are simply given by the fibre surfaces (described in Chapter 2) associated with the forbidden subwords. For this to make sense, recall that if β' is a subword of a positive braid β, then $\Sigma(\beta')$ is a surface minor of $\Sigma(\beta)$.

Consider the positive braid monoid on $16c + 33$ strands. By Higman's Lemma, the words in a finite alphabet are well-quasi-ordered by the partial order induced by subwords [**28**]. In particular, the positive braid monoid on $16c+33$ strands is well-quasi-ordered by the partial order induced by subwords. Since $g - g_4^{\text{top}} > c$ of the closure is inherited from subwords, $g - g_4^{\text{top}} \leq c$ is characterised by finitely many forbidden subwords for the positive braid monoid on $16c + 33$ strands.

Now, let K be a prime knot obtained as the closure of a positive braid β of minimal positive braid index b, where b can be arbitrarily large. We argue that if $g - g_4^{\text{top}} > c$ holds for K, then β contains one of the finitely many forbidden subwords characterising $g - g_4^{\text{top}} \leq c$ for the positive braid monoid on $16c + 33$ strands. To see this, note that $g - g_4^{\text{top}} > c$ for K implies $g - g_4^{\text{top}} > c$ for $\widehat{\beta}_{\{1,\dots,16c+32\}}$ by Lemma 7.12. In particular, $\beta_{\{1,\dots,16c+32\}}$, and hence β, contains one of the forbidden subwords characterising genus defect $g - g_4^{\text{top}} \leq c$ for the positive braid monoid on $16c + 33$ strands. □

Since half the signature is a lower bound for the topological 4-genus [**33**], the genus defect $g - g_4^{\text{top}}$ is a lower bound for half the signature defect $2g - |\sigma|$. From this, it

follows that Theorem 7.3 implies the same quantitative result (up to a factor 2) for the signature defect, and hence also Lemma 7.12. In particular, we can use the proof of Theorem 7.1 to show the analogous result for the signature defect $2g - |\sigma|$. This yields Theorem 7.2.

Bibliography

[1] N. A'Campo: *Sur les valeurs propres de la transformation de Coxeter*, Invent. Math. **33** (1976), no. 1, 61–67.

[2] N. A'Campo: *Planar trees, slalom curves and hyperbolic knots*, Inst. Hautes Etudes Sci. Publ. Math. **88** (1998), 171–180 (1999).

[3] S. Baader: *Positive braids of maximal signature*, Enseign. Math. **59** (2013), no. 3–4, 351–358.

[4] S. Baader: *On the stable* 4*-genus of knots with indefinite Seifert form*, Comm. Anal. Geom. **24** (2016), no. 2, 301–305.

[5] S. Baader, P. Dehornoy: *Minor theory for surfaces and divides of maximal signature*, `http://arxiv.org/abs/1211.7348`.

[6] S. Baader, P. Dehornoy, L. Liechti: *Signature and concordance of positive knots*, accepted for publication in Bull. London Math. Soc. (2017).

[7] S. Baader, P. Feller, L. Lewark, L. Liechti: *On the topological 4-genus of torus knots*, accepted for publication in Trans. Amer. Math. Soc. (2016).

[8] S. Baader, C. Graf: *Fibred links in* S^3, Expo. Math. **34** (2016), no. 4, 423–435.

[9] S. Baader, L. Lewark: *The stable* 4*-genus of alternating knots*, `https://arxiv.org/abs/1505.03345`.

[10] S. Baader, L. Lewark, L. Liechti: *Plane graph monodromies*, preprint (2017).

[11] R. Billet, L. Liechti: *Teichmüller polynomials of fibered alternating links*, `https://arxiv.org/abs/1611.05685`.

[12] L. Bessières, G. Besson, S. Maillot, M. Boileau, J. Porti: *Geometrisation of* 3*-manifolds*, EMS Publishing House, Zürich, 2010.

[13] M. Borodzik, S. Friedl: *The unknotting number and classical invariants, I*, Algebr. Geom. Topol. **15** (2015), no. 1, 85–135.

[14] A. E. Brouwer, W. H. Haemers: *Spectra of graphs*, Springer, New York, 2012.

[15] G. Burde, H. Zieschang, M. Heusener: *Knots*, De Gruyter, Berlin, 2014.

[16] P. R. Cromwell: *Positive braids are visually prime*, Proc. London Math. Soc. (3) **67** (1993), no. 2, 384–424.

[17] S. K. Donaldson: *An application of gauge theory to four-dimensional topology*, J. Differential Geom. **18** (1983), no. 2, 279–315.

[18] B. Farb, D. Margalit: *A primer on mapping class groups*, Princeton University Press, Princeton, NJ, 2012.

[19] A. Fathi, F. Laudenbach, V. Poénaru, editors: *Travaux de Thurston sur les surfaces*, volume 66 of *Astérisque*, Société Mathématique de France, Paris, 1979.

[20] P. Feller: *The signature of positive braids is linearly bounded by their genus*, Internat. J. Math. **26** (2015), no. 10, 1550081.

[21] P. Feller: *The degree of the Alexander polynomial is an upper bound for the topological slice genus*, Geom. Topol. **20** (2016), no. 3, 1763–1771.

[22] P. Feller: *A sharp signature bound for positive four-braids*, `http://arxiv.org/abs/1508.00418`.

[23] P. Feller, L. Lewark: *On classical upper bounds for slice genera*, `https://arxiv.org/abs/1611.02679`.

[24] M. H. Freedman: *The topology of four-dimensional manifolds*, J. Differential Geom. **17** (1982), no. 3, 357–453.
[25] D. Gabai: *The Murasugi sum is a natural geometric operation*, Low Dimensional Topology AMS Cont. Math. Studies **20** (1983), 131–144.
[26] Y. Gerber: *Positive tree-like mapping classes*, PhD Thesis, University of Basel (2006).
[27] P. M. Gilmer, C. Livingston: *Signature jumps and Alexander polynomials for links*, Proc. Amer. Math. Soc. **144** (2016), no. 12, 5407–5417.
[28] G. Higman: *Ordering by divisibility in abstract algebras*, Proc. London Math. Soc. (3) **2** (1952), 326–336.
[29] E. Hironaka: *Mapping classes associated to mixed-sign Coxeter graphs*, `http://arxiv.org/abs/1110.1013`.
[30] M. Hirasawa, K. Murasugi: *Various stabilities of the Alexander polynomial of knots and links*, `http://arxiv.org/abs/1307.1578`.
[31] E. Hironaka, L. Liechti: *On Coxeter mapping classes and fibered alternating links*, Michigan Math. J. **65** (2016), 799–812.
[32] P. Hubert, E. Lanneau: *Veech groups without parabolic elements*, Duke Math. J. **133** (2006), 335–346.
[33] L. H. Kauffman and L. R. Taylor: *Signature of links*, Trans. Amer. Math. Soc. **216** (1976), 351–365.
[34] J. C. Cha, C. Livingston: *KnotInfo: Table of Knot Invariants*, `http://www.indiana.edu/~knotinfo`, 12.11.2015.
[35] P. B. Kronheimer, T. S. Mrowka: *The genus of embedded surfaces in the projective plane*, Math. Res. Lett. **1** (1994), no. 6, 797–808.
[36] E. Lanneau, J.-L. Thiffeault: *On the minimum dilatation of pseudo-Anosov homeomorphisms on surfaces of small genus*, Ann. Inst. Fourier **61** (2011), 105–144.
[37] C. Leininger: *On groups generated by two positive multi-twists: Teichmüller curves and Lehmer's number*, Geom. Topol. **8** (2004), 1301–1359.
[38] J. Levine: *Knot cobordism groups in codimension two*, Comment. Math. Helv. **44** (1969), 229–244.
[39] L. Liechti: *Signature, positive Hopf plumbing and the Coxeter tranformation*, Osaka J. Math. **53** (2016), no. 1, 251–267.
[40] L. Liechti: *Positive braid knots of maximal topological 4-genus*, Math. Proc. Cambridge Philos. Soc. **161** (2016), no. 3, 559–568.
[41] L. Liechti: *Minimal dilatation in Penner's construction*, accepted for publication in Proc. Amer. Math. Soc. (2016).
[42] R. A. Litherland: *Signatures of iterated torus knots*, Topology of low-dimensional manifolds (Proc. Second Sussex Conf., Chelwood Gate, 1977), 71–84, Lecture Notes in Math. **722**, Springer, Berlin, 1979.
[43] C. Livingston: *The stable 4-genus of knots*, Algebr. Geom. Topol. **10** (2010), no. 4, 2191–2202.
[44] M. Marden: *The geometry of the zeros of a polynomial in a complex variable*, Mathematical Surveys, no. 3, American Mathematical Society, New York, 1949.
[45] B. Martelli: *An Introduction to Geometric Topology*, `https://arxiv.org/abs/1610.02592`.
[46] C. T. McMullen: *Coxeter groups, Salem numbers and the Hilbert metric*, Publ. Math. Inst. Hautes Études Sci. **95** (2002), 151–183.
[47] F. Misev: *On the plumbing structure of fibre surfaces*, PhD thesis, University of Bern (2016).
[48] F. Misev: *Hopf bands in arborescent Hopf plumbings*, `https://arxiv.org/abs/1601.01933`.
[49] K. Murasugi: *On a certain numerical invariant of link types*, Trans. Amer. Math. Soc. **117** (1965), 387–422.
[50] R. C. Penner: *A construction of pseudo-Anosov homeomorphisms*, Trans. Amer. Math. Soc. **310** (1988), 179–197.
[51] G. Perelman: *The entropy formula for the Ricci flow and its geometric applications*, `https://arxiv.org/abs/math/0211159`.

[52] G. Perelman: *Finite extinction time for the solutions to the Ricci flow on certain three-manifolds*, `http://arxiv.org/abs/math/0307245`.

[53] G. Perelman: *Ricci flow with surgery on three-manifolds*, `http://arxiv.org/abs/math/0303109`.

[54] M. Powell: *The four-genus of a link, Levine-Tristram signatures and satellites*, J. Knot Theory Ramifications **26** (2017), no. 2, 1740008.

[55] I. Rivin: *Walks on groups, counting reducible matrices, polynomials, and surface and free group automorphisms*, Duke Math. J. **142** (2008), no. 2, 353–379.

[56] D. Rolfsen: *Knots and links*, A.M.S. Chelsea Publishing, 1976.

[57] L. Rudolph: *Nontrivial positive braids have positive signature*, Topology **21** (1982), 325–327.

[58] L. Rudolph: *Some topologically locally-flat surfaces in the complex projective plane*, Comment. Math. Helv. **59** (1984), no. 4, 592–599.

[59] L. Rudolph: *Quasipositivity as an obstruction to sliceness*, Bull. Amer. Math. Soc. (N.S.) **29** (1993), no. 1, 51–59.

[60] L. Rudolph: *Hopf plumbing, arborescent Seifert surfaces, baskets, espaliers, and homogeneous braids*, Topology Appl. **116** (2001), no. 3, 255–277.

[61] H. Shin, B. Strenner: *Pseudo-Anosov mapping classes not arising from Penner's construction*, Geom. Topol. **19** (2015), no. 6, 3645–3656.

[62] H. Smith: *On Systems of linear indeterminate equations and congruences*, Phil. Trans. R. Soc. Lond. **151** (1861), 293–326.

[63] J. Stallings: *Constructions of fibred knots and links*, Algebraic and Geometric Topology, 55–60, Proc. Sympos. Pure Math. **32** (1978) Amer. Math. Soc., Providence, R.I.

[64] R. Steinberg: *Finite reflection groups*, Trans. Amer. Math. Soc. **91** (1959), 493–504.

[65] A. Stoimenow: *Some applications of Tristram-Levine signatures and relation to Vassiliev invariants*, Adv. Math. **194** (2005), no. 2, 463–484.

[66] A. Stoimenow: *Bennequin's inequality and the positivity of the signature*, Trans. Amer. Math. Soc. **360** (2008), 5173–5199.

[67] B. Strenner: *Galois conjugates of pseudo-Anosov stretch factors are dense in the complex plane*, `https://arxiv.org/abs/1702.05424`.

[68] L. R. Taylor: *On the genera of knots*, Topology of low-dimensional manifolds (Proc. Second Sussex Conf., Chelwood Gate, 1977), Lecture notes in Math. vol. 722, Springer, Berlin, 1979, 144–154.

[69] W. Thurston: *On the geometry and dynamics of diffeomorphisms of surfaces*, Bull. Amer. Math. Soc. **19** (1988), 417–431.

[70] W. P. Thurston: *Hyperbolic structures on 3-manifolds, II: Surface groups and 3-manifolds which fiber over the circle*, `http://arxiv.org/abs/math/9801045`.

[71] A. G. Tristram: *Some cobordism invariants for links*, Proc. Cambridge Philos. Soc. **66** (1969), 251–264.

[72] H. F. Trotter: *Homology of group systems with applications to knot theory*, Ann. of Math. (2) **76** (1962), 464–498.

[73] C. G. Wagner: *Newton's inequality and a test for imaginary roots*, Two-Year College Math. J. **8** (1977), no. 3, 145–147.

Erklärung

gemäss Art. 28 Abs. 2 RSL 05

Name/Vorname: Liechti Livio

Matrikelnummer: 08-117-004

Studiengang: Mathematik, Dissertation

Titel der Arbeit: On the spectra of mapping classes and the 4-genera of positive knots

Leiter der Arbeit: Prof. Dr. Sebastian Baader

Ich erkläre hiermit, dass ich diese Arbeit selbständig verfasst und keine anderen als die angegebenen Quellen benutzt habe. Alle Stellen, die wörtlich oder sinngemäss aus Quellen entnommen wurden, habe ich als solche gekennzeichnet. Mir ist bekannt, dass andernfalls der Senat gemäss Artikel 36 Absatz 1 Buchstabe r des Gesetzes vom 5. September 1996 über die Universität zum Entzug des auf Grund dieser Arbeit verliehenen Titels berechtigt ist. Ich gewähre hiermit Einsicht in diese Arbeit.

Bern, 6. Juni 2017

Livio Liechti